PREDIS

Deliverable 5.3
Technical report: Synthesis of conditioning matrix performances studies

03.07.2024 Version Final

Dissemination level: Public

Matthieu Briffaut (Centrale Lille Institut)
Ecole Centrale de Lille
Cité Scientifique – CS20048
59651 Villeneuve d'Ascq Cedex
Matthieu.briffaut@centralelille.fr
+ 33 320434333

This project has received funding from the Euratom research and training programme 2019-2020 under grant agreement No 945098.

Project acronym PREDIS	Project title PRE-DISposal management of radioactive waste		Grant agreement No. 945098
Deliverable No. D5.3	Deliverable title Report on Synthesis of conditioning matrix performances studies		Version Final
Type Report	Dissemination level Public		Due date M45
Lead beneficiary Ecole Centrale de Lille (ECL)			WP No. 5
Main author Matthieu Briffaut (ECL)	Reviewed by Arnaud Poulesquen (CEA) and John Provis (PSI). External reviewers Thierry Mennecart (SCK CEN) and Céline Cau dit Coumes (CEA).	Accepted by Maria Oksa and Erika Holt (VTT), Coordinators	
Contributing authors Sara Koubeissy (ECL, France), Anna Sears (CV Rez, Czech Republic), Borys Zlobenko (SIIEG NAS, Ukraine), Gabriele Magugliani (POLIMI, Italy), Ilaria Moschetti (IMT, France), Eros Mossini (POLIMI, Italy), Lara Esperanza (CIEMAT, Spain), Nguyen Thi Nhan (SCK CEN, Belgium), Monika Kiselova (UJV, Czech Republic), Rosa Lo Franco (UNIPI, Italy) Quoc Tri Phung (SCK CEN, Belgium)			Pages 119

Abstract

WP5 “Innovations in liquid organic waste treatment and conditioning” of the PREDIS project focused on the investigation and development of innovative technologies for direct conditioning of radioactive liquid organic waste (RLOW). A part of this work package was Task T5.4 “Study of conditioning matrix performances” dedicated to the study of performances of conditioning matrix developed during task 5.3 “Study of direct conditioning process”.

During this Task, the partners have first investigated the long-term performances of three formulation families based on Metakaolin (MK), Blast Furnace Slag (BFS) and a mixture of fly ash (FA), BFS and MK (MIX) formulation. The durability of materials in various conditions (endogeneous, aerated, acid & alcaline liquid lixiviation) was studied with formulation containing different type of waste surrogate. Moreover, materials behaviour under irradiation and high temperature (including fire hazard) have also been studied. Finally, radionuclides binding and leaching on real waste have been investigated.

This technical report “Synthesis of experimental results on long term matrices performances for direct conditioning of liquid organic waste” describes all the work and results achieved by the partners in the scope of Task T5.4 “Study of conditioning matrix performances”.

This report version has included comments from the external reviewers Thierry Mennecart (SCK CEN) and Céline Cau dit Coumes (CEA).

Keywords

Radioactive liquid organic waste, RLOW, long-term performance, formulation, metakaolin, blast furnace slag, fly ash, materials behaviour, irradiation, high temperature

Coordinator contact

Maria Oksa
VTT Technical Research Centre of Finland Ltd
Kivimiehentie 3, Espoo / P.O. Box 1000, 02044 VTT, Finland
E-mail: maria.oksa.@vtt.fi
Tel: +358 50 5365 844

Acknowledgement

This project has received funding from the Euratom research and training programme 2019-2020 under grant agreement No 945098.

TABLE OF CONTENTS

ABBREVIATIONS

AAM – Alkali Activated Material

ACRIA – Belgian waste acceptance criteria

BFS – Blast Furnace Slag

CT – Computed Tomography

GC – Gas Chromatography

GEOIL – Geopolymer + Oil

GP – Geopolymer

MK – Metakaolin

NPP – Nuclear Power Plant

OPC – Ordinary Portland cement

PREDIS – Pre-Disposal Management of Radioactive Waste

RLOW – Radioactive liquid organic waste

RW – Radioactive waste

TBP – Tri-butyl phosphate

TSO – Technical and Scientific Support Organization

VT – Volcanic Tuff

WP – Work package

1 Introduction

The "**PREDIS** – **Pre-Disposal Management of Radioactive Waste**" project is a 4-year cooperative research and innovation action initiated by Euratom in September 2020. The project's main aim is to develop and improve treatment and conditioning options of low- and intermediate level radioactive waste for which no adequate or industrially mature solutions are currently available. This involves waste such as metallic materials, liquid organic waste and solid organic waste. Additionally, the PREDIS project also targets innovation in cemented waste handling and assessing for extended interim surface storage using digitalisation solutions. This includes the use of digital twin and artificial intelligence for big data mining from non-destructive evaluation methods.

Work package 5 (WP5) "Innovations in liquid organic waste treatment and conditioning" of the PREDIS project addresses the lack of available technologies for radioactive liquid organic waste (RLOW) treatment and conditioning by investigating and developing innovative technologies for direct conditioning of RLOW. The work package is divided into Tasks focused on exploring the possibility of using geopolymers and related alkali-activated materials.

Task 5.4 "Study of conditioning matrix performances" is dedicated to the performance of direct conditioning matrix. The main objective of this Task is to study the long-term performances of the most promising reference formulations developed in the Task 5.3 "Study of direct conditioning process" that can be used for treatment and conditioning of various types of RLOW identified during Task 5.2 (Collection & Review of Waste, Regulatory, Scientific & Technical Data). The work within Task T5.4 was split into different Sub-tasks which are presented below:

- Sub-task T5.4.1 – Definition of experimental protocols
- Sub-task T5.4.2 – Study of matrix durability in endogeneous conditions
- Sub-task T5.4.3 – Study of conditioning matrix durability in aerated conditions
- Sub-task T5.4.4 – Study of conditioning matrix durability in acid & liquid lixiviation conditions
- Sub-task T5.4.5 – Study of conditioning materials behaviour under irradiation
- Sub-task T5.4.6 – Study of radionuclides binding and leaching
- Sub-task T5.4.7 – Study of Thermal behaviour and Fire hazard.

The list of partners involved in T5.4 describing the type of partner organisation and its involvement in different Sub-tasks is presented in Table 1. It is important to note that this Task involved various types of organisations, ranging from TSO's, waste management organisations and service providers to research organisations and universities.

Table 1. List of partners involved in PREDIS Task T5.4 Study of conditioning matrix performances.

Project partner		Country	Type of organisation	Sub-task
Abbreviation	**Full name**			
ECL	Ecole Centrale de Lille	France	University	All - Task leader
IMT	Institut Mines Telecom Nantes	France	University	T5.4.5
NUCLECO	Nucleco Societa Per L'Ecoingegneria	Italy	Service provider	T5.4.6
USFD	University of Sheffield	UK	University	All – Task co-leader (supporting ECL)
UNIPI	University of PISA	Italy	University	T5.4.7
CIEMAT	Centro de Investigaciones Energeticas, Medioambientales y Tecnologicas	Spain	TSO	T5.4.2 - T5.4.3, T5.4.4
SCK CEN	Belgian Nuclear Research Center	Belgium	Research	T5.4.2 - T5.4.3, T5.4.4
UJV Rez	ÚJV Rez, a.s.	CZ	TSO	T5.4.2 - T5.4.3, T5.4.4
POLIMI	Politecnico di Milano	Italy	University	T5.4.6 - T5.4.5
CV Rez	Centrum Vizkumu Rez	CZ	Research	T5.4.2 - T5.4.3, T5.4.4
SIIEG	SI "Institute of Environmental Geochemistry" NAS of Ukraine	Ukraine	Research	T5.4.2 - T5.4.3, T5.4.4

1.1 Objective

This Technical report is the result of final Sub-task T5.4.8 created with an objective of describing, summarizing, highlighting and analyzing the key results, information and data generated by the different partners in Task T5.4. This report includes all necessary results obtained in the different Sub-tasks, for the different conditioning performance and formulations.

1.2 Structure of the report

The structure of the report is divided into two main parts. The first part is devoted to the presentation of the preparation of the sample, curing and characterization (macroscopic and microstructural ones) before the test and the second part consists in experimental results during and after tests (durability, irradiation and high temperature behaviour). The organization of the WP 5.4 task is summarized in the Table 2.

Table 2. Organization of the subtask for each formulation and each experiment type

Task	Formulation MK (NNL)	Formulation BFS (SCK CEN)	Formulation MIX (KIPT)	RLOW surrogate
T5.4.2 to 5.4.4	CIEMAT + ECL	SCK CEN / IRSN + CV Rez	SIIEG	TBP Dodecane/scintill/oil
T5.4.5	IMT + POLIMI			TBP Dodecane/scintill/oil
T5.4.6	UJV + POLIMI			TBP Dodecane/scintill/oil
T5.4.7	UNIPI			TBP Dodecane/scintill/oil

2 PREPARATION OF SAMPLES and CURING CONDITIONS

2.1 Reminder of the formulation selected by WP 5.3

Various types of organic liquids are used in the nuclear industry, especially during nuclear reactor operations, in the field of nuclear medicine, at various nuclear research centers and during the decontamination of facilities. The waste types of RLOW arising from these operations can be classified as lubricants, organic solvents, scintillation liquids and decontamination liquids. In most cases these types of radioactive waste (RW) amount to a small part of the total liquid waste generated. In the past, conventional treatment methods used in the industry, such as cementation and incineration were used in some countries to treat this kind of RW. However, due to their organic nature, the RLOW treatment process is oftentimes difficult and requires either an additional treatment step or a different treatment and conditioning methodology altogether.

RLOW are very mobile. They will drain under gravity and contribute to the spread of contamination, so they need to be effectively immobilized. Many are volatile and combustible or will support combustion of other wastes. They can also provide a source of nutrients for microbial activity. Many organic fluids are immiscible with water and can be classed as nonaqueous phase liquids which require special care due to their potential to migrate rapidly in the environment (the lighter fraction can float on water whereas the dense fraction cannot). This distinction is significant for waste collection, storage and processing. Furthermore, some of the decontaminants (chelating agents) can form water soluble complexes with radionuclides (especially the actinides).

As a consequence of the complex physico-chemical properties of the RLOW, many countries, partly including the EU Member States, still have their RLOW in storage and are trying to develop an adequate treatment method.

Table 3 contains the available information on the types of RLOW stored by different organizations in EU member countries (adapted from the results of data collected using a specific questionnaire in the scope of Task 5.2 – D5.1). As can be seen, the most common waste types are lubricants, organic solvents and scintillation cocktails. The description of the different RLOW waste types as well as a further look on their origin is given in Table 3 below.

Table 3. Types of RLOW stored by organizations in EU member states

Organization	Country	Lubricants	Organic solvents	Scintillation cocktail	Decontamination liquids	Sludge
KIPT	Ukraine	Y				
Sellafield Ltd.	UK		Y			
CV Rez	Czech Republic	Y	Y	Y	Y	
ÚJV Rez	Czech Republic	Y	Y	Y		
SOGIN	Italy	Y	Y			
RATEN	Romania	Y		Y		
Cernavoda NPP	Romania	Y	Y	Y		Y

More information about each kind of RLOW can be found in the synthesis report of WP 5.3.

The final composition of the matrices selected by the WP 5.3 can be found in Table 4.

Table 4. References formulation (without RLOW) proposed by T5.3

NNL formulation – MK based

- **Row material:**
  - Metamax® - RC: Al_2O_3 = 43.99%, SiO_2 = 52.48%
- **Alkaline activator:**
  - K silicate (K120): K_2O = 21.3 wt.% SiO_2 = 30.38 wt.% H_2O = 48.32 wt.%
- **Optimized formulation:**
  - SiO_2:K_2O = 1.2
  - K_2O: Al_2O_3 = 1.2
  - H_2O_2:K_2O = 13
- **RLOW:**
  - Nevastane Oil (20% vol.)

SCK CEN formulation – BFS based

- **Row material:**
  - BFS = 46.6 wt.% (Al_2O_3 = 11.10%, SiO_2 = 32.40%)
  - Sand = 28 wt.%
- **Alkaline activator:**
  - $Na_2O.2SiO_2.xH_2O$ – 1.5 wt.%
  - NaOH (10M) – 5.5 wt.%
  - Additional water – 18.4 wt.%
- **RLOW:**
  - Ionic liquid (Aliquat 336) – 9.9 wt.%(1)
  - TBP – 19.1 wt.%

(1) Tween 80 surfactant used: 0.5% and 0.95% relative to the waste volume

KIPT formulation – MIX based

- **Row material:**
  - FA = 34 wt.% (Al_2O_3 = 18%, SiO_2 = 46.12%)
  - BFS = 20 wt.% (Al_2O_3 = 6.02%, SiO_2 = 40.6%)
  - MK = 14 wt.% (Al_2O_3 = 35.50%, SiO_2 = 51%)
- **Alkaline activator:**
  - K_2SiO_3 = 11 wt.%
  - KOH – 9 wt.%
  - Water – 12 wt.%
- **RLOW:**
  - ShellSpirax: from 10% to 40% vol. (2)

(2) Castament FW 10 (solid Polyethylene glycol-based additive) used to improve several properties: 0.5%

It should be noted that due to the raw material availability, some participants have slightly adapted the formulation proposed by WP 5.3. Consequently, the real used formulation is described in the following sub-chapter. This slight modification allows also to test the robustness of a given formula and their capacity to be transposed to other country.

2.2 Metakaolin formulation

To produce sample, CIEMAT used Metakaolin (BASF) and Betol (K5020) as activator enriched with potassium hydroxide solution to achieve the K_2O concentration desired. The activator is a mixture of K-Betol, KOH (pellets) and water. K-Betol is a commercial potassium silicate (31.5% SiO_2 and 20.5% K_2O) supplied by Woellner. KOH pellets (85% purity) were obtained from Scharlab. The activator is prepared by adding the pellets slowly (since it is an exothermic reaction) in the marked amounts of water and K-Betol. The mixture is stirred for 4 hours at 500 rpm and left to rest until the next day. This manufactured activator has the following molar ratios: Silica modulus (Ms)=1.2 and H_2O/K_20=13. Its overall chemical composition is 86.3% H_20, 7.7% SiO_2 and 6% K_2O.

The wastes immobilized were oil (Repsol Taurus) and liquid scintillation (Instagel Plus).

POLIMI adopted the formulation and mixing protocol developed by NNL. Raw materials employed for the preparation of samples are reported in Table 5.

Table 5. Raw materials employed by POLIMI for the preparation of MK-based formulation.

Material	Concentration (wt%)
MK (Metamax, BASF)	32.5
KOH	10.0
Betol K 5020 T	40.5
Water	17.0

POLIMI considered two types of organic liquids:

- TBP/dodecane (30:70 mix by volume)
- Ultima Gold liquid scintillation cocktail (Perkin Elmer)

A constant waste loading factor of 30 %v. was adopted for all studies. In case of TBP/dodecane, Tween 80 was used as a surfactant at 3 %w. with respect to waste mass. For encapsulation of LSC no added surfactant was used, as this organic liquid already contains a surfactant by design.

The mixing protocol adopted for the preparation of MK-based samples is illustrated in Figure 1. Both high-shear and low-shear (planetary) mixers are adopted at various stages of the preparation protocol. Also, the order of addition of precursor and activator is different depending on the waste considered, as optimized by NNL. After casting, samples were cured for 28 days in endogenous conditions at room temperature (20 ± 2 °C).

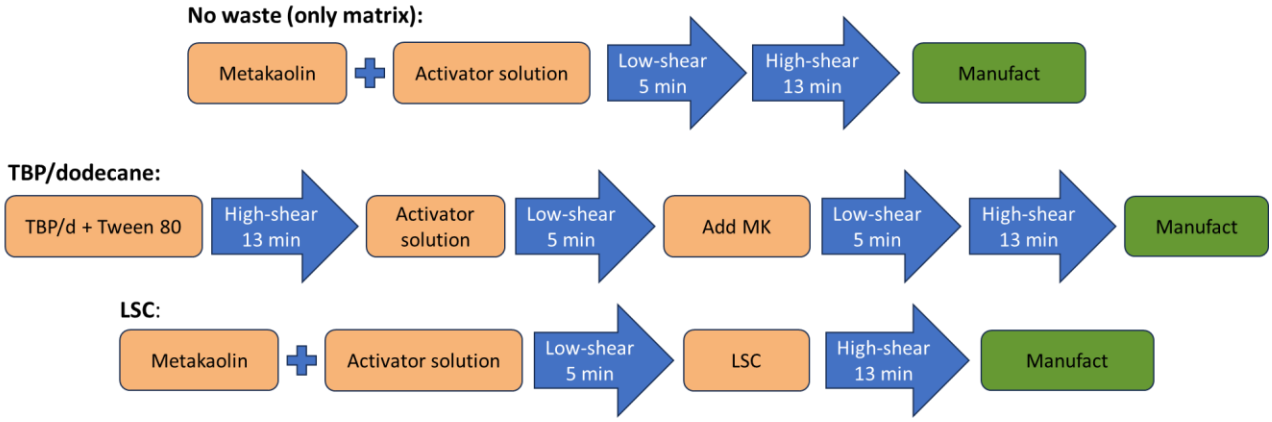

Figure 1. Mixing protocol adopted by POLIMI to prepare MK-based samples with LSC and TBP/dodecane wastes.

Two sample geometries were adopted:

- 5 cm equilateral cylinders for compressive strength testing after curing (> 90% RH, 20 ± 2 °C) and after immersion in osmotic water (28 days) and/or irradiation at 200 kGy (Co-60 source, 2.5 kGy/h).
- Cylinders of 2.5 cm diameter and 4 cm height employed for leaching tests (both irradiated and non-irradiated).

In this latter type of sample geometry employed for the study of leaching behaviour, specimens were doped with known amounts of elements of interest. In particular, stable Cs, Sr, Ni, Co, Ce, Eu and Nd were used as surrogates of their radioactive counterparts and of tri/tetravalent actinides. Th and U were also included as radioactive contaminants.

UJV MK based Geopolymer sample, composed of Metakaolin 60% in mass + Activator Mefisto L05 from Czech Shale Plants Company Nove Straseci (40% in mass), were used as the reference matrices. When RLOW are added (with ^{63}Ni or ^{14}C)– a scintillation cocktail and an ionic solution, they reached respectively 8,6wt% and 11,8 wt%.

Metakaolin and activator properties:

- Workability at temperature of 20°C: up to 60 minutes
- Expected maximum application temperature: 1200 °C
- Bending strength: 11 MPa
- Shrinkage after 28 days at a temperature of 20 °C: max 0.5 %
- Density of the geopolymer binder: 1.8 - 1.9 g/ cm3
- Efflorescence: minimal

The mixing procedure used by UJV is the following:

- Mixing of MK and activator
- Addition of RLOW
- Mixing of all components for 5 minutes

Samples of the materials (cubes of 50 x 50 x 50 mm, 20 ml cylinders) were cured under controlled wet conditions in a closed box for 28 days (Figure 2), following which the samples were removed from the molds and subjected to testing (Figure 3).

Figure 2. Curing of the samples in a closed box with the addition of water

Figure 3. Matured samples (mixtures with ^{14}C radionuclide)

The following tests were performed on the samples:

- Compressive strength
- ^{63}Ni and ^{14}C radionuclide sorption tests
- ^{63}Ni and ^{14}C radionuclide leaching tests

ECL is testing the MK based geopolymer activated with potassium silicate (we are reproducing the same formulation but replacing the alkaline activator solution K120 by BETOL 5020T, available in France). The adapted formulation with the quantities used for each component is shown in the Figure 4.

NNL Formulation - MK based

- **Raw material:**
- Metamax®-RC: $Al_2O_3 = 43.99\%$ $SiO_2 = 51.48\%$
- **Alkaline activator:**
- K120 :$K_2O = 21.3wt\%$ $SiO_2 = 30.38wt\%$ $H_2O = 48.32wt\%$
- **Optimized formulation:**
- $SiO_2 : K_2O$ = 1.2
- $K_2O : Al_2O_3$ = 1.2
- $H_2O : K_2O$ = 13

Adapted NNL Formulation - MK based

- **Raw material:**
- Metamax®-RC: $Al_2O_3 = 43.99\%$ $SiO_2 = 51.48\%$
- **Alkaline activator:**
- BETOL 5020T: $K_2O = 18.5wt\%$ $SiO_2 = 30wt\%$ $H_2O = 51.5wt\%$
- **Optimized formulation:**
- $SiO_2 : K_2O$ = 1.2
- $K_2O : Al_2O_3$ = 1.2
- $H_2O : K_2O$ = 13

Figure 4. Quantities used for the adapted MK formulation using BETOL5020T

POWDER CHARACTERISATION:

The metakaolin powder used in the formulation is 'Metamax' provided by BASF. Below, XRD (Figure 5), XRF (Table 6) and SEM images (Figure 6) are provided for a better characterization of the powder used.

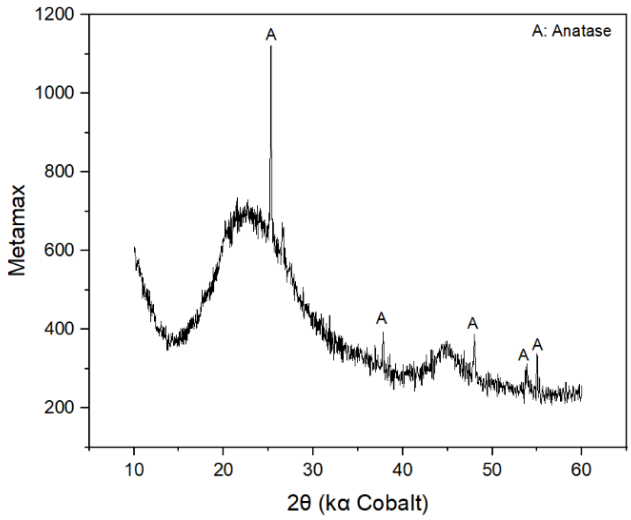

Figure 5. XRD patterns obtained from Metamax® with a Bruker Advance D8 diffractometer, in Bragg-Brentano configuration, for 2θ angles between 5° and 60°, a step size of 0.05° and an acquisition time of 20 seconds per step. Results were analyzed using DIFFRAC.EVA software.

Table 6. XRF composition of Metamax® powder

Weight percentage showing the composition of Metamax powder									
SiO_2	Al_2O_3	Fe_2O_3	TiO_2	K_2O	CaO	MgO	SO_3	ZrO_2	Fire loss
51,48	43,99	0,34	1,47	0,06	0	0	0	0	2,66

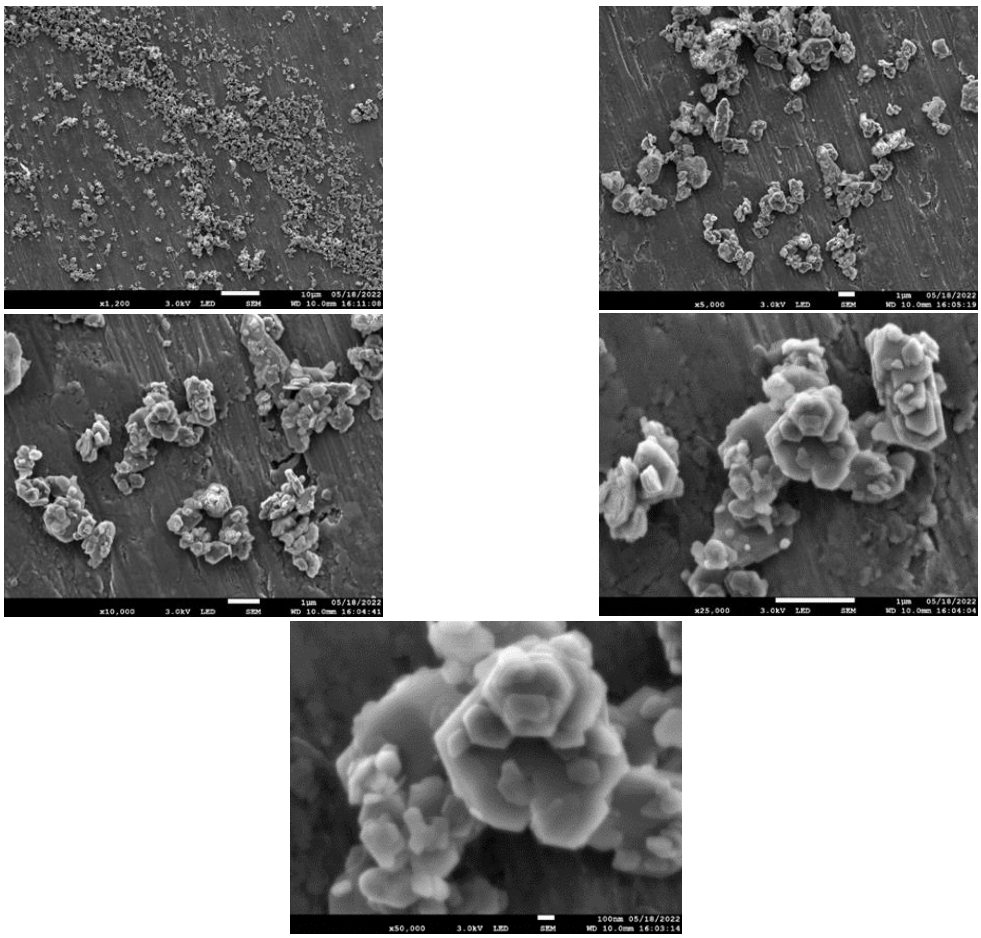

Figure 6. SEM images for Metamax powder (mean particle size: about 1μm)

The XRD graph shows only peaks assigned to anatase, as well as a broad hump due to the disordered metakaolin material. XRF confirms the high purity of Metamax powder where no additional crystalline phases containing SiO_2 have been detected. SEM images have shown the size and the shape of powder particles for a better understanding of the fresh state workability of the metakaolin-based matrices.

The alkali-activated solution combined a commercial potassium silicate solution provided by WOELLNER and KOH pellets. The surrogate waste used in the experiments is **Nevastane EP 100** provided by Total; the volume of the surrogate waste was chosen according to NNL suggestion (20%-40%); 30% vol. of Nevastane has been incorporated in the specimens.

The sample preparation protocol was conducted on a laboratory scale. The activating solution (potassium silicate + potassium hydroxide pellets + deionized water) was prepared 24 hours before the sample preparation to avoid the high heat release problems at an early age. For the reference sample, where no oil is added, the activating solution and the metakaolin powder are mixed for 5 min at 1200 rpm. For the GEOIL samples, the metakaolin is mixed with the activating solution for 5 min, then the Nevastane oil is added over 2 min while stirring and finally the whole mix is blended for 13 min at 1200 rpm.

Figure 7. Agitator with helical propeller used to stir the formulations

Once the samples are cast, they are left to harden. After that, they are demolded, weighted and cured for the required time in a climatic chamber at 20°C, RH >90%.

Figure 8. Climatic chamber used to cure the specimens

2.3 Blast furnace slag formulation

As shown in WP5.3, in SCK CEN, we comprehensively investigated the waste-forms containing alkali activated slag (AAS) and lubricating oils by a robustness test. Nevastane EP100 and Shellspirax (S2 80W90) oils provided by Lubricant Supplies (UK) were used. Tween 80 was used as a surfactant for enhancement of the mixing between AASs and oils. Among 14 formulations (Table 7) of the robustness test, four formulations (DoE 11 – DoE 14) were selected to study their durability (carbonation and leaching).

Table 7. Robustness test of waste-forms containing AASs and lubricating oils

Sample ID	SS	NH	WB	WL, vol. %	SF, wt.%	Oil type
DoE 1	2.79	4.2	0.45	30	3	NEV
DoE 2	2.59	4	0.35	30	5	NEV
DoE 3	2.59	4.2	0.35	25	3	SHE
DoE 4	2.69	4	0.45	25	4	SHE
DoE 5	2.79	3.8	0.35	30	4	SHE
DoE 6	2.59	4.2	0.55	20	4	NEV
DoE 7	2.69	3.8	0.35	20	3	NEV
DoE 8	2.59	3.8	0.55	30	3	SHE
DoE 9	2.69	4.2	0.55	30	5	SHE
DoE 10	2.69	4	0.45	25	4	NEV
DoE 11	2.79	3.8	0.55	25	5	NEV
DoE 12	2.59	3.8	0.45	20	5	SHE
DoE 13	2.79	4	0.55	20	3	SHE
DoE 14	2.79	4.2	0.35	20	5	NEV

SS and NH: sodium silicate and NaOH (g per 100 g BFS), respectively
WB: water/binder ratio
WL: waste loading (vol.%, volume of oil per total volume of waste-form)
SF: surfactant Tween 80, (wt.%, w.r.t. mass of oil)

Waste-form mixing and curing: The activating solution (SS, NH and water) was poured into a bowl containing precursor BFS, and they were mixed for 2 minutes at low speed. The mixing was then stopped to scrape everything from the bowl wall. The mixture containing Tween 80 and oil, which was prepared by adding and mixing gradually Tween 80 into oil for 5 min, was poured into the bowl. All components were then mixed for 8 min at high speed. Afterwards, sand was added, and mixing was continued for 4 more minutes at low speed. The obtained waste-from slurry was cast, and then sealed, and cured at 20 ℃ for 28 days.

In CV Rez, two series of experiments with different surrogate wastes were conducted. In Series A, a finely ground granulated BFS (Ecocem Benelux, Belgium) provided by SCK CEN was used with locally sourced quartz sand as the added component. The alkali binder combined sodium silicate (Sigma-Aldrich) and sodium hydroxide (Penta). The waste oil used in the experiments was Mogul TB 32 and we evaluated the performance of three distinct surfactants: Tween® 80, sodium dodecyl sulphate (SDS), and Glucopone 600 CS UP solution (all Sigma-Aldrich) while using Mogul TB 32 as surrogate waste. In the Series B experiments, a finely ground granulated BFS sourced from Trinec Iron and Steel Works (Czech Republic) was used with locally sourced quartz sand. The alkali binder was the same as in Series A. Total Nevastane EP 100 oil was used as a surrogate waste and Tween® 80 as a surfactant.

Diffraction patterns from XRD analysis in CV Rez were collected with a Malvern PANalytical Empyrean, series 3 diffractometer equipped with a conventional X-ray tube (Co K_α radiation, 40 kV, 30 mA, line focus), multicore optics and a linear position sensitive detector PIXCel3D detector. In this case, we used conventional Bragg Brentano geometry with the iCore optical module set with a 0.03 rad Soller slit, a 0.25° divergence slit and a 14 mm mask in the incident beam. The dCore optical module set with a 0.25° anti scatter slit and 0.04 rad Soller slit was used in the diffracted beam.

X-ray patterns were collected in the range of 5 to 85 deg. 2theta with the step of 0.013 deg and 600 sec/step producing a scan of about 4 hours 11 minutes. Samples were adjusted for analysis in the standard sample holder with “backloading”. XRD patterns were not pre-treated before interpretation as no background correction was needed. Qualitative analysis was performed with the HighScorePlus software package (Malvern PANalytical, The Netherlands, version 5.2.0) and PDF-4+ database.

XRD analysis was conducted on the BFS raw materials. BFS obtained from Ecocem Benelux, Belgium (Figure 9) primarily contained amorphous SiO_2 with traces of $CaCO_3$. In BFS supplied by Trinec Iron and Steel Works, the Czech Republic also contained amorphous SiO_2, traces of $CaCO_3$ and minerals containing calcium, magnesium, and silicon (Figure 10).

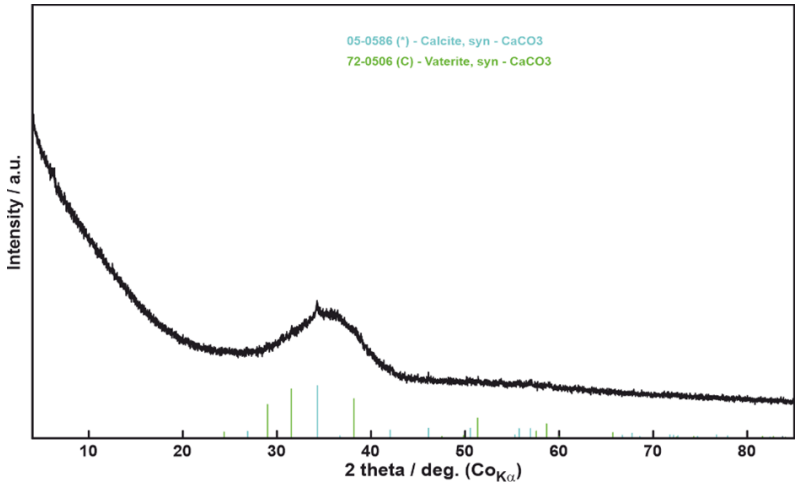

Figure 9. XRD analysis of BFS raw material from Ecocem Benelux, Belgium

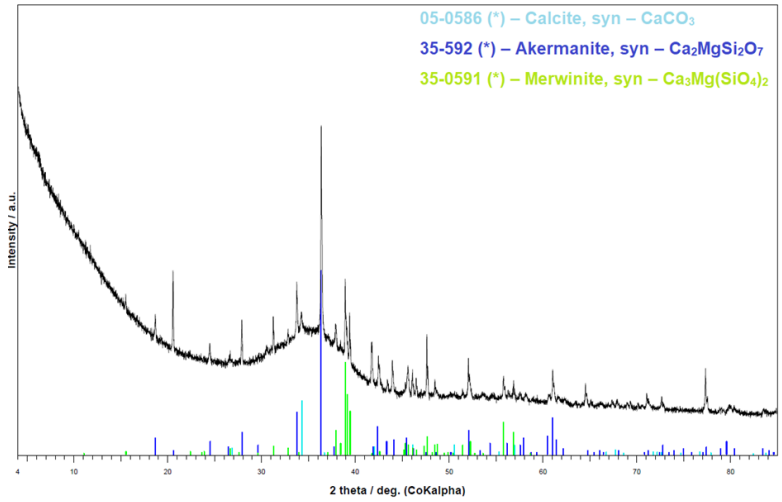

Figure 10. XRD analysis of BFS raw material from Trinec Iron and Steel Works, Czech Republic

The sample preparation protocol was conducted on a laboratory scale. The activating solution was prepared 24 hours before the actual preparation of the sample. This involved the dissolution of sodium silicate in a solution of 10M sodium hydroxide and demineralised water. Before the main sample preparation, a mixture of oil and a surfactant was mixed for 10 minutes. Subsequently, BFS and activating solution were mixed for 3 minutes, after which the oil-surfactant emulsion was incorporated, and the mixture was further mixed for 10 minutes. Subsequently, the sand was added to the mixture and mixed for 3 minutes.

A thoroughly mixed geopolymer paste was cast into cubic molds (see Figure 11), each with dimensions of 50×50×50 mm. After casting, the samples were left to harden on air at the laboratory temperature for two days. Following this, the samples were demolded, weighted and subjected to a controlled curing process for 28 days. The controlled conditions were: one in a dry environment and the second in a sealed bag environment, both maintained at laboratory temperature (series A) and in a sealed bag environment at laboratory temperature (series B). The sealed bag conditions were established by placing the samples in a sealed container positioned above the surface of the demineralised water, ensuring that the sample remained untouched by the water.

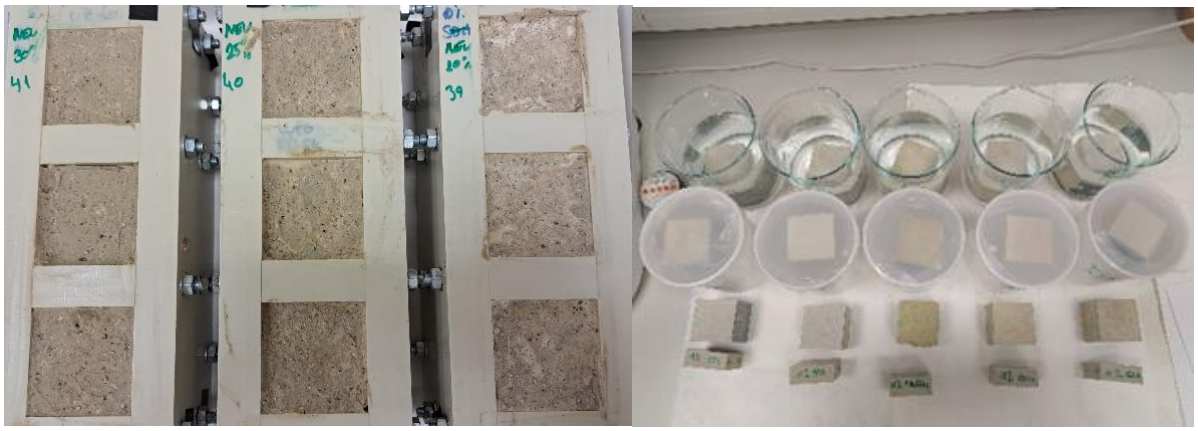

Figure 11. Prepared BFS samples by CV Rez

Series A

In our initial experimentation phase, we used a waste load of 5 wt.% while investigating the performance of three different surfactants - SDS, Glucopone, and Tween® 80 - at varying concentrations of 0.15, 0.3, 0.45 and 0.75 wt.% (Table 8).

Table 8. The composition of samples with waste load of 5 wt.%.

Sample	Waste (wt.%)	Waste type	Surfactant type	Surfactant (wt.%)
M1	5	Mogul oil	SDS	0.45
M2	5	Mogul oil	SDS	0.75
M3	5	Mogul oil	Tween® 80	0.45
M4	5	Mogul oil	Tween® 80	0.75

Initial trials using 0.15 and 0.3 wt.% of these surfactants produced unsatisfactory results. Although the samples demonstrated sufficient hardening, a significant oil release was noticeable. In response to this issue, we increased the surfactant levels to 0.45 and 0.75 wt%, resulting in increased homogeneity and decreased oil release from the sample during the hardening period.

During these experiments, challenges arose regarding the surfactant Glucopone. As we increased the surfactant quantity, we encountered difficulties in effectively mixing the oil and Glucopone. Furthermore, an additional complication arose as the Glucopone within its original container solidified over time, thus requiring heating to restore it to its liquid state.

After samples with 5 wt.% we investigated the higher waste load of 10 and 20 wt.%. As the performance of the SDS surfactant was not satisfactory with a greater waste load than 10 wt%, we proceeded with Tween® 80 only. All samples in Series A (M1-M7, cf. Table 9) were dimensionally stable during the curing period and no visible cracking was observed.

Table 9. The composition of samples with waste load 10 and 20 wt.%.

Sample	Waste (wt.%)	Waste type	Surfactant type	Surfactant (wt.%)
M5	10	Mogul oil	SDS	1.5
M6	10	Mogul oil	Tween® 80	1.5
M7	20	Mogul oil	Tween® 80	3

Series B

In Series B, we prepared samples with the gradual increase of added Total Nevastane oil together with the increase of the added surfactant Tween® 80 as shown in Table 10 and samples with the gradual increase of added Total Nevastane oil and constant Tween® 80 amount (Table 11).

Table 10. The composition of samples with increasing waste load

Sample	Waste (wt.%)	Waste type	Surfactant type	Surfactant (wt.%)
N1	5	Total Nevastane EP l00	Tween® 80	0.75
N2	10			1.5
N3	15			2.25
N4	20			3
N5	25			3.75
N6	30			4.5
Standard	-	-	-	-

Table 11. The composition of samples with increasing waste load and constant surfactant amount

Sample	Waste (wt.%)	Waste type	Surfactant type	Surfactant (wt.%)
N7	5	Total Nevastane EP l00	Tween® 80	1.5
N8	10			
N9	15			

All samples showed good homogeneity with negligible to no oil release after casting. From each composition, we prepared three samples; all were cured in sealed bags for 28 days. After 28 days of curing, one sample was used for stereoscopic microscope investigation, one sample for compressive strength test, and one for leaching. No shrinkage or swelling was observed during the curing phase.

POLIMI adopted the formulation and mixing protocol developed by SCK CEN. Raw materials employed for the preparation of samples are reported in Table 12. BFS and sand were directly provided by SCK CEN to guarantee reproducibility of the formulation.

Table 12. Raw materials employed by POLIMI for the preparation of BFS-based formulation.

Material	Concentration (wt%)
BFS	46.5
Na_2SiO_3	1.5
NaOH 10 M	6.0
Sand	18.0
Water	28.0

POLIMI considered two types of organic liquids:

- TBP/dodecane (30:70 mix by volume)
- Ultima Gold liquid scintillation cocktail (Perkin Elmer)

A constant waste loading factor of 10 wt% was adopted for all studies, plus an additional 5 wt% with respect to waste mass of Tween 80 surfactant. The loading factor was not compliant with the target of 30 v% but limited to 10 wt% as suggested by SCK CEN to cope with the scarce compatibility with these organic liquids.

The mixing protocol adopted for the preparation of BFS-based samples is illustrated in Figure 12, and is unchanged regardless of the organic liquid considered. After mixing of activator, raw materials and RLOW simulant, oven curing is adopted to facilitate waste incorporation, as suggested by SCK CEN colleagues. The heterogeneous mixture is placed in an oven at 50 °C for a few minutes (between 2 and 10, depending on the size of the batch and the progression of setting). It is then removed from the oven and immediately mixed for 1-2 minutes. This alternate process is repeated until the waste is fully incorporated by the paste. The number of times required to obtain a homogeneous sample directly depends on the scale of the batch.

Once homogeneous, specimens are cast and allowed to cure for 28 days in endogenous conditions at room temperature (20 ± 2 °C). Oven curing was not necessary (hence not adopted) for specimen with no waste.

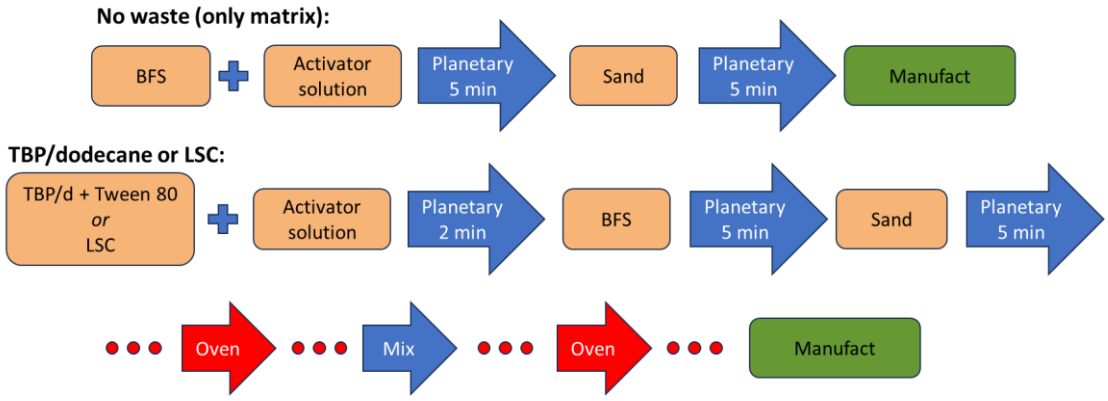

Figure 12. Mixing protocol adopted by POLIMI to prepare BFS-based samples with LSC and TBP/dodecane wastes.

Two sample geometries were adopted:

- 5 cm equilateral cylinders for compressive strength testing after curing (>90% RH, 20 ± 2 °C) and after immersion in osmotic water (28 days) and/or irradiation at 200 kGy (Co-60 source, 2.5 kGy/h).
- Cylinders of 2.5 cm diameter and 4 cm height employed for leaching tests (both irradiated and non-irradiated)

In this latter type of sample geometry employed for the study of leaching behaviour, specimens were doped with known amounts of elements of interest. In particular, stable Cs, Sr, Ni, Co, Ce, Eu and Nd were used as surrogates of their radioactive counterparts and of tri/tetravalent actinides. Th and U were also included as radioactive contaminants.

UJV used Blast furnace slag (BFS) from Moravia Steel company Trinec. X- ray qualitative analyses show that it structure is composed by:

- Calcite $CaCO_3$
- Akermanite $(Ca_{1.53}\ Na_{0.51})\ (Mg_{0.39}Al_{0.41}Fe_{0.16})Si_{2.007}$

A summary of the used materials and their weights is provided in the Table 13.

Table 13. Materials used for the BFS mixtures by UJV

Matrix		MK	Activator	RLOW (addition of 1.5 ml ^{63}Ni/^{14}C)			$Na_2O.3SiO_2$	10M NaOH		Sand	Add. water	wt% of RLOW fulfillment
	g	g	g		ml	g	g	ml	g	g	g	
BFS	465.44			scintilliation cocktail	100.0	86.3	15.15	46.87	62.33	279.93	50.0	9.9
	465.44			ionic liquid	100.0	118.0	15.15	46.87	62.33	279.93	50.0	13.5

Mixing procedure in small scale using the laboratory mixer

- Production of an NaOH 10M solution from NaOH pellets and the cooling of the solution to room temperature
- Dissolution of sodium silicate in the NaOH solution
- Mixing of the BFS + NaOH solution + RLOW + water for 10 minutes
- Addition of sand and mixing for a further 3 minutes
- Mixing of the GP + RLOW for 10 minutes

Blast furnace slag (BFS) is used as the matrices, and RLOW prepared by UJV – a ***scintillation cocktail*** and an ***ionic solution*** – were fixed into the selected matrices. As for MK based matrices, the RLOW was treated via the addition of small amounts (1.5 ml) of ^{63}Ni and 1.5 ml of ^{14}C solutions due to the low levels of radioactivity of the monitored radionuclides (0.56 Bq/ml of ^{14}C and 0.84 Bq/ml of ^{63}Ni in the scintillation cocktail and 12.05 Bq/ml of ^{14}C and 11.04 Bq/ml of ^{63}Ni in the ionic solution).

The final radioactivity values of the treated RLOW in „CPM“ (counts per minute) were:

- 37 380 597 CPM/100 ml: ^{63}Ni in the scintillation cocktail (~ 0.8 MBq/100 ml)
- 37 420 944 CPM/100 ml: ^{63}Ni in the ionic solution (~ 0.81 MBq/100 ml)
- 150 003 114 CPM/100 ml: ^{14}C in the scintillation cocktail (~ 2.5 MBq/100 ml)
- 150 069 489 CPM/100 ml: ^{14}C in the ionic solution (~ 2.56 MBq/100 ml)

Counts per minutes (CPM) values were measures on “Hidex” scintillation spectrometer (which detects sources of both α and ß radiation), Figure 13.

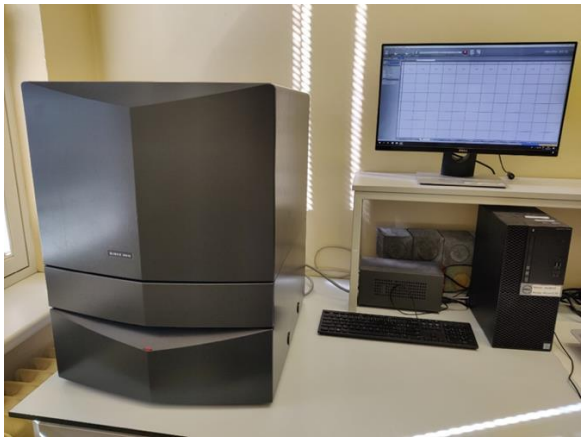

Figure 13. Hidex liquid scintillation spectrometer

Suitable additives (alkali activators, sand, water) were added so as to create homogeneous mixtures. Inactive BFS mixtures were also prepared for compressive strength and sorption testing purposes.

UJV followed recipes recommended by CV Rez (Research Centre Rez) for the preparation of the inactive mixtures. The matrix materials (of Czech origin) were also provided by colleagues from CVR.

2.4 Mix formulation

The SIIEG NASU has performed the sub-tasks on reference formulations of the KIPT on received two batches of cylinders 16-millimetre size samples with different amounts of waste oil simulant and without organic oils for reference (cf. Figure 14). On 21 December 2021, the MIX formulation samples were received in SIIEG NASU from KIPT. The beginning of 2022 must have been the start of the durability testing campaign under endogenous, aerated leaching conditions, but since February 24th 2022, after the invasion of russian troops on the territory of Ukraine the Institute has closed, all experiments have stopped, and the installations were switched off. In September, after opening work, SIIEG NASU had a problem with electricity, and some of the staff were refugees from Kyiv. Nevertheless, leaching experiments began, although it was impossible to maintain a temperature of 20 degrees in winter.

Procedure description of samples obtaining (experimentations performed of KIPT):

- Alkaline activators preparation: addition of KOH and K_2SiO_3 in distilled water and mixing with Castament FW 10 (BASF) - 0,5%wt
- Mixing dry powder components in the planetary mill (30 min)
- Mixing alkaline activators (1) with powders mixture (2) (30 min) = fresh geopolymer
- Waste: oil Nevastane and ShellSpirax -10, 20, 30 and 40% vol.
- Casting (formation) samples into plastic mold

(a) (b)

Figure 14. Specimen of MIX formulation used by SIIEG NASU (a) batches of samples with oil, (b) the 16mm size sample

Ukrainian raw materials used: Blast Furnace Slag (BFS), CemBudService (Kam'yanske, Dnipro region); Fly Ash (FA), Thermal Power Station (Burshtin, Ivano Frankivsk region) and a Metakaolin (MK), kaolin calcined at 800^{o}C, whose oxide compositions are reported in Table 14. The raw materials have sifted through 600 microns.

Three series of samples were prepared in KIPT (see Table 15 for the formulation): 1) without organic oils for reference; 2) containing 10-30 %wt. of oil Shell Spirax; 3) containing 10-30 %wt. of oil Nevastane. Unfortunately, to SIIEG NASU has not been transmitted of the starting BFS, FA and metakaolinite, and investigation of raw materials was impossible.

Table 14. Main oxide content of raw materials

Raw Mat.	Oxide content													
	LI	SiO2	Al20₃	CaO	MgO	SO3	Na2O	Ka2O	TiO2	Na2O + K2O	P2O5	MnO	Fe2O3	C
BFS	0,97	40,6	6,02	45,1	3,61	1,74	0,42	0,40	0,30	-	0,01	0,17	0,62	-
FA	1,42	46,1	18,0	4,10	1,46	0,21	2,50	2,10	1,78	2,10	-	0,14	22,17	2,50
MK	10,8	51,0	35,5	0,25	0,16	-	0,15	0,27	0,78	-	-	0,14	1,05	-

Table 15. Mix formulation composition of samples (KIPT formulation).

Fly ash	34 %wt	K2SiO3	11 % wt
Slag	20 %wt	KOH	9 %wt
Metakaolin	14 %wt	Water	12%wt

POLIMI adopted the formulation and mixing protocol developed by KIPT and reviewed by CEA. Raw materials employed for the preparation of samples are reported in Table 16 and are the same as those used by CEA.

Table 16. Raw materials employed by POLIMI for the preparation of MIX-based formulation.

Material	Concentration (wt%)
FA	0.32
BFS	0.19
MK (Metamax, BASF)	0.14
Betol K 5020 T	0.14
KOH	0.08
Water	0.144

POLIMI considered two types of organic liquids:

- TBP/dodecane (30:70 mix by volume)
- Ultima Gold liquid scintillation cocktail (Perkin Elmer)

To prepare sample with TBP/dodecane, Tween 80 was used as a surfactant at 5 wt.%. with respect to waste mass. For LSC, no added surfactant was used, as this organic liquid already contains a surfactant by design.

The mixing protocol adopted for the preparation of MIX-based samples is illustrated in Figure 15. Both high-shear and low-shear (planetary) mixers are adopted at various stages of the preparation protocol. Also, order of addition of precursors and activator is different depending on the waste considered. After casting, samples were cured for 28 days in endogenous conditions at room temperature (20 ± 2 °C).

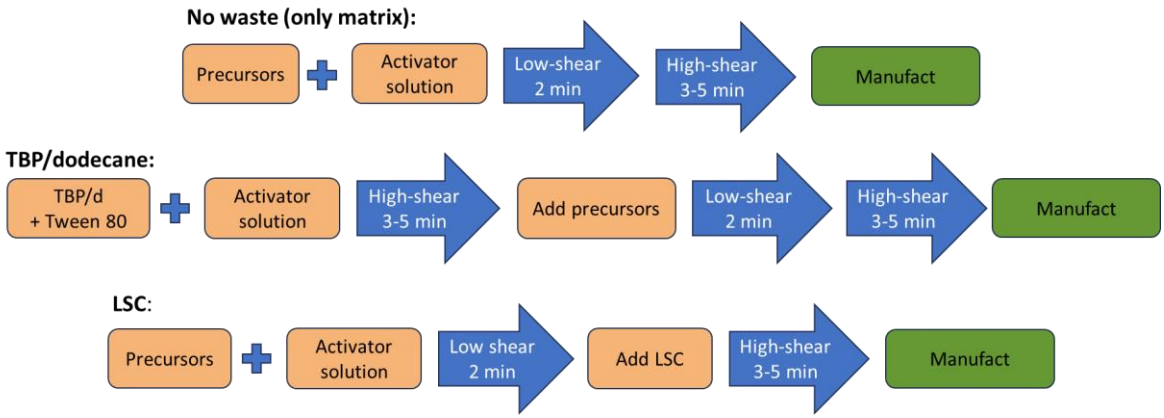

Figure 15. Mixing protocol adopted by POLIMI to prepare MIX-based samples with LSC and TBP/dodecane wastes.

Despite the presence of surfactant, encapsulation of TBP/dodecane, using Tween 80 as surfactant, proved unsuccessful since the mixture underwent immediate phase separation, with essentially negligible waste incorporation (see Figure 16). Due to the large amount of waste bleeding, representative samples could not be prepared. Hence, the study of MIX-based formulation by POLIMI was limited only to LSC waste. The reason for this ineffective encapsulation is unclear and should be further investigated to provide robustness to the formulation.

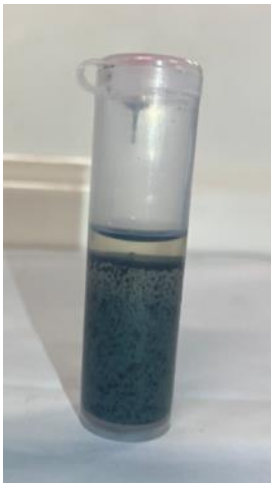

Figure 16. MIX-based samples with TBP/kerosene prepared by POLIMI. Severe organic liquid bleeding and large porosities caused by ineffective encapsulation are visible.

Two sample geometries were adopted:

- 5 cm equilateral cylinders for compressive strength testing after curing (>90% RH, 20 ± 2 °C) and after immersion in osmotic water (28 days).
- Cylinders of 2.5 cm diameter and 4 cm height employed for leaching tests.

In this latter type of sample geometry employed for the study of leaching behaviour, specimens were doped with known amounts of elements of interest. In particular, stable Cs, Sr, Ni, Co, Ce, Eu and Nd were used as surrogates of their radioactive counterparts and of tri/tetravalent actinides. Th and U were also included as radioactive contaminants.

2.5 Samples received from partners

UNIPI investigated the thermal behaviour of metakaolin (MK) based materials, the main parameters of which are summarised in Table 17, to determine changes in the important matrix properties, such as strength, durability, fire resistance, and non-combustibility properties.

The cylindrical samples (Φ=50 mm) tested were prepared by POLIMI, and NUCLECO, and SCK CEN are:

1) MK-based formulation (as developed by NNL): 2 samples without waste plus 2 samples loaded with 30% wt. of kerosene and TBP (cf. Figure 17).

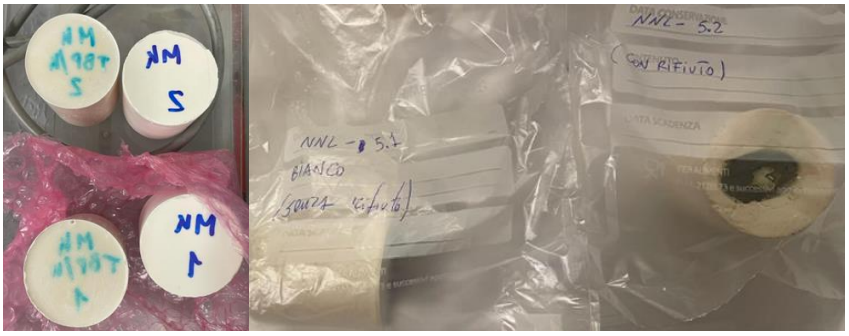

Figure 17. MK formulation samples used by UNIPI

Two samples per each formulation were tested in a two-stage approach to determine both the fresh paste properties and the hardened matrix properties (e.g., compressive strength).

2) KIPT formulation: 2 samples (without waste) and 2 samples loaded with Nevastane oil (cf. Figure 18).

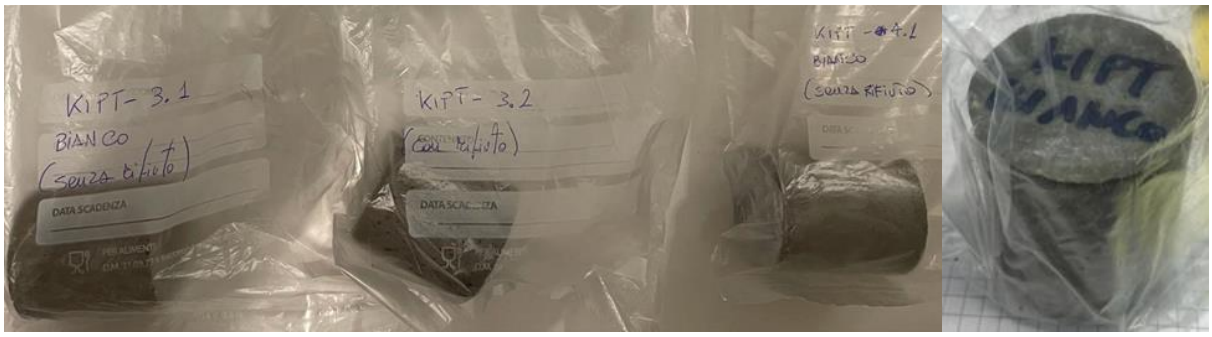

Figure 18. MIX formulation samples received by UNIPI

3) BFS formulation: 4 samples (without waste) and 1 sample loaded with oil (cf. Figure 19).

Figure 19. BFS formulation samples received by UNIPI

Table 17. Formulation of the samples used by UNIPI

NLL formulation – MK based	**SCK CEN formulation – BFS based**	**KIPT formulation – MIX based**
Row Material: Metamax© RC: Al_2O_3 = 43.99% SiO_2 = 51.48%	**Row materials**: BFS = 46.5 wt% (Al_2O_3 = 11.10%, SiO_2 = 32.40%) Sand = 28 wt%	**Row materials**: FA = 34 wt.% (Al_2O_3 = 18%, SiO_2 = 46.12% BFS = 20 wt.% (Al_2O_3 = 6.02%, SiO_2 = 40.6% MK= 14 wt% (Al_2O_3 = 35.50%, SiO_2 = 51%)
Activator: K silicate (K120): K_2O = 21.3 wt% SiO_2 = 30.38 wt% H_2O = 48.32 wt%	**Activator:** $Na_2O.2SiO_2.xH_2O$ – 1.5wt. % NaOH (10M) – 5.5 wt% Additional water – 18.4 wt.%	**Activator**: K_2SiO_3 = 11 wt.% KOH – 9 wt.% Water – 12wt.%
RLOW: Nevastane Oil (20% vol)	**RLOW**: Ionic liquid (Aliquat 336) – 9.9 wt% (1) TBP – 19.1 wt%	**RLOW**: ShellSpirax: from 10% to 40% vol(2)
Optimized formulation: SiO_2:K_2O = 1.2 K_2O:Al_2O_3 = 1.2 H_2O: K_2O = 13		

(1) Tween 80 surfactant used: 0.5% and 0.95% relative to the waste volume.
(2) Castament FW10 (solid Polyethylene glycol-based additive) used to improve several properties: 0.5%

Different formulations were used for the study of behaviour under gamma irradiation from IMT Atlantique. The samples were produced by other laboratories following the shape specification needed for the irradiation experiments. Silicon moulds of around 1x1x1 cm^3 were used.

Table 18 summarizes the information regarding the different GPs studies, i.e. the name, the producer laboratory, the formulation, and the v% of oil added in the samples with surrogate waste. After the preparation, samples were sent to IMT Atlantique laboratory and stored in close plastic bags at laboratory conditions until the irradiation.

Table 18. Formulation and producer of the samples used by IMT

Name	**Metakaolin based**	**Blast furnace slag based**	**Mix based without surfactant**	**Mix based with surfactant**
Abbreviation	MK GP	BFS GP	MIX GP	MIX GP (S)
Producer	École Centrale Lille	SCK CEN	CEA	SOGIN
Formulation [w%]	Metamax – 32% Betol K 5020 T – 41% KOH – 10% Water – 17%	BFS – 46.5% Sodium silicate – 1.5% NaOH 10 M – 6.2% Water – 17.7% Sand – 27.9%	Fly Ash – 33.3% BFS – 19.6% Metakaolin – 13.7% Betol K 5020 T – 15% KOH – 8.2% Water – 9.8%	Fly Ash – 33.3% BFS – 19.6% Metakaolin – 13.7% Betol K 5020 T – 15% KOH – 8.2% Water – 9.8% SLS – 0.5%
Aspect				
v% of surrogate waste	30% NEV	20% SHE	30% NEV	-

2.6 Partial conclusion about sample preparation and curing

The objective of this first chapter was to present the production of the geopolymer samples prepared by the various participants and to present, when necessary, a characterization of the raw materials. It should be noted that some of the partners involved in this task also participated in task 5.3, thus facilitating this first stage. From the three formulations proposed by task 5.3, some participants had to slightly modify the formulation to adapt to the availability of materials. For the metakaolin-based geopolymer, ECL, CIEMAT and POLIMI modified the alkaline solution, while maintaining the molar ratios. For the formulation based on blast furnace slag, POLIMI worked with slag supplied by SCK CEN (formulation developer), while UJV and CV Rez worked with local blast furnace slag. For the MIX formulation, SIIEG studied samples directly from KIPT (formulation developer). It should also be noted that IMT and UNIPI worked with samples manufactured by other partners who are not directly the formulation developers.

In terms of protocol, certain adaptations were also made (linked to the alkaline solution for ECL, CIEMAT and POLIMI) since the alkaline solution had to be prepared in advance (exothermic preparation). At POLIMI, the mixing protocol was modified to incorporate TBP/dodecane leading to a protocol that is difficult to industrialize and for which the homogeneity of the composite (AAM + LOW) is questionable (results obtained with these formulations should consequently be analyzed carefully). The results of this first chapter also show that the use of a surfactant is sensitive because, unlike the CEA which had succeeded in task 5.3 in incorporating TBP/dodecane into the MIX formulation using Glucopon, POLIMI was unable to obtain a homogeneous mixture with Tween 80 (LOW = TPB/kerosene).

Curing conditions are also extremely important, especially for formulations based on metakaolin. At both CIEMAT and ECL, a very high sensitivity to the drying/wetting cycle was detected (violent appearance of intense cracking when immersed in water after drying). This sensitivity means that this material must be cured in very humid conditions (above 90% RH).

3 CHARACTERISATION BEFORE DURABILITY TESTING

To be able to compare the properties of the matrix between them but also to measure the impact of ageing during tests (durability, sensibility to irradiation and thermal loadings), properties of geopolymers matrices (MK based, BFS based and MIX one) must be characterize before testing. Two different families of tests can be performed and are classified in this report as macroscopic measurements and microstructural investigations.

3.1 Macroscopic measurements (porosity, density and strength)

3.1.1 Metakaolin formulation

Compressive strength tests were performed at UJV for both inactive and radioactive samples, using a „MEGA 11-300 DM1-S“ press, see Figure 20. 3 or 4 of the cube shaped samples were tested for each mixture.

Figure 20. MEGA 11-300 DM-1-S Presser

Table 19. Results of the compressive strength tests of UJV samples

Compressive Strength [MPa]			addition of ^{63}Ni	addition of ^{14}C
inactive BFS matrix	**20.64**	BFS + scintillation cocktail	**19.88**	**13.28**
		BFS + ionic liquid	**21.37**	**21.59**
inac MK atrix	**21.11**	GP + scintillation cocktail	**25.71**	**18.6**
		GP + ionic liquid	**21.93**	**16.51**

As indicated by the results shown in Table 19, only moderate differences were determined between the radioactive and inactive mixtures after 28 days of curing, with the ionic liquid in particular having only a small effect. Both inactive matrices based on MK or BFS compressive strength reach close to 20 MPa on cubic samples. Same results were obtained by UNIPI for samples at about 28 days age.

CIEMAT investigated both density, heat of reaction, rheology and compressive strength. Regarding the density of the hardened specimens, several pieces were manufactured, the dimensions were measured with calipers and they were weighed to obtain the density. It is this last density value that is used to carry out Oil volume % calculations. The density of the geopolymer calculated was 1.63 g/cm^3. In terms of rheological characterization, the measurements were carried out in the rotational rheometer model MCR 72 MCR 92 SmartPave 92 in Figure 21. It is formed by a Peltier heating system cooled by a water bath.

Figure 21. Rotational rheometer MCR 72 MCR 92 SmartPave 92

To carry out the measurements, a sample container called Cup (volume=1L) is used, which is placed on the Peltier plate. The stirring blade (Vane stirrer) is used as the upper measurement geometry.

This blade has two ways of moving or acting, rotational or oscillatory. The results are obtained from the interaction of the blade with the sample in software. These results can also be analyzed through the software using models that make the corresponding adjustments to obtain the graphs and rheological values.

3 different types of samples have been analyzed in the rheometer:
• K-0%: The typical formulation of potassium geopolymer (MK based without RLOW).
• K-20%: with 20% oil.
• K-40%: with 40% oil.

The conditions to carry out the test were the following:

- Preparation of the sample in the mixer by the usual procedure (15 minutes of stirring the geopolymer and 1 hour of oil).
- Introduction of 0.5 L of sample in the cup.
- Rheometer conditions:
  • Gap = below 1mm (distance from the blade to the bottom of the cup)
  • Peltier temperature = 20°C
  • Bath temperature = 20°C

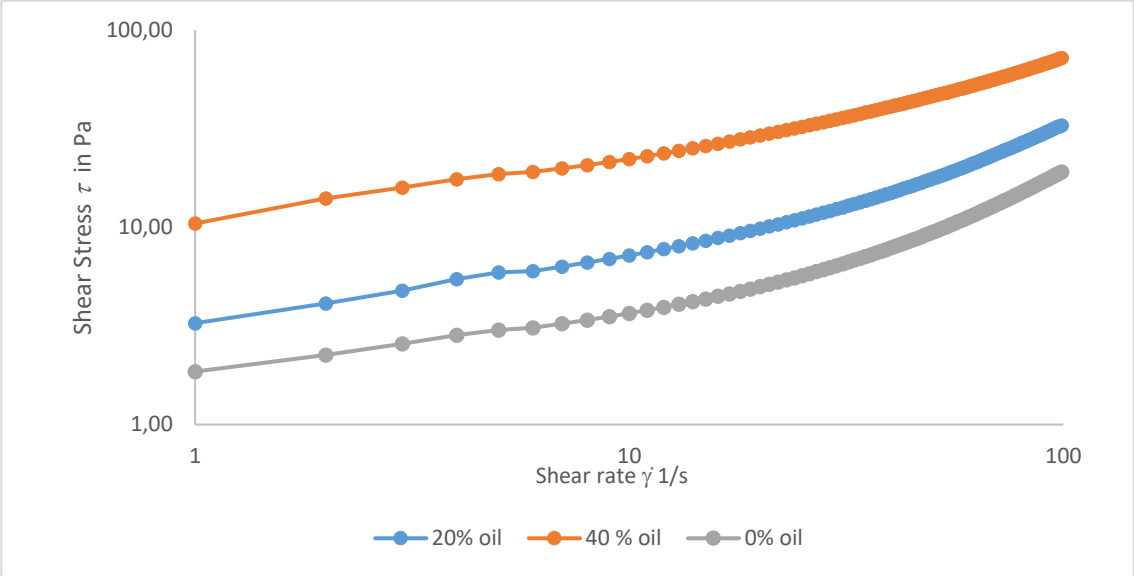

Figure 22. Flow curve of MK based geopolymer with Oil.

The Figure 22 represents the flow curve (shear rate vs shear stress) for 0, 20 and 40 % of oil. It can be observed that the shear stress increases with the introduction of oil into the samples.

It was calculated the viscosity in the mixer (with stirring). At high shear rates the viscosity decreases as would be expected and stabilizes at the following values:

40%=0.72 Pa s
20%=0.32 Pa s
0%=0.18 Pa s

The static viscosity (viscosity after mixing) calculated was:

40% = 431,2 Pa s
20%= 93,3 Pa s
0%= 57,05 Pa s

It is possible to calculate the percentage of viscosity recovery at 30 seconds. The mixture that needs more time to recover the initial viscosity is the sample with 40% of waste.

The Yield point can also be measured with this apparatus. This is the point where the sample goes from elastic to plastic behaviour. It is related to the force that must be applied to break bonds and go from a solid/gel type behaviour to a more liquid/fluid behaviour. This point corresponds to the maximum shear stress. For the times of 10, 20 and 30 min, this maximum is perceived very clearly but not so much for time 0. (see Figure 23)

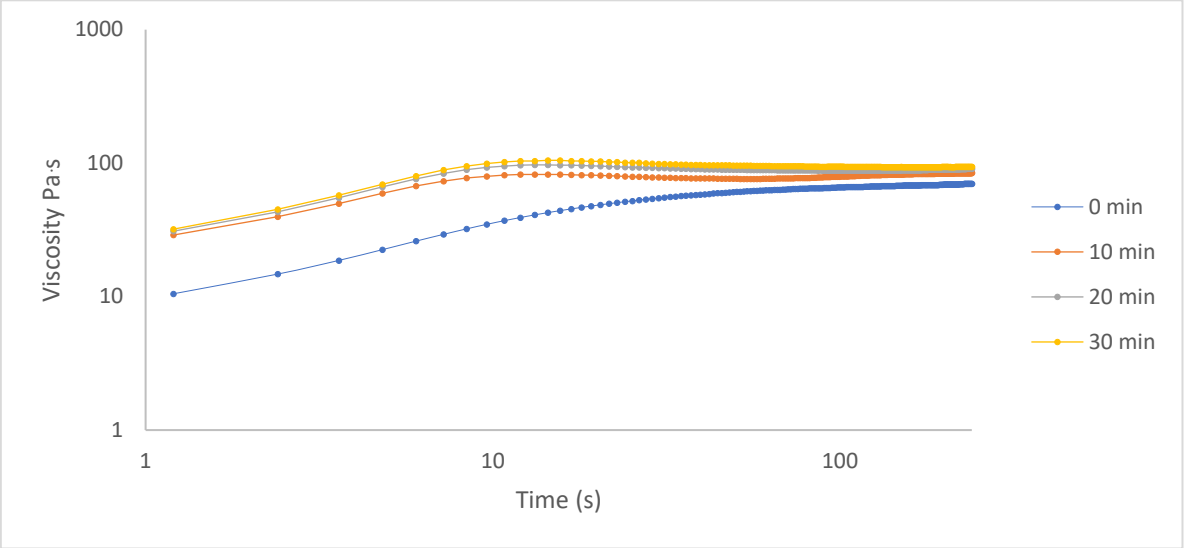

Figure 23. Viscosity at 0 min (blue), 10 min (orange), 20 min (grey) and 30 min (yellow) of potassium geopolymer with 40 % of waste.

Table 20. Yield stress (Pa) with different mixing times and different waste concentrations

Time (min)	0	10	20	30
0 %	0.84	1.22	1.34	1.38
20 % oil	1.34	2.06	2.27	2.39
40 % oil	6.51	8.24	9.7	10.45

The mechanical strength tests were performed with 3 prismatic samples of 4x4x16 cm, dividing the samples in two parts to obtain 6 measurements. The results obtained after different times of curing are shown in Table 21.

Table 21. Mean compressive strength for MK based formulation (CIEMAT)

	Compressive strength (MPa)
REF 7days	23.8
REF 28days	25.5
REF 90days	29.3

ECL measured the compressive and flexural strength (Table 22) and the setting time. Compressive and flexural strength measurements were performed using an INSTRON 5500R machine. Flexural resistance was determined using a 3-point bend test with a load applied at a normalized speed of 3000 N/min on 4x4x16 cm specimens. Compressive strength fc is performed on 4 cm cubic samples, with a normalized applied load rate of 144 kN/min. Note that flexural strength has not been tested after durability testing since this would require an important increase in the sample volume used in leaching experiments.

Table 22. Mean mechanical compressive strength for MK based formulation (ECL)

	Compressive strength (MPa)	Flexural strength (MPa)
REF 7days	24.58	3.1
REF 28days	32.5	3.5
30% 7days	22.22	Not tested
30% 28days	25.5	Not tested

According to NF EN 196-3, the initial setting time (IST) refers to the time when the needle is 6 ± 3 mm away from the base plate (corresponding to 34 ± 3 mm penetration). To determine the final setting time (FST), it corresponds to 39.5 mm between the needle and the base of the plate (corresponding to 0.5 mm penetration). The used device by ECL is presented on Figure 24.

Figure 24. Vicat setting time apparatus

The results obtained (Figure 25) show an initial setting time (IST) of 5.37 hours for the samples with no oil and a final setting time (FST) of 6.46 hours. However, after the oil is added, the required time for the samples to set has been increased for two hours approximately with the following values: 7.36 hours for IST and 9 hours for FST.

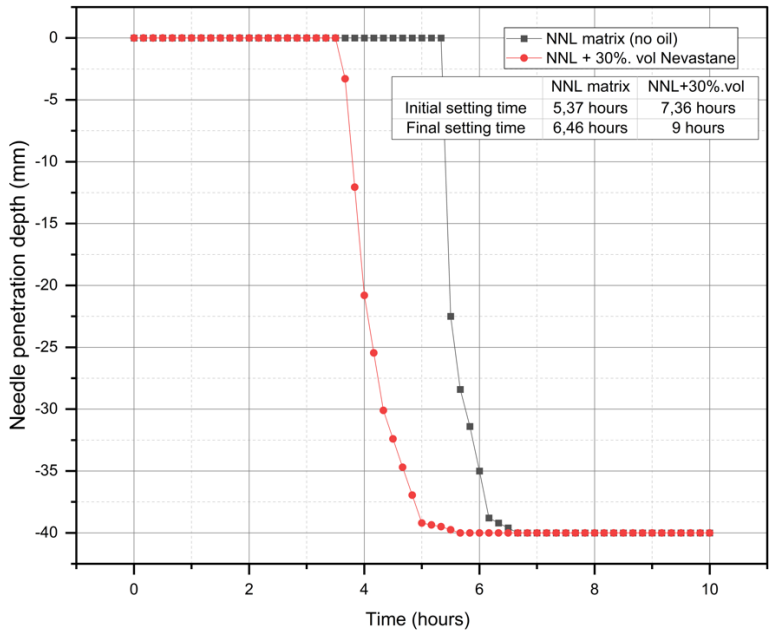

Figure 25. Setting time curves for NNL GP (MK Based) without and with oil showing the penetration depth in mm in function of the time in hours.

At UNIPI, compression tests were carried out to evaluate the strength of samples before and after thermal treatment. Compression tests were performed on all samples at the age of about 28 days. Figure 26 (a) and (b) show the execution of the compression tests: the brittle rupture mode with projection of fragments is visible. The mean maximum value of the compression stress obtained, e.g. for samples without oil, was 11.07 MPa but with a high standard variation on three samples.

Formulation	Fresh	Crush load [kN]
MK Based	Without Oil	29.80
	Oil 20% vol.	16.06
	Without Oil	14.85
	Oil 20% vol.	19.77
	Without Oil	20.57

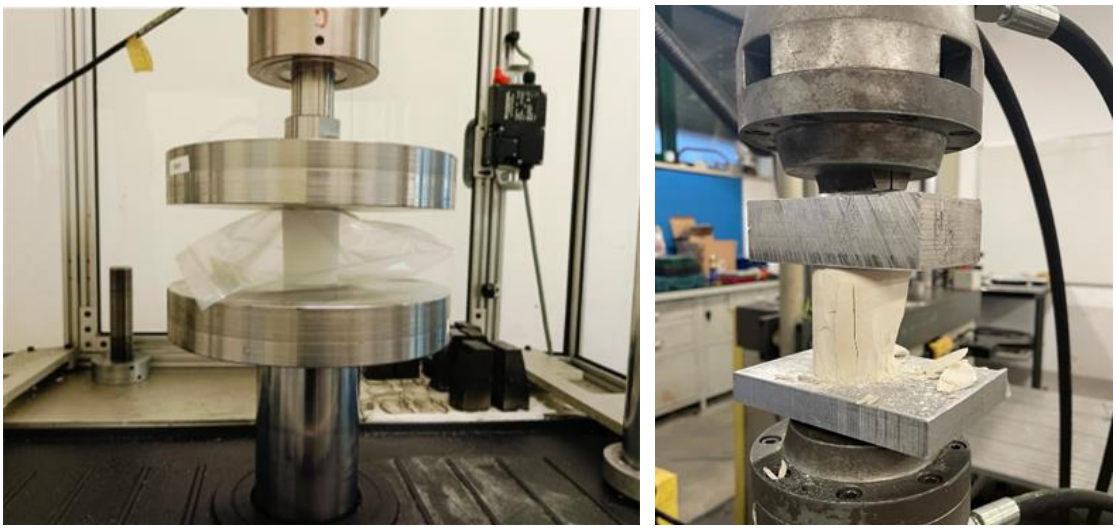

Figure 26. Compression test execution: (a) initial loading phase, (b) brittle rupture

POLIMI also performed some compressive strength measurement on the MK-based formulation in conjunction with NUCLECO after 28 days of curing under endogenous conditions. Obtained results are reported in Table 23.

Compressive strength of the non-loaded matrix is halved in presence of RLOW simulants at 30 vol.% loading, with similar results for both LSC and TBP/dodecane wastes.

Table 23. Compressive strength of MK-based samples with and without waste (POLIMI).

Sample	Compressive strength (MPa)
No waste	18.6 ± 0.9
LSC – 30 v%	8.9 ± 0.4
TBP/dodecane – 30 v%	10.0 ± 0.5

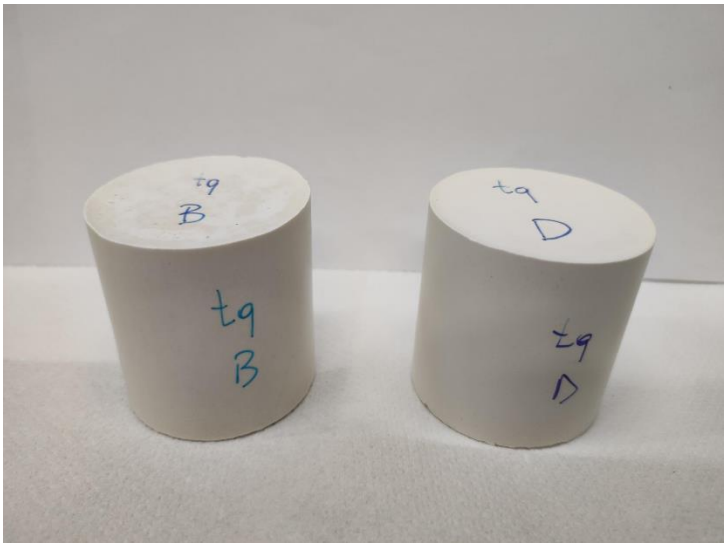

Figure 27. MK-based samples prepared by POLIMI after 28 days of curing.

Following the prescribed curing period, all samples appeared dense and homogeneous. Qualitative visual inspection evidenced no macroscopic porosities or cracks. Slight bleeding after curing was noted for all samples, amounting to approximately 1-2 v%. The composition of the bleeding liquid was qualitatively assessed as 50% water and 50% waste. Notably, also samples with no added waste presented a similar amount of bleeding (1 v%), in this case being only water.

3.1.2 Blast furnace slag formulation

In SCK CEN, four selected waste-forms containing AAS and oils were tested to determine their setting time and mechanical strengths before durability tests. The setting time was measured by a Vicat apparatus device, following the ASTM C191 standard, which was controlled at 20 ℃ and setup with a 20 min measurement interval. The results are illustrated in Figure 28. The increase in w/b ratio delayed the hardening of reference AASs, from ~2.5h to ~13h of initial setting time and from ~7.5h to ~18.5h of final setting time when the w/b ratio increased from 0.35 to 0.55, respectively. Generally, the presence of oil in AAS's matrix relatively delayed the setting, depending on the w/b ratio, alkali content, oil type, oil loading. The statistical analysis (presented in WP5.3 report) showed that NaOH content, w/b ratio, and waste loading are three major factors impacting the setting of waste-forms. However, the setting times of the waste-forms were in a reasonable range, suggesting their practical application at ambient temperature.

In reference AASs, the compressive strength increased from ~30 to 66 MPa, and the flexural strength increased from ~4 to 11 MPa when reducing w/b ratio from 0.55 to 0.35, respectively. Incorporating lubricating oils induced a significant loss in both strengths, depending not only on the w/b ratio but also on the type of oil. The oil type can attribute to the oil distribution in the matrix and the size of oil droplets. However, although the strengths were significantly decreased, most of them met the ACRIA (2 MPa of flexural strength and 8 MPa of compressive strength, see Figure 29).

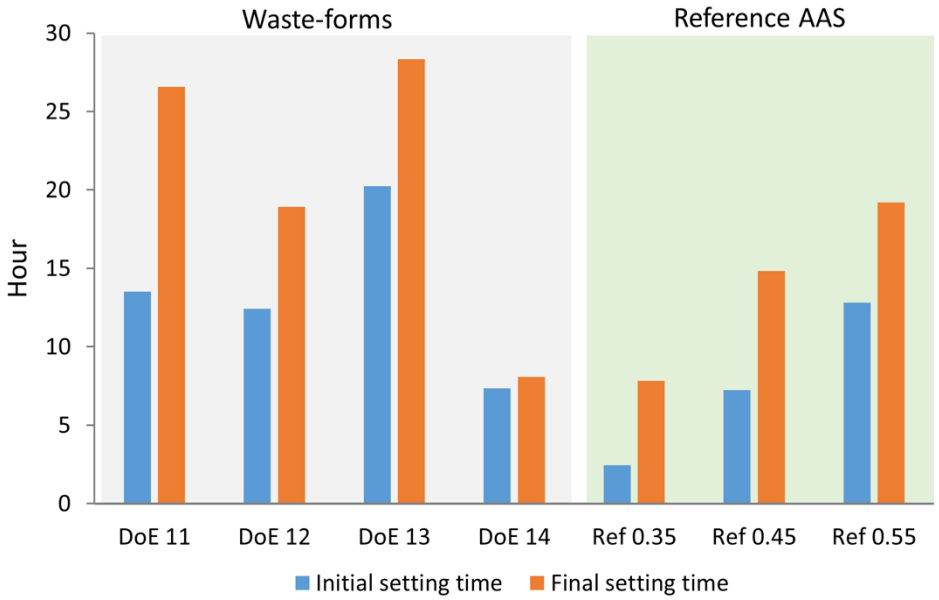

Figure 28. Setting time of reference AASs (Ref 0.35, Ref 0.45, and Ref 0.55 correspond to the w/b ratio of 0.35, 0.45, and 0.55) and 4 waste-forms (DoE)

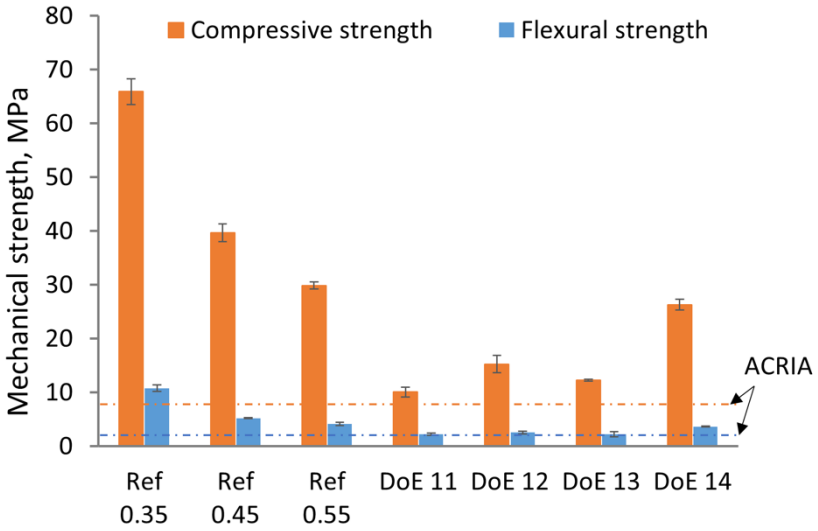

Figure 29. Mechanical strength of reference AASs (Ref 0.35, Ref 0.45, and Ref 0.55 correspond to the w/b ratio of 0.35, 0.45, and 0.55) and 4 waste-forms (DoE)

At CV Rez center, the compressive strength of the cured samples was tested using a MTS 300 Exceed® device according to the Czech National Standard CSN EN 12390-3 (Testing hardened concrete - Part 3: Compressive strength of test specimens).

Series A

The compressive strength of the samples with different surfactants and the surfactant concentration cured under sealed bag conditions is shown in Figure 30. The introduction of surfactant-free waste oil has resulted in a reduction in compressive strength compared to the standard sample, which exhibited a compressive strength of 48.25 MPa. The compressive strength values ranged from 18.77 to 26.76 MPa, depending on the type and concentration of the surfactant. The average compressive strength value decreases as the concentration of surfactant increases. This suggests that higher concentrations of surfactants could lead to weaker overall strength in the samples.

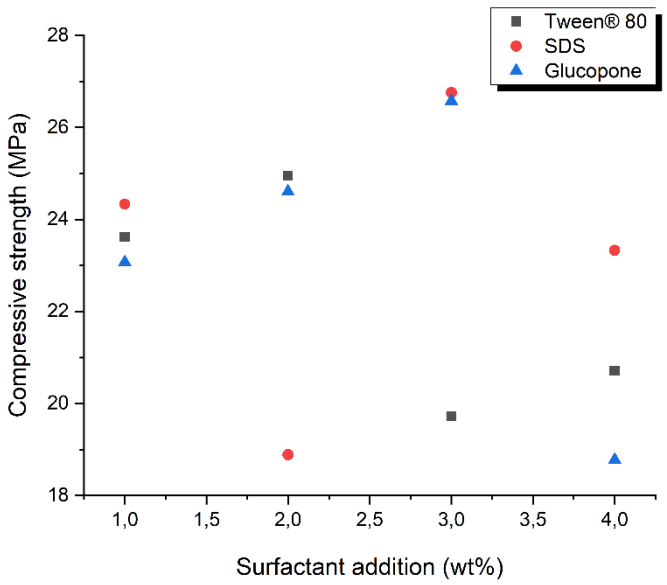

Figure 30. Compressive strength of samples with different surfactants and surfactant concentration under sealed bag curing conditions.

Series B

Samples N1-N6 and the Standard sample (the composition of samples in Table 10) were cured in sealed bags conditions and tested for compressive strength. We observed the reduction of the compressive strength (Table 24. The compressive strength analysis) with the increase of waste oil (see Figure 31). Only one sample (N1 with 5 wt.% added oil) had a compressive strength higher than 10 MPa.

Table 24. The compressive strength analysis

Sample	Compressive strength (MPa)
N1	19.29
N2	8.63
N3	3.52
N4	2.15
N5	0.93
N6	1.27
Standard (without RLOW)	34.30

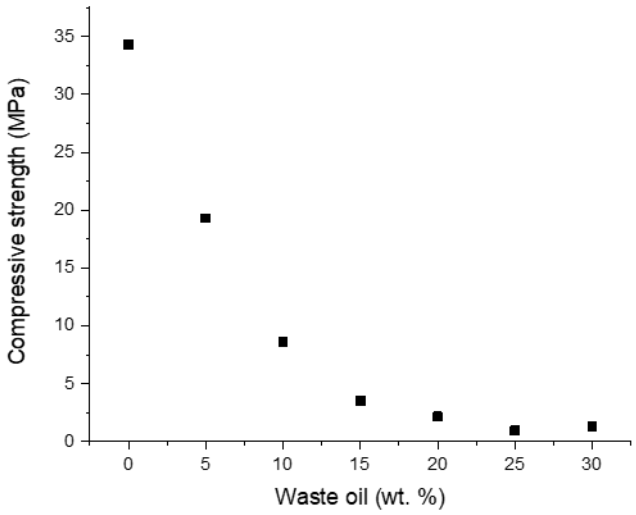

Figure 31. Compressive strength of samples with increase amount of waste oil

Compressive strength of the BFS-based formulation was assessed by POLIMI in conjunction with NUCLECO after 28 days of curing under endogenous conditions. Obtained results are reported in Table 25. Compressive resistance is drastically lowered by the presence of the waste, even at the small loading factors considered (10 wt%). Notably, no bleeding was noted after the prescribed curing period.

Table 25. Compressive strength of MK-based samples with and without waste.

Sample	Compressive strength (MPa)
No waste	55.0 ± 5.1
LSC – 10 wt%	3.8 ± 0.4
TBP/dodecane – 10 wt%	5.6 ± 0.6

Such a significant decrease of mechanical resistance is likely attributable to the preparation protocol necessary to incorporate the organic liquid. The alternate in-oven curing/mixing necessary to achieve effective incorporation of the waste also hinders an effective setting of the microstructure. Moreover, macroscopic porosities are difficult to avoid due to the high viscosity of partially set paste, as illustrated in Figure 32.

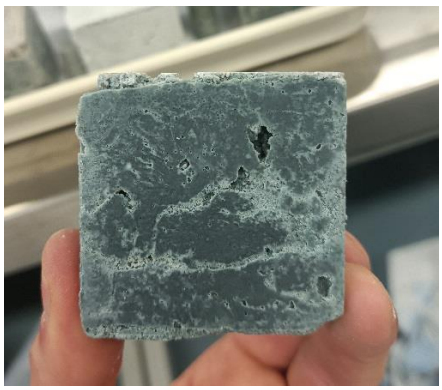

Figure 32. BFS-based specimen loaded with 10 wt% LSC, where visible voids can be seen.

3.1.3 Mix formulation

SIIEG investigates the macroscopic porosity (weighting technique) and the compressive strength of Mix formulation-based samples. To prevent cracking due to heating, the samples were dried at a temperature of 90°C until they reached a constant mass. Later, the oil was fired at 350°C- 500°C, and the cooled samples were weighed and placed in kerosene for one day. After repeat weighing, the volume of kerosene in the samples was determined, and taking into account the volume of the samples, the pore volume (%) was determined, Table 26.

Table 26 shows the relationships between the compressive strength and porosity of alkali-activated slag/fly ash/MK blends. It can be seen that the compressive strength decreases at constant porosity, confirming again the inverse relationship between strength and oil in materials.

Table 26. Porosity and compressive strength of geopolymer matrices with Shell Spirax oil.

Sample number	Porosity [%]	Compressive strength [MPa]
Mix Formulation with 10%	27	17
Mix Formulation with 20%	29	12
Mix Formulation with 30%	28	8

Compressive strength of the MIX-based formulation was assessed by POLIMI in conjunction with NUCLECO after 28 days of curing under endogenous conditions. The obtained results are reported in Table 27. Compressive resistance of the non-loaded matrix is essentially halved in presence of LSC waste. Nonetheless, compressive strength of the loaded MIX formulation is well above WAC commonly adopted in Europe. As discussed earlier, samples with TBP/dodecane could not be manufactured due to severe bleeding. Hence, compressive resistance in presence of this waste could not be assessed.

Table 27. Compressive strength of MIX-based samples with and without waste.

Sample	Compressive strength (MPa)
No waste	44.1 ± 2.3
LSC – 30 v%	23.1 ± 1.2
TBP/dodecane	N/A due to bleeding

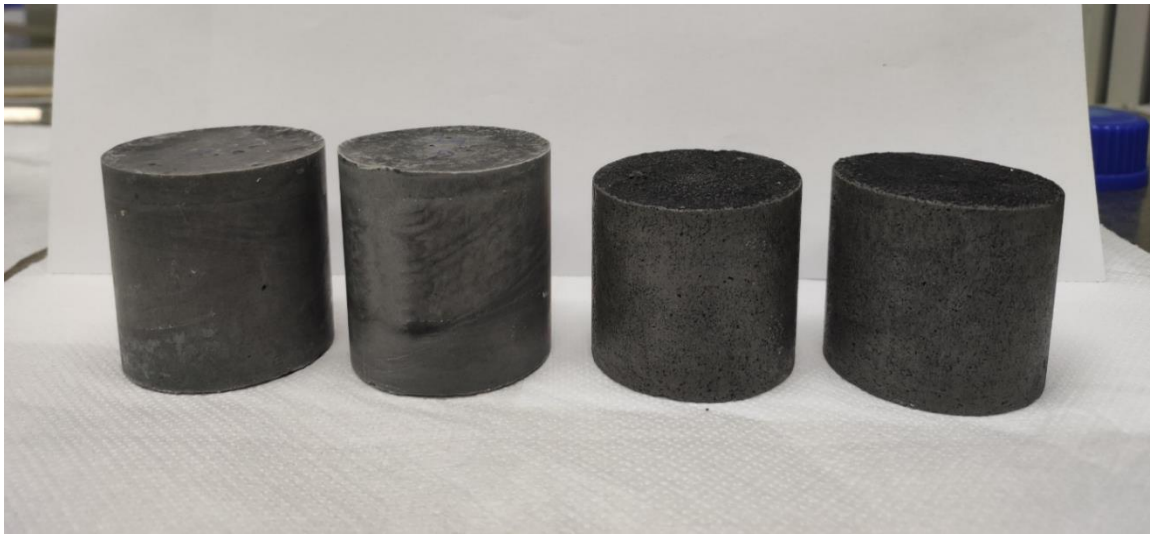

Figure 33. MIX-based samples prepared by POLIMI (first two: no waste; last two with 30 v% LSC).

Following the prescribed curing period, samples with no waste and with 30% LSC appeared dense and homogeneous. Qualitative visual inspection evidenced no macroscopic porosities or cracks. Slight bleeding was noted for samples containing LSC, amounting to approximately 2-5 v% with respect to waste volume. Samples with no waste presented negligible water bleeding.

3.2 Microstructural investigation

3.2.1 Metakaolin formulation

Pore size distribution and porosity of MK based samples were measured by Mercury Intrusion Porosimetry (MIP) after 28 days of curing. The results are shown in Table 28.

Table 28 . Results of MIP in potassium geopolymer samples.

Sample	Median pore diameter (nm)	Average pore diameter (nm)	% porosity
Geopolymer aerated	13.8	16.4	37.5
Geopolymer endogenous	15.4	32.4	45.0

It was observed that contact with air (and potential carbonation) did not cause a significant change in the median pore diameter, but it seems to cause a significant change in the average pore diameter. The porosity of the aerated samples is lower than the endogenous samples. A possible explanation is that the carbonation capacity could densify the microstructure of the geopolymer.

ECL performed X-ray diffraction (XRD) spectra on solid sample of MK based formulation. The results are obtained with a Bruker Advance D8 diffractometer, in Bragg-Brentano configuration, for 2θ angles between 5° and 60°, a step size of 0.05° and an acquisition time of 20 seconds per step. Results were analyzed using DIFFRAC.EVA software.

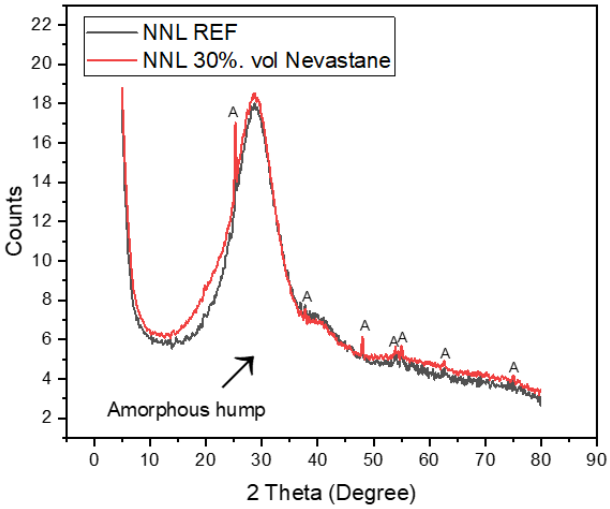

Figure 34. XRD pattern of 28 days cured samples NNL REF and NNL 30%. Nevastane

XRD patterns (Figure 33) have shown no differences in crystalline phases for the samples with and without oil. Anatase is the unique crystalline phase detected in XRD and is from the metakaolin precursor. Although, this shows that oil does not cause changes on the crystalline phases. Also, this XRD pattern will be considered as a reference for future comparison with the specimens after durability testing.

Specific surface and the pore distribution has also been determined using a Micromeritics instrument. The specific surface area value obtained for the reference sample is 24.4 m^2/g. However, the pore size distribution shows a concentration of pores around a diameter of 6.5 nm which corresponds to the mesoporous family (2-50 nm) with an almost monomodal distribution.

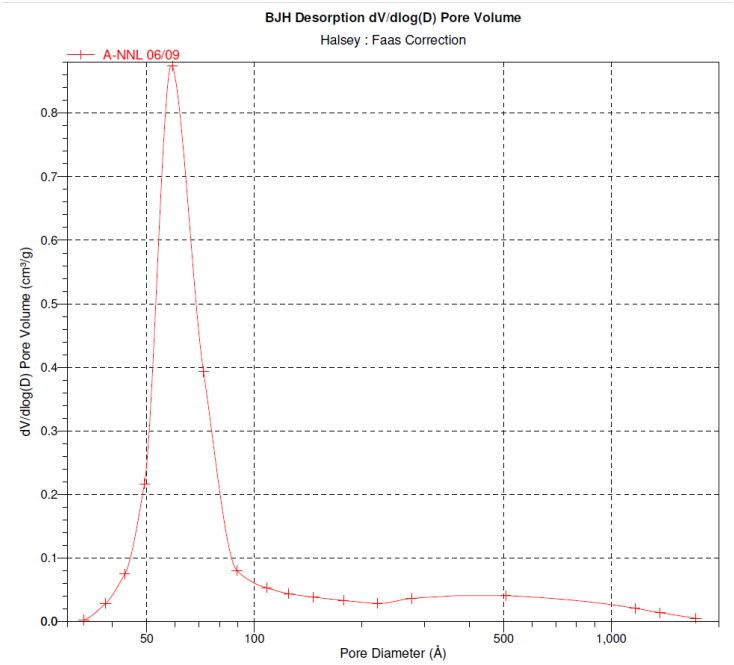

Figure 35. Pore size distribution of MK based formulation without oil

The water porosimetry was conducted following standard NF P¨18-459. Once the samples are cured, they are placed in deionized water in the desiccator. The evacuation is done after that for at least 4 hours. This low pressure is maintained for 44 hours approximately. To determine the mass % porosity, the following masses are required:

- The humid mass in the air: the samples are wiped are weighed
- The humid mass in the water: the samples are placed in the suspension system of the hydrostatic balance
- The dry mass: determined after drying the samples at 40°C until stabilization.

Table 29. Sample porosity (accessible to water) measured by ECL on MK based samples

Reference samples	Samples with 30%. vol
7 days of curing: 48.9% **28 days of curing: 41.7%**	7 days of curing: 35.9% 28 days of curing: 33.5%

The results show that oil added to the samples helps in reducing their open porosity. This may be explained by the fact that the oil clogs the pores and therefore the pores will not be accessible to the water to penetrate.

Gas permeability is an excellent indicator of durability and microstructural modification. Cylindrical specimens whose diameter and height are 37 mm and 50 mm respectively have been used for the permeability measurement. The jacketed samples are placed in a confined cell.

In order to highlight to determine the intrinsic permeability value, a constant confinement pressure of 5 MPa has been used under injection pressures equal to 0.5, 1 and 2.5 MPa.

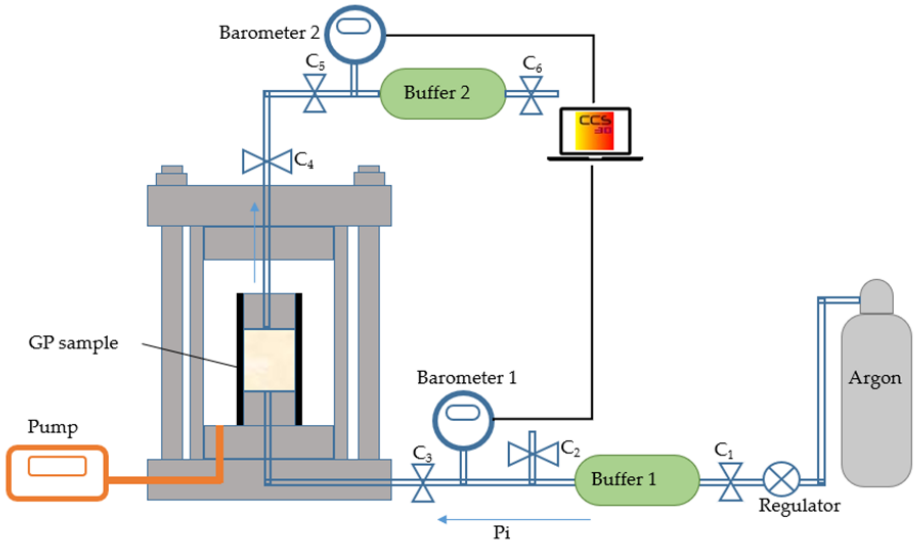

Figure 36. Scheme of permeability cell used by ECL

The permeability is calculated by using Darcy's Law (see for instance Loosveldt et al., 2002[1]):

$$K = \frac{\mu . Q_m}{S} \frac{2.h.P_m}{(P_1^2 - P_0^2)}$$

- Where: Q_m is the mean volume flow rate,
- P_m is the mean injection pressure which is equal to $P_1 - (\Delta P_1)/2$ (ΔP_1=0.1 MPa due to a loss on the upper side),
- P_1 is the gas pressure at the injection side,
- P_0 is the atmospheric pressure at the outer side,
- μ, S and h denote the gas viscosity, the cross-sectional area and the height of sample.

Assuming a unidimensional and quasi-static gas flow through a dry sample, Klinkenberg's equation is written as follows:

$$K_{app} = K_{eff} = K_{int} . \left(1 + \frac{\beta}{P_m}\right)$$

Where:

- K_{app} is the apparent permeability measured at the average pressure P_m,
- K_{int} is the intrinsic permeability. It is determined as the Y-intercept in a diagram plotting apparent gas permeability $K_{app} = K_{eff}$ vs. $(1/P_m)$,
- β is Klinkenberg's coefficient.

[1] Loosveldt, H., Lafhaj, Z., Skoczylas, F., 2002. Experimental study of gas and liquid permeability of a mortar. Cem. Concr. Res. 32, 1357–1363. https://doi.org/10.1016/S0008-8846(02)00793-7

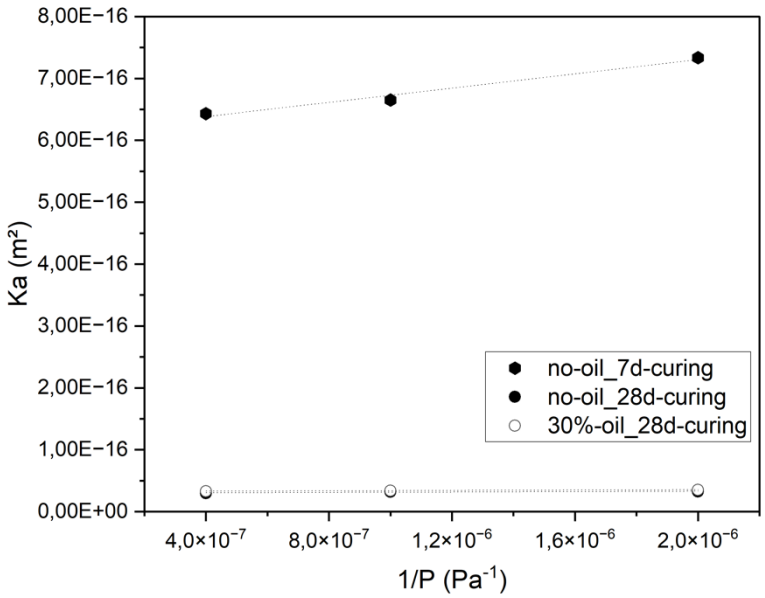

Figure 37. Intrinsic permeability measurement for MK based sample with and without oil

The permeability measurement has been conducted on samples with and without oil at 7 days and 28 days (7 days cured samples with oil cracks after drying, thus it is not possible to test its permeability). Permeability measurements of the three samples has shown the same slope at 28 days for both samples with and without oil resulting in a same behaviour in terms of transfer properties under 50 bars confinement (at 50 bars, all the cracks are closed due to the important pressure). Those values, in the case of cementitious materials, are considered as indicators for low to medium durability.

UNIPI also performed the XRD analysis using a Bruker D8 Venture X-ray diffractometer with dual micro-focused source, Photon III counting detector with mixed mode technology, and cryostat system for low temperature collections (up to 100 K). It allowed the qualitative determination of crystalline phases on micro-samples in θ-2θ Bragg-Brentano configuration. Similar results than those achieved by ECL are obtained for MK based formulation.

The morphological and compositional analyzes (SEM-EDS) were done by UNIPI by using a FEI Quanta 450 FEG field emission gun – scanning electron microscope (FEG-SEM). Analyses were carried out for samples reference without oil/RLOW. The SEM micrographs of MK based materials (Figure 38) showed the samples phase composition and surface, which are used as a reference for thermally aged ones.

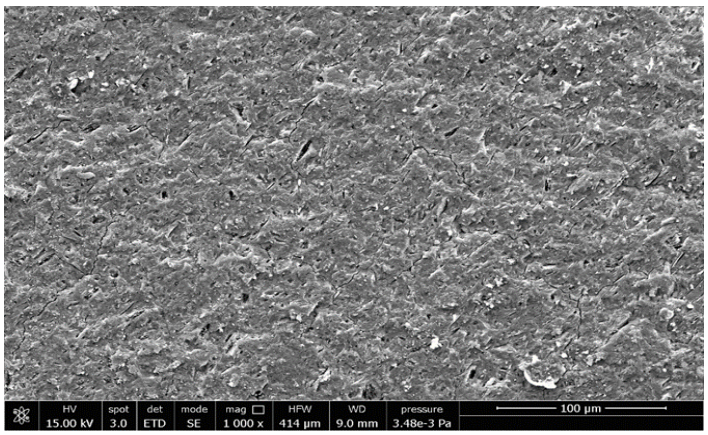

Figure 38. SEM micrographs of MK-based sample without oil

POLIMI also conducted XRD analyses on MK-based specimens to study their phase compositions. Collected data confirm that all samples, both without organic liquid and with TBP/dodecane or LSC at 30 v% loading, present a completely amorphous structure with pattern very closed to those of UNIPI and ECL.

Porosity (namely water porosity) after curing was assessed according to Day *et al*[2]. Results are reported in Table 29.

Table 29 . Water porosities determined for MK-based samples without waste and with LSC or TBP/dodecane. Uncertainty of the method was assessed at 3%.

Sample	Porosity
No waste	34.9%
LSC	36.0%
TBP/dodecane	34.5%

No significant differences were noted among all samples, irrespective of waste type.

3.2.2 Blast furnace slag formulation

In SCK CEN, a variety of techniques has been tried to study the microstructure of waste-forms, including N_2-adsorption, MIP, SEM. We found difficulty when applying N_2-adsorption and MIP measurements to the waste-forms because oil in the samples was not completely removed, even trying with different drying methods (e.g., oven drying, solvent exchange, and freeze drying). The obtained results were then not really representative to the samples. However, the SEM images can visualize the morphology of waste-forms and the oil distribution in the matrices.

Figure 39. presents the SEM images of DoE 11 and DoE 13 corresponding to the waste-form of Nevastane and Shellspirax, respectively. Nevastane oil dispersed as coalesced, irregular, and non-spherical droplets in the waste-form matrix. In contrast, The Shellspirax oil did not disperse as droplets as seen in DoE 11 but tended to create connected, even isolated oil zones. This is probably due to how difference in the viscosity between oil and AAS slurries. The closer the viscosities are, the more homogeneous the oil distribution is.

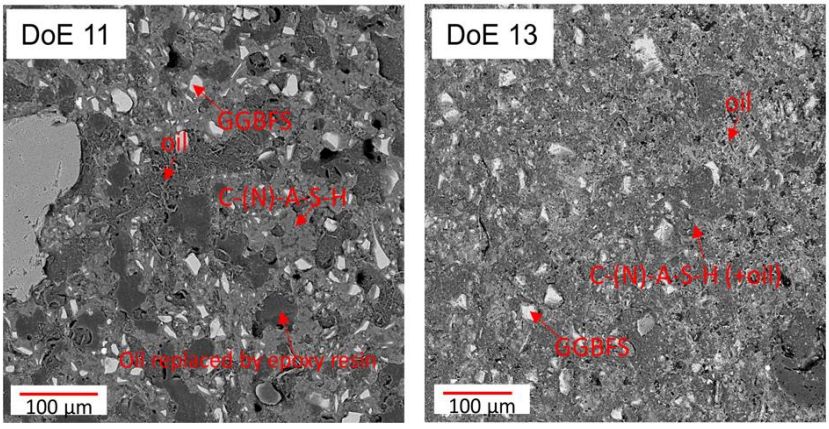

Figure 39. SEM images of DoE 11 (25 vol.% Nevastane) and DoE 13 (20 vol.% Shellspirax)

[2] Robert L. Day, and Bryan K. Marsh. "Measurement of porosity in blended cement pastes." Cement and Concrete Research 18.1 (1988): 63-73

In addition, SCK CEN also investigated the permeability as a microstructure-related physical property of waste-forms. The water permeability was conducted on DoE 12 and DoE 13 with the same waste loading of 20 vol.% Shellspirax. The main difference in the formulations between these waste-forms is the w/b ratio (the w/b ratio of 0.45 and 0.55 corresponds to DoE 12 and DoE 13, respectively). The permeability coefficients of DoE 12 and DoE 13 were 3.71×10^{-12} and 1.90×10^{-11} m/s, respectively. Compared to the permeability of reference AASs with the same w/b ratios, both DoE 12 and DoE 13 showed a ~17-time higher permeability than that of AAS 0.45 and AAS 0.55.

Further analysis in CV Rez with XRD analysis involved the Standard sample, prepared without any added oil or surfactant (Figure 40) and the sample where Mogul oil and a 0.75 wt. % concentration of Tween® 80 were added (Figure 41).

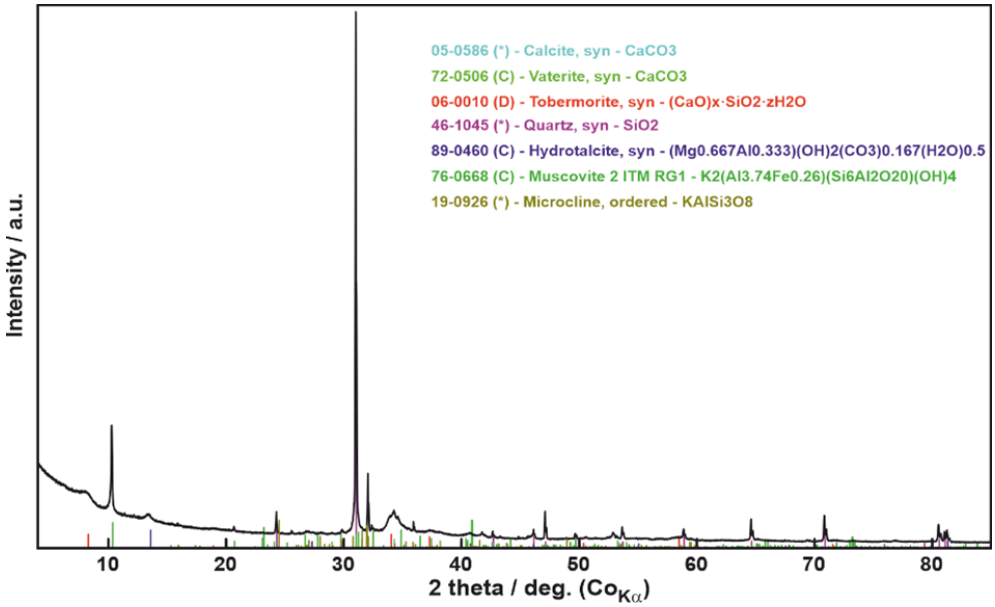

Figure 40. XRD analysis of a Standard sample prepared without oil and surfactant addition.

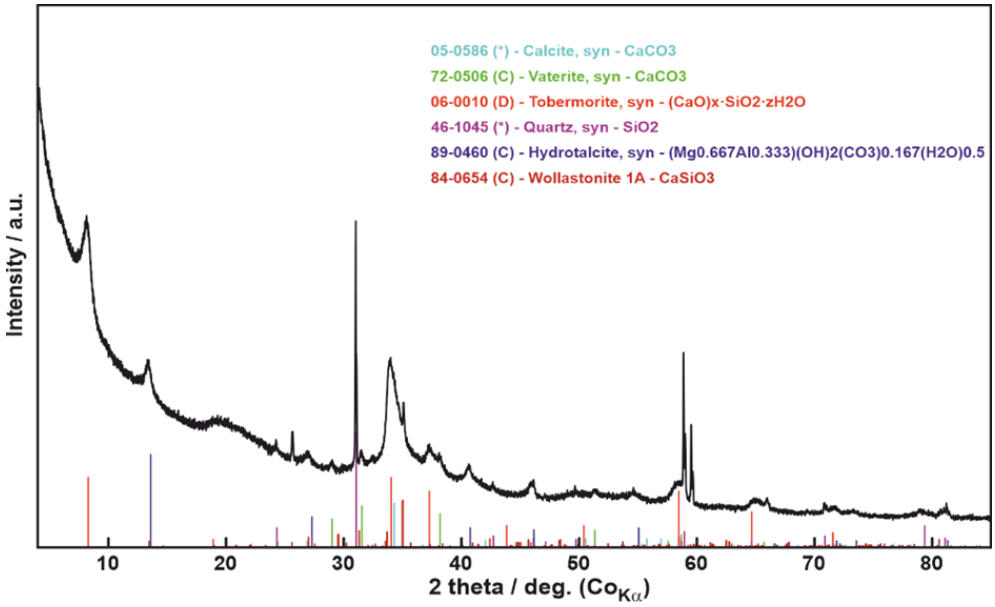

Figure 41. XRD analysis of sample with 5 wt.% Mogul oil and 0.75 wt.% Tween® 80

In geopolymer samples, minerals like quartz, feldspar, and mica can be associated with incorporated sand. Additionally, tobermorite and hydrotalcite are commonly associated with the reaction products of the geopolymerisation process forming as a result of alkali activation of the BFS. The presence of these minerals signifies the formation of a stable geopolymer matrix. Identifying wollastonite in the sample suggests a specific reaction during synthesis and curing. However, it should be noted that wollastonite typically forms at elevated temperatures, which are not typically achieved during the geopolymerisation process. It is therefore likely that this was either a contaminant or an experimental artefact.

In our analysis, we used a stereoscopic microscope, specifically the Motic SMZ 171 T-LED model, equipped with a MOTICAM S12 camera to examine the samples (Figure 42).

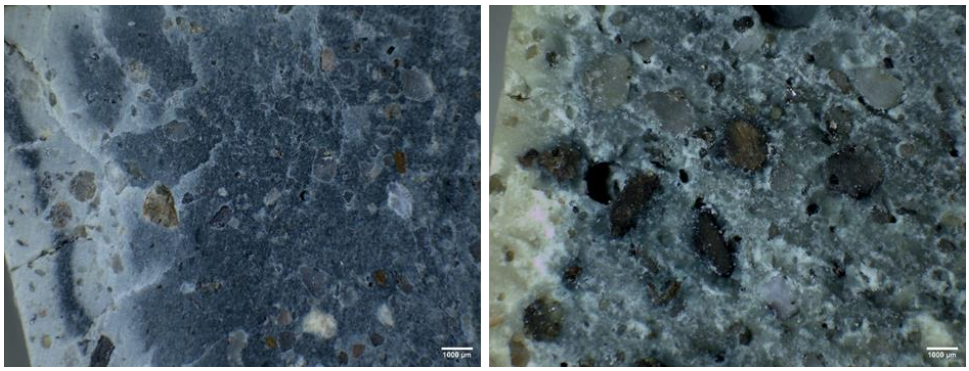

Figure 42. The stereoscopic microscope images of the sample (serie A) without added Mogul oil (left) and with 5 wt.% Mogul oil and 0.75 wt.% Tween® 80 (right) both cured in sealed bag condition.

In both images a magnified view of the grains of quartz sand incorporated into the samples was visible. We detected the presence of fractures within the samples, particularly concentrated towards their edges. A contrast in colour is evident between the surface and near-surface regions of the samples, likely due to the influence of air during drying before the analysis (oxidation of polysulfide species). The pore structures in the samples were also examined. The Standard sample displayed significantly smaller and less frequent pores than those with added waste oil. The sample with added waste oil exhibited larger and more pronounced pores.

Small fractures within the Standard sample of serie B (Figure 43) were visible mainly near the sample surface. As with previous samples, a magnified view of the grains of quartz sand incorporated into the samples was visible.

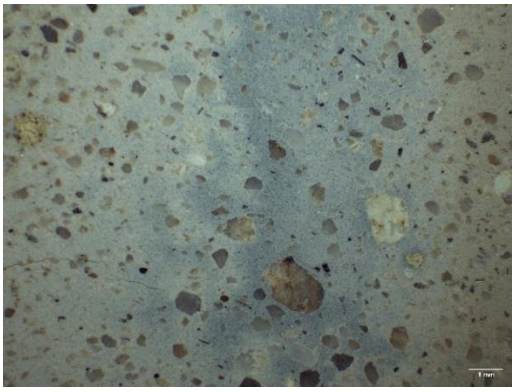

Figure 43. Stereoscopic microscopy image of the standard sample

On the samples with Total Nevastane oil (Figure 44) we observed a contrast in colour between the surface and near-surface regions of the samples as we did in Series A. The samples were dried after curing to be cut and analysed under the microscope, therefore the contrast in colours is likely due to the influence of air during drying. The samples with oil displayed significantly larger and more frequent pores than the Standard and this was also confirmed by the porosity analysis.

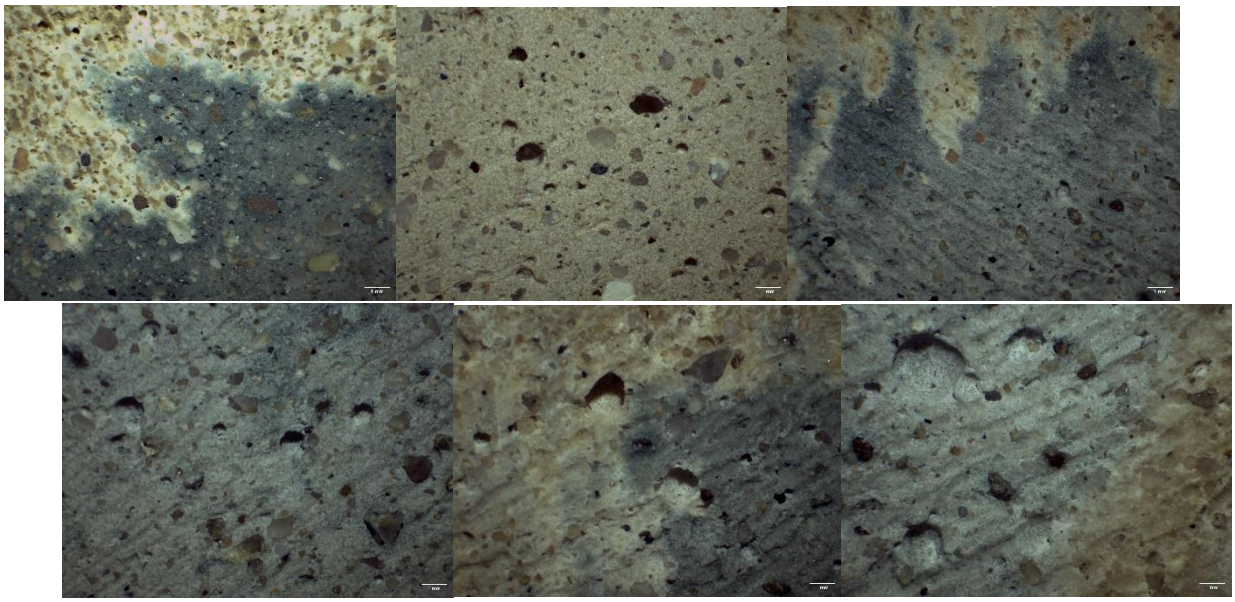

Figure 44. Stereoscopic microscope images of the samples with oil N1-N6 (top row form the left N1, N2 and N3, bottom row from the left N4, N5 and N6)

The porosity of the samples (series A) was measured using the AutoPore IV 9500 mercury porosimeter. The pores of 1 and 0.001 µm in size were predominant within the sample matrix and the results of the porosity analysis are shown in Figure 45.

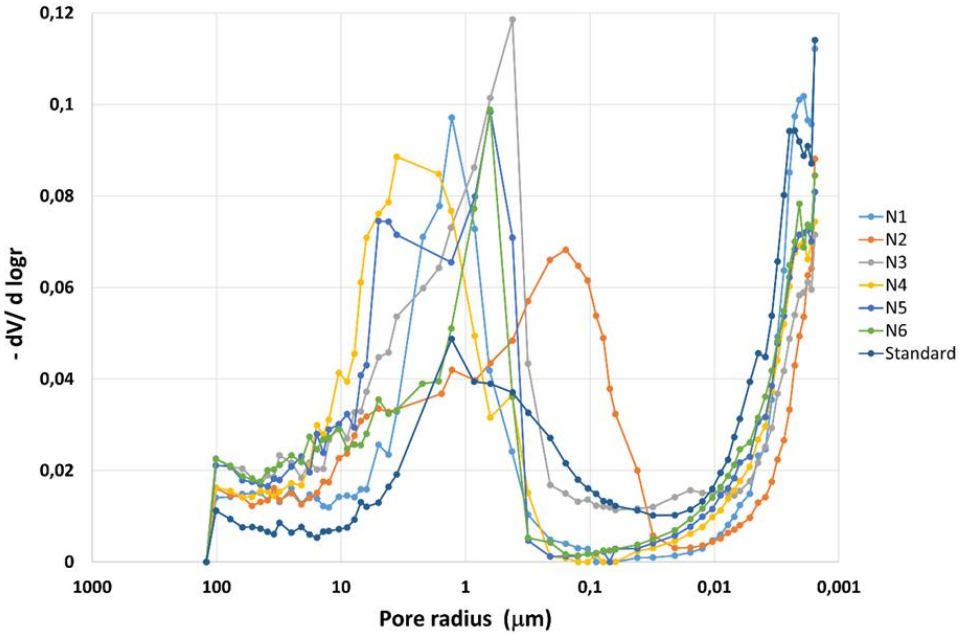

Figure 45. Porosity of samples N1-N6 and Standard

Each sample was analysed for the specific surface area using the 3Flex Adsorption Analyser, Micromeritics. The corresponding results are shown in Table 30.

Table 30 . The results of the surface area and pore volume analysis

Sample	BET surface area (m^2/g)	D-H Desorption cumulative surface area of pores between 1.7 - 300 nm diameter (m^2/g)	D-H Desorption cumulative volume of pores between 1.7 - 300 nm diameter (cm^3/g)	D-H Desorption average pore diameter (nm)
N1	0.1008	0.0369	0.000018	1.9349
N2	0.6209	0.5836	0.000774	5.3077
N3	0.5274	0.3324	0.002551	30.6988
N4	0.1696	0.0932	0.000060	2.5689
N5	0.2608	0.2749	0.000508	7.3895
N6	0.1429	0.0378	0.000019	1.9984
Standard	2.8317	6.1938	0.018331	11.8380

The compressive strength of the samples (series B) that were cured in sealed bag is shown in the Table 31). We observed a reduction of compressive strength with an increase in waste oil.

Table 31 . The compressive strength analysis of series B

Sample	Compressive strength (MPa)
N7	2.82
N8	1.89
N9	0.95

The porosity of the samples was measured using the AutoPore IV 9500 mercury porosimeter and the results of the porosity analysis are shown in Figure 46.

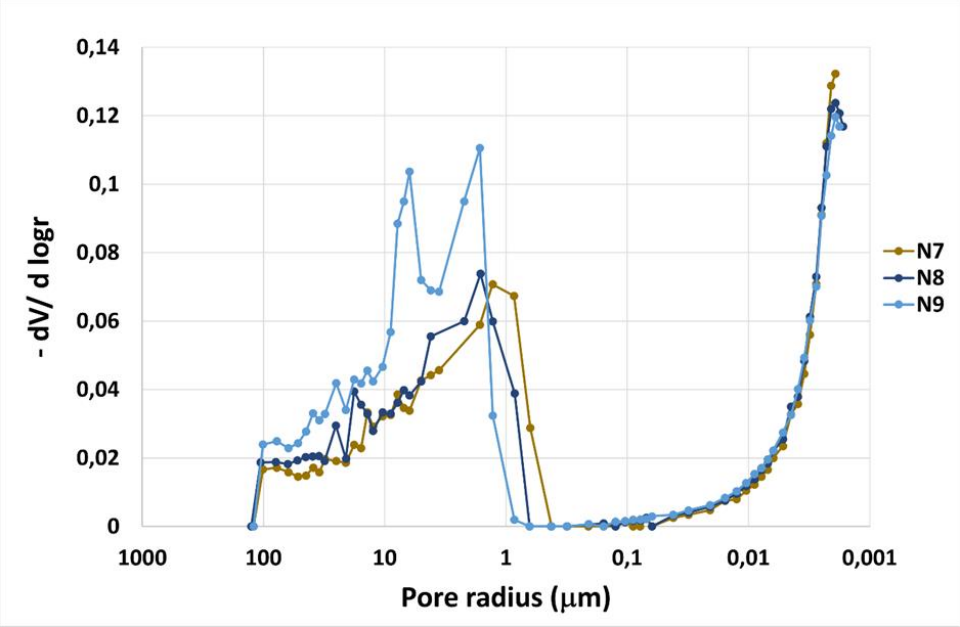

Figure 46. Porosity of samples N7-N9

Samples were also analysed for the specific surface area using the 3Flex Adsorption Analyser, Micromeritics. The corresponding results are shown in Table 32. It was unfortunately not possible to measure the pore volume of samples N7-N9.

Table 32 . The results of the surface area and pore volume analysis

Sample	BET surface area (m^2/g)
N7	0.1021
N8	0.0706
N9	0.1350

3.2.3 Mix formulation

The analyses on the GP matrix (MIX formulation) with ROLW have been conducted by SIIEG. The microstructural properties of the hardened matrix have been thoroughly characterised.

The XRD study (Figure 47) and SEM micrographs (Figure 48) showed the phase composition and surface of the geopolymer matrices for reference. The specific XRD patterns observed depend on various factors, including the composition of the starting materials, the concentration of KOH and K_2SiO3, curing conditions, and any additives present in the geopolymerization mixtures. The amorphous hump in the XRD pattern, observed between 10° and 40° 2θ, represents the formation of amorphous geopolymer phases. Peaks corresponding to various geopolymer phases include sodalite, zeolites, and other aluminosilicate phases resulting from BFS, FA, and MK polymerization in the presence of KOH and K_2SiO_3. Also, peaks corresponding to crystalline phases in raw materials - mullite and quartz phases - were observed.

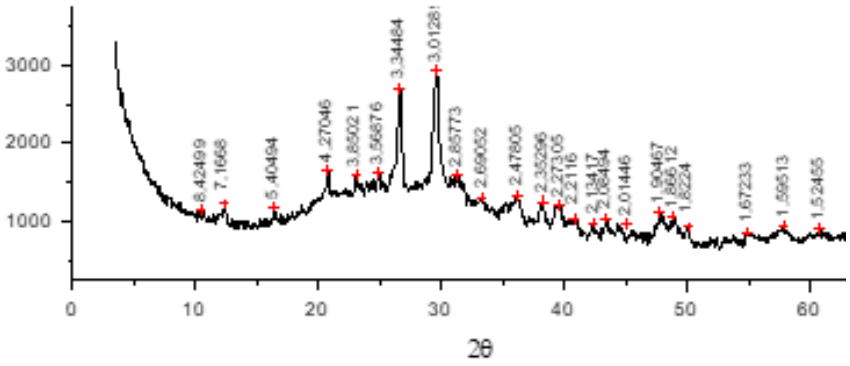

Figure 47. XRD of MIX formulation without organic oils

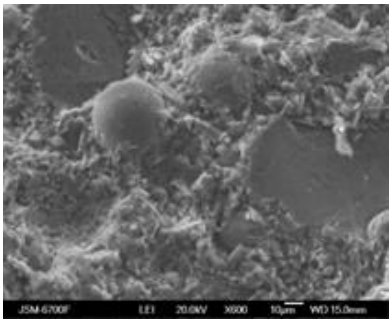

Figure 48. SEM micrographs of MIX formulation matrix

The mineralogical composition of the MIX formulation has been analyzed by X-ray diffraction (XRD) using DRON-4-07 diffractometers with a Cu anticathode. The interpretation of XRD patterns from geopolymers is complex. The XRD study (Figure 49) showed that potassium-calcium silicate hydrates represented a phase composition of the geopolymer under study. The amorphous hump in the XRD pattern, observed between 10° and 40° 2θ, represents the formation of amorphous geopolymer phases. The phases such as quartz (SiO_2), mullite ($Al_6Si_2O_{13}$), and other phases depend on the composition of the precursors in the activation process.

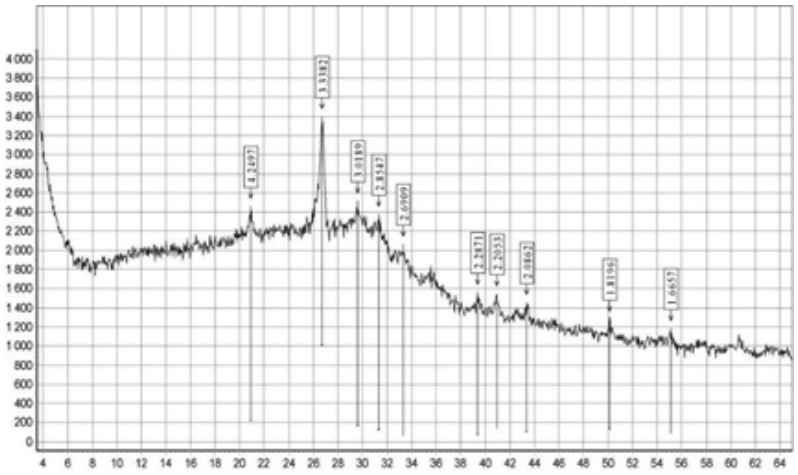

Figure 49. XRD of geopolymer matrices with oil (Nevastane - 30% vol)

Thermogravimetric analyses (TGA) studied on the mix formulation was also performed on the geopolymer matrix with different Shell Spirax (Figure 50)and Nevastane oil quantities (Figure 51). TGA was performed using a Thermal instrument Q-1500, and curves were recorded simultaneously in a static air and flow nitrogen atmosphere at a heating rate of 5°C/min.

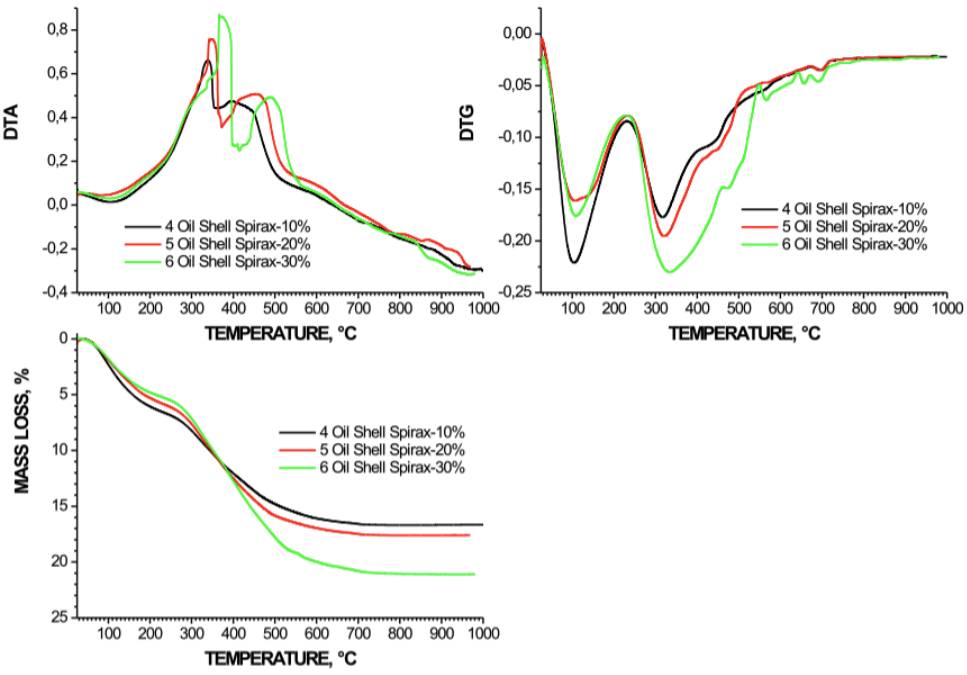

Figure 50. TGA of MIX formulation matrices # 4 with 10%, #5 with 20%, and #6 with 30% of the oil Shell Spirax.

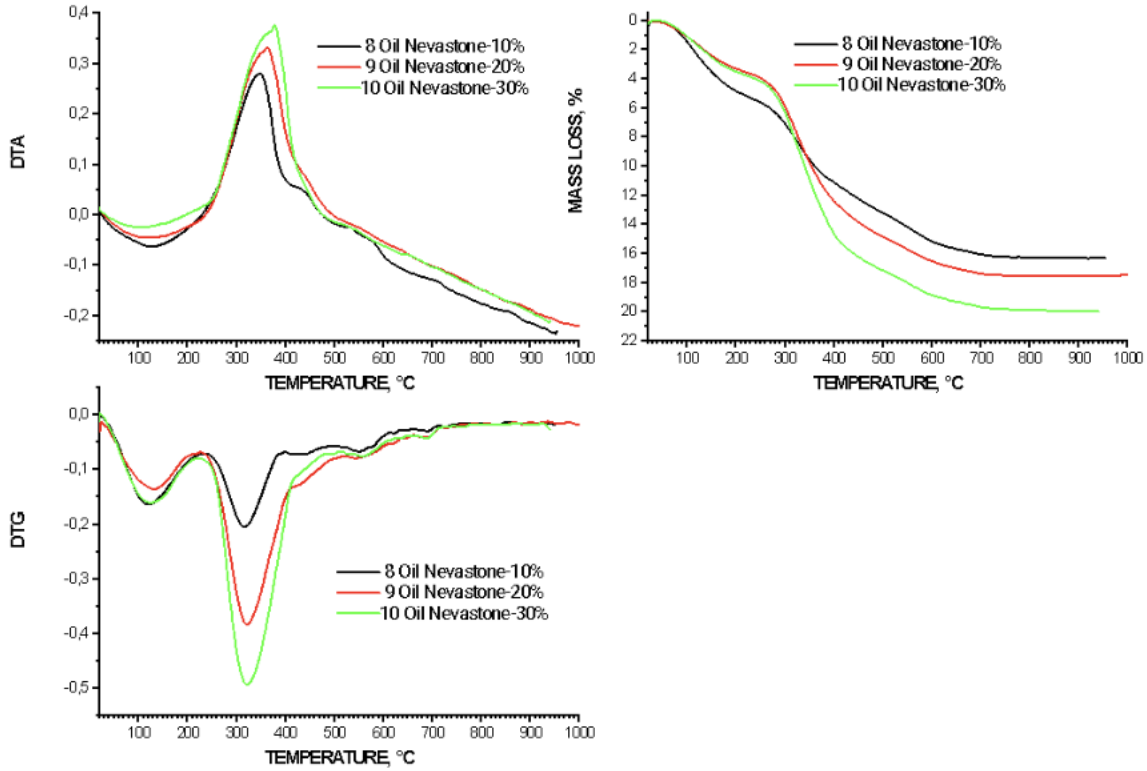

Figure 51. TGA of MIX formulation matrices with the Oil Nevastane - 10, 20, 30 % vol.

The analyses were done on samples aged for 287 days at room temperature. The research was conducted up to 1000°C. On the TG curves of all compounds, there is an intense decrease in weight up to a temperature of 200°C; the sample in this temperature range releases absorbed water and water in the sample's pores. The DTG curves show mass loss rate maxima in the region of 120°C and 320°C, which are associated with the release of bonded water of the investigated compounds and oil. It should be emphasized that there is a significant difference between the samples, including the different volumes of oil in their structure.

The structural nature of geopolymer matrices was studied using the FTIR spectroscopy method. The 4000-400 cm^{-1} frequency range FTIR reflection spectra were recorded on a Thermo Nicolet Nexus FTIR spectrometer. The FTIR spectra of geopolymer samples aged for 287 days in the air are shown in Figure 52. The FTIR spectra of geopolymers showed several peak shifts.

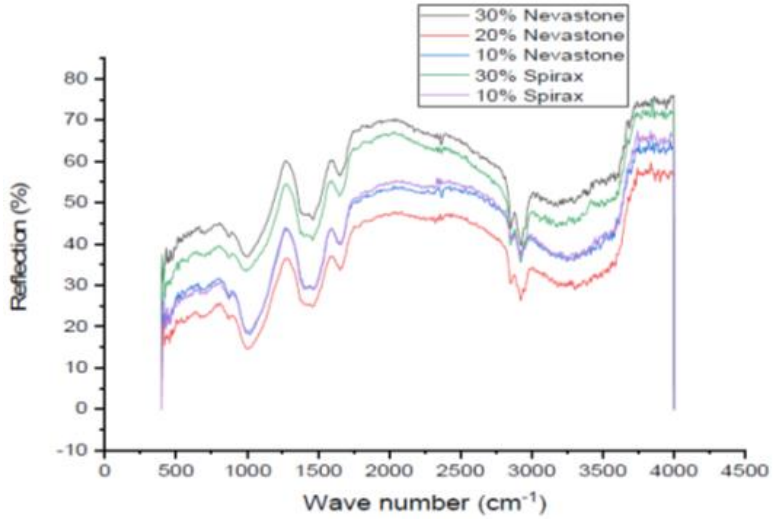

Figure 52. FTIR spectra of geopolymer matrices with different amounts of waste oil simulant.

Depending on the nature of the oils added, additional peaks or shifts in peaks related to organic compounds might be visible. These are challenging to interpret without further analysis, as they may overlap with peaks from other materials. POLIMI and UNIPI also conducted XRD analyses on MIX-based specimens to study their mineralogical structures. Collected data confirm that all samples, both without waste and with LSC at 30 v% or Oil at 30v% (Shellspirax), show an essentially amorphous structure, with a small presence of quartzite, mullite and calcite. The presence of calcite could also be ascribed to the reaction with atmospheric CO_2. A representative XRD pattern is reported in Figure 53. As for other formulation, the XRD with and without RLOW are virtually identical, meaning that there is no chemical encapsulation of waste in crystalline phases.

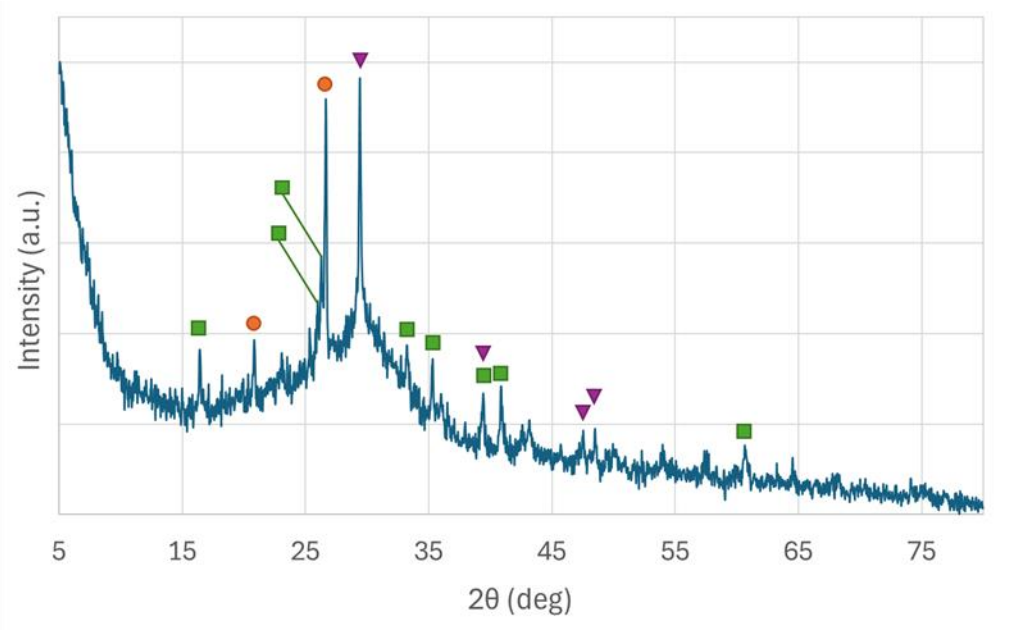

Figure 53. XRD pattern of MIX-based sample loaded with 30 v% LSC prepared by POLIMI.

Highlighted peaks can be assigned to mullite (squares), quartzite (circles) and calcite (triangles).
The porosity (namely water porosity) after curing was assessed and reported Table 33 in No significant differences were noted between the two sample types.

Table 33. Water porosities determined for MIX-based samples with no waste and with LSC. Uncertainty of the method was assessed at 3%.

Sample	Porosity
No waste	26.1%
LSC	27.9%

The SEM micrographs on MIX formulation (Figure 54) revealed that they are mainly composed of oxygen, silicon, calcium, potassium and aluminum. After thermal treatment (TTa), compression tests were carried out and the obtained results compared to those obtained from reference samples. The results obtained were compared to the strength value for fresh showed an average strength loss of about 27.66%.

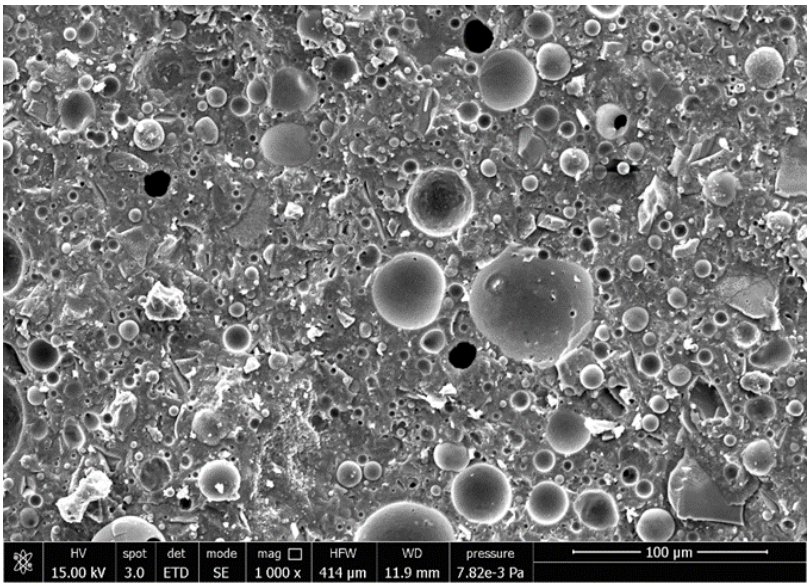

Figure 54. SEM micrographs of MIX -based formulation samples

Table 35. Ultimate stress of reference and TTa samples of KIPT formulation

Formulation	Fresh	Ultimate Stress [MPa]	TTa	Ultimate Stress [MPa]	Strength loss [%]
MIX formulation	Without Oil	10.48	Without Oil	12.01	14,60%
	Oil 20% vol	6.00	Oil 20% vol	4.2	22,15%
	Without Oil	10.23	Without Oil	17.10	67,07%
	Oil 20% vol	6.23	Oil 20% vol	6.65	6,80%

3.3 Partial conclusion about characterization before durability tests

The behaviour of materials incorporating liquid organic waste were characterized by the various partners through macroscopic and microscopic analysis.

Macroscopic analyses were based mainly on compressive strength measurements, although some partners provided additional analyses of porosity and/or fresh-state properties. For all three formulations, the strength results are generally acceptable when the materials are tested without liquid organic waste (except for one partner who found relatively low values). The addition of LOW in all cases results in a significant reduction in compressive strength, but this seems more limited for the metakaolin-based formulation, since it is possible to incorporate up to 30% by volume of waste while maintaining a strength greater than 10 MPa. For the formulation based on blast furnace slag, the initial mechanical performance (without waste) seems better (over 40 MPa), but the drop is greater and to maintain a strength of 10 MPa, the waste loading must be limited to 20% by volume. It should be noted that POLIMI and CV Rez obtained very low values with waste, attributable to the protocol and the difficulty to obtain homogeneous samples.

Microstructural analyses provide interesting additional data. On the one hand, XRD analyses show that, whatever the formulation, no major modification of the crystalline structure is brought by the incorporation of liquid organic waste, thus indicating that the incorporation of oil is mainly due to a physical and not a chemical effect.

Furthermore, the porosity and pore size distribution analyses proposed in this chapter, supplemented by SEM images, show that the porosity of the MK-based formulation is globally higher (between 35 and 45% depending on the partners, curing conditions and measurement methods) than the other formulations, but with a thinner pore size distribution. In fact, whether on the pore size distribution measured by ECL through nitrogen adsorption, on the mercury intrusion measurements carried out by CIEMAT or on the SEM images from UNIPI, none of the data show the existence of pores with sizes between 1 and 100 μm as is the case for the BFS and MIX formulations.

4 STUDY OF CONDITIONING MATRIX DURABILITY DURING AND/OR AFTER TESTS

4.1 Study of conditioning matrix durability in endogenous conditions

4.1.1 Metakaolin formulation

In CIEMAT, the immobilisation of the organic waste was carried out by adding the liquid waste to the prepared geopolymer (direct method). The main variables that affect the formation of the geopolymer are the time and speed of stirring. The optimized time of stirring was 15 minutes for the geopolymer preparation. Then the waste was added at low speed until reaching one hour of stirring. A homogeneous mixture of geopolymer and waste was obtained, so it was not necessary to use surfactants. For endogenous conditions, samples were wrapped with films to avoid the exchange of water with the surrounding environment (without re-saturation or evaporation of water) to simulate the real case of use of the geopolymer during the encapsulation of radioactive waste.

The studies carried out for the characterisation of the manufactured geopolymers in endogenous conditions were planned to monitor mechanical strength evolution.

The mechanical strength results with the immobilised waste are shown in Figure 55. In the case of the oil samples, the results are shown for 30 and 40 % vol. of waste and the geopolymer without waste, while for the liquid scintillation samples, the results are shown for 10, 20 and 30 % vol. and the geopolymer without waste.

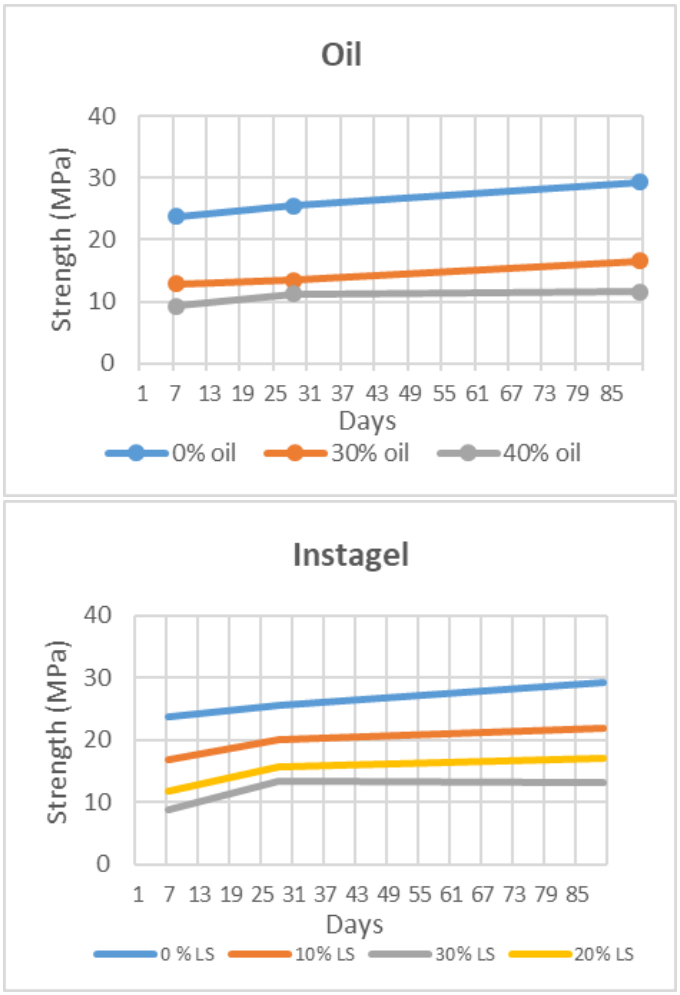

Figure 55. Mechanical strength results at different curing days and different volume of OIL and Instagel Plus as waste in endogenous conditions.

Both types of samples showed an increase in the strength as a function of time and a decrease of strength when increase the amount of waste immobilized.

4.2 Study of conditioning matrix durability in aerated conditions

4.2.1 Metakaolin formulation

The samples were prepared in the same way as endogenous conditions and cured in a climatic chamber at 20°C and 90 % humidity until performing the mechanical strength test. A slight increase of the mechanical strength is found in aerated but humid curing conditions (Figure 56).

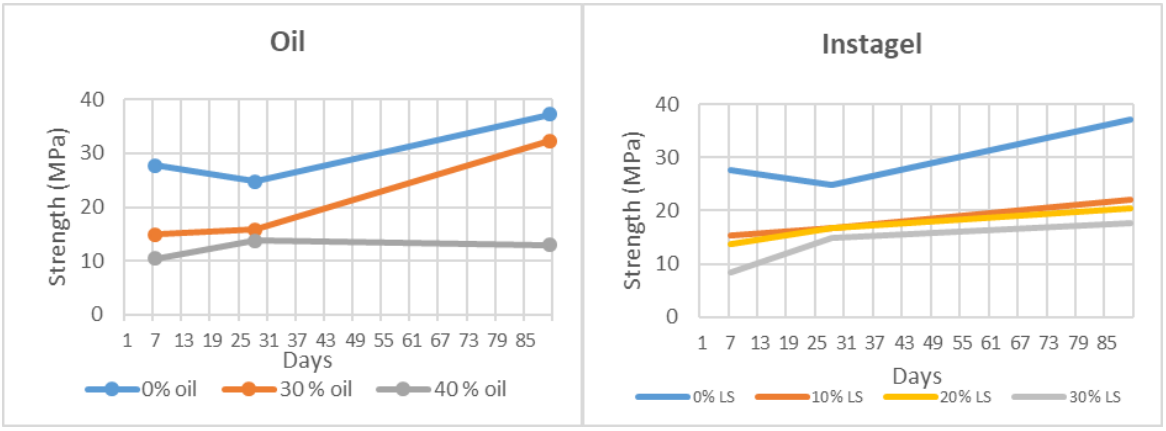

*Figure 56. Mechanical strength results at different curing days and different volumes of **OIL** and **INSTAGEL** as waste in aerated conditions.*

At ECL, to study the behaviour of MK based GP in aerated conditions, both natural and accelerated carbonation have been studied on 7 days cured samples. Natural carbonation has been tested on specimens up to 14 days in a carbonation chamber 0.1 % CO_2, 20°C, 65%RH. Accelerated carbonation was done in a carbonation chamber under the following conditions:

- 1% CO_2, 20°C, 65%RH
- 3% CO_2, 20°C, 65%RH
- 5% CO_2, 20°C, 65%RH
- 1% CO_2, 50°C, 65%RH

For the several conditions, the 2.7 cm diameter cylindrical specimens are split as is shown in Figure 57.

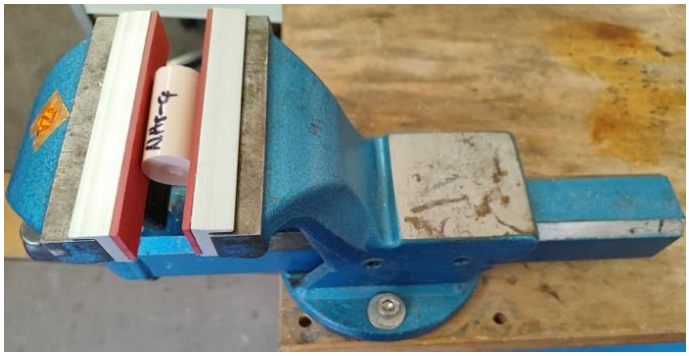

Figure 57. Splitting of the specimens for carbonation studies

<u>Accelerated carbonation:</u>

Phenolphthalein and Alizarine yellow were tested at GP to detect the carbonation depth. The follow-up to 7 days shows that the carbonation depth is more and more important over time. Other conditions of carbonation have shown the same effect of time and were illustrated in Figure 58 and Figure 59.

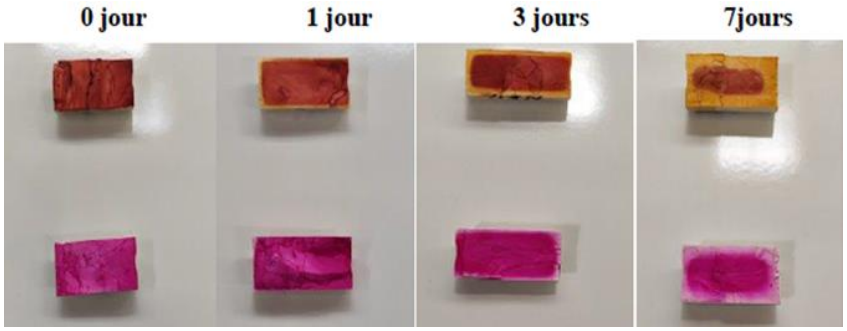

Figure 58. Split samples with color indicators showing the carbonation depth for GP samples with no oil, carbonated at 1% CO_2, 20°C, 65%RH

Figure 59. Split samples with color indicators showing the carbonation depth for GP samples with no oil, carbonated at 1% CO_2, 40°C, 65%RH

Since the carbonation depth varies depending on the colour indicator used (Table 34), alizarine yellow values were taken into consideration for the calculation of the depth that are reported into Figure 60.

Table 34. Transition pH and colors for the color indicators used

Indicator solutions					
Phenolphthalein	pH < 9	x	x	pink	pH > 9
Alizarine yellow	pH < 10.2	Orange	10.2 < pH < 12	Red	pH > 12

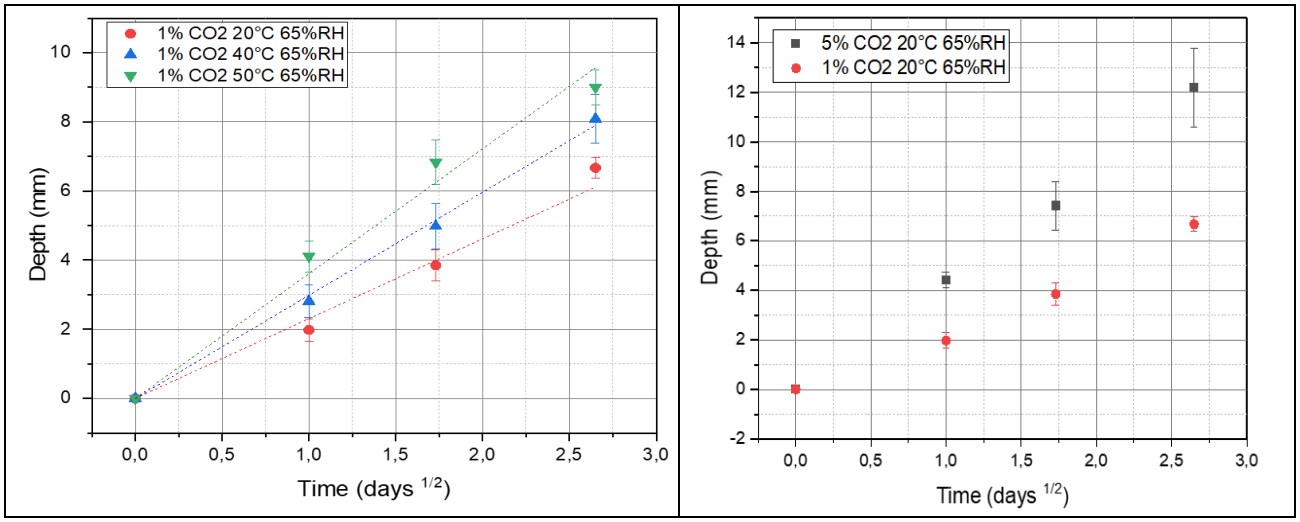

Figure 60. Graphs showing the kinetics of carbonation for samples with oil (Diffusive process)

Natural carbonation:

No oil- NC 0D	30% oil- NC 0D
	
No oil- NC 7D	30% oil- NC 7D
	
No oil- NC 14D	30% oil- NC 14D
	

Figure 61. Table showing the carbonation depth in natural carbonation conditions (NC)

Like accelerated carbonation samples, the carbonation depth increased with time. However, the photographs taken at 14 days of natural carbonation show that samples with oil carbonate less than the reference samples. This may explain that the oil is clogging the pores, thus not letting the entire carbonation proceed to the core of the GP.

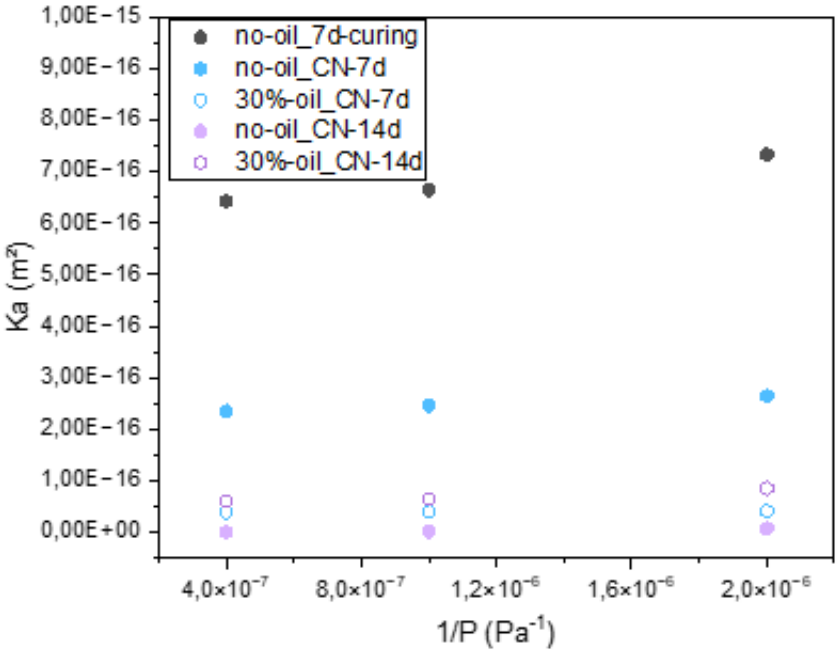

Figure 62. Permeability measurements after natural carbonation

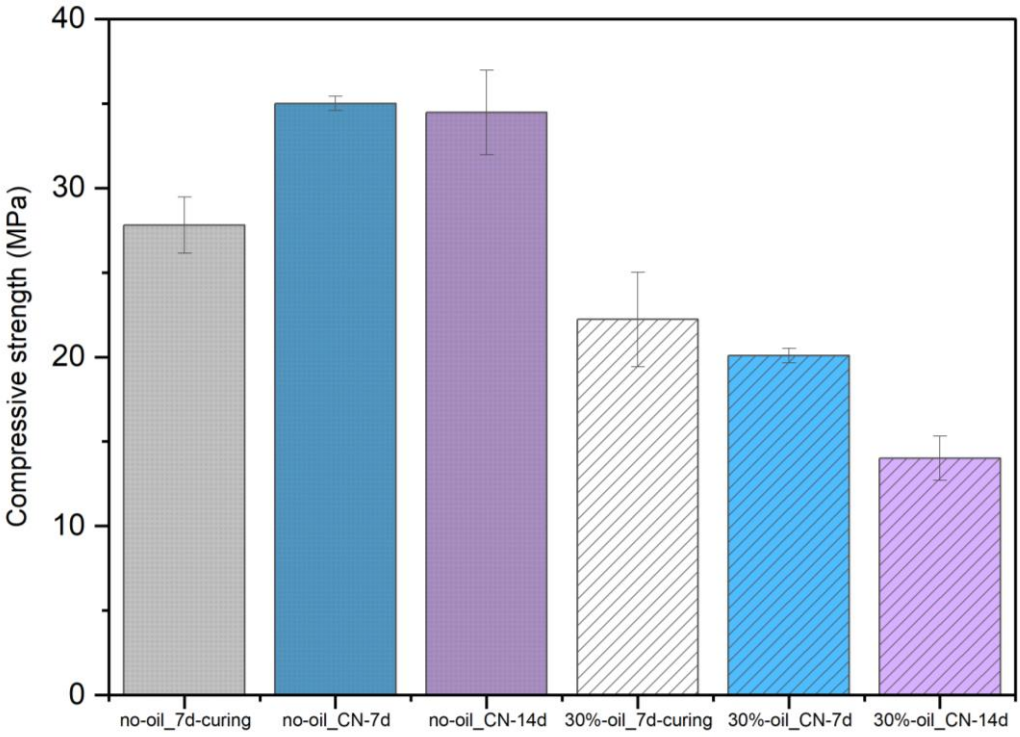

Figure 63. Compressive strength for GP under natural carbonation

Samples with and without surrogate oil wastes show fair permeability values with no differences at 14 days of carbonation. However, in Figure 63 a variation in the compressive strength of the samples is detected: Increase of 5 MPa for the sample with no oil and decrease of 5 MPa for samples with 30 vol.% Nevastane

4.2.2 Blast furnace slag formulation

In SCK CEN, accelerated carbonation and leaching tests were conducted in the four waste-forms containing AASs and oils. The accelerated carbonation is shown in this part while the accelerated leaching in acid is shown in the next section.

The waste-form mortar bars (40×40×160 mm) after 28 days of curing were preconditioned at 20℃ and RH of 60 % in a climate chamber until achieving a stable mass (~1 month). After that, six bars of each waste-form were placed in a climate chamber for accelerated carbonation testing. The carbonation conditions were set at 20 ℃, 60% RH, and 1% CO_2, which followed EN standard 13295. After 7, 14, and 28 days of carbonation, carbonation depth and mechanical strength were determined, while the 28-day carbonated samples were further characterized.

Carbonation depths (Figure 64) of the waste forms increased linearly with the square root of time, which was also witnessed in the AASs' carbonation. However, the carbonation depths of waste-forms were less strictly correlated to the carbonation time than that of AASs (smaller R^2). Additionally, the carbonation depths of the waste-forms were smaller than that of AASs with the same w/b ratios (e.g., the ~3 mm depth of AAS 0.35 compared to the ~0 mm of DoE 14). The presence of oil may clog the connected pores in the matrices of waste-forms and then diminish the CO_2 diffusion into the matrices. Interestingly, the DoE samples with Shellspirax (DoE 12 and DoE 13) showed a higher susceptibility to carbonation compared to the ones with Nevastane (DoE 11 and DoE 13).

The mechanical strengths of the four waste-forms before and after 7, 14, and 28 days of carbonation are shown in Figure 65. In addition, the strengths of samples (Ref-DoE, end carb), which were cured at the same temperature, RH, and duration (28 days after precondition process), were tested to compare with the 28d-carbonated samples. In general, both compressive strength and flexural strength of the waste-forms withstood the carbonation, again suggesting the better carbonation resistance of waste-forms than reference AASs.

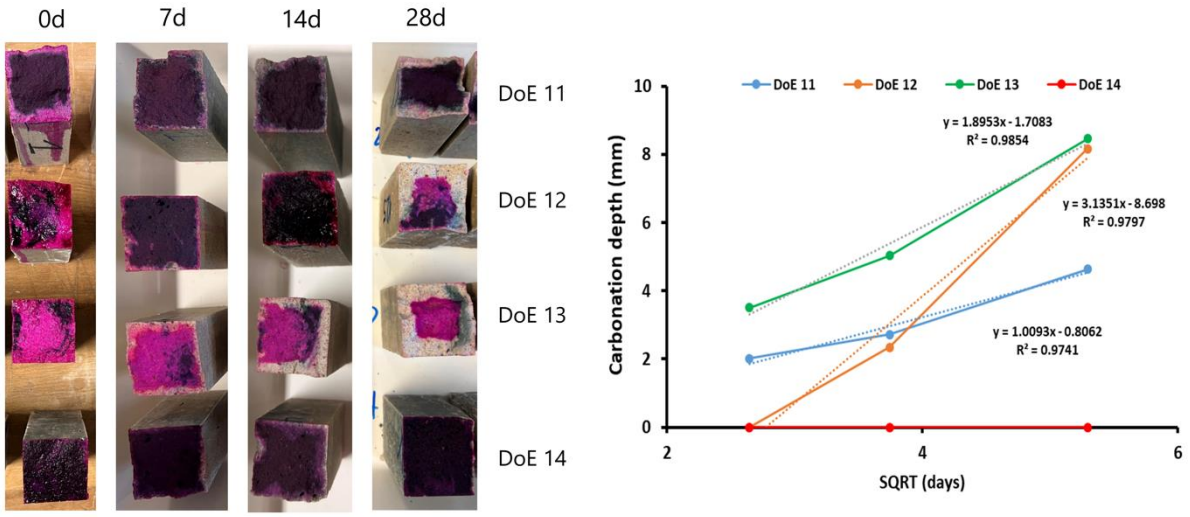

Figure 64. Carbonation depth of waste-forms containing AASs and oils over 0, 7, 14, and 28 days of CO_2 exposure (0d, 7d, 14d, and 28d)

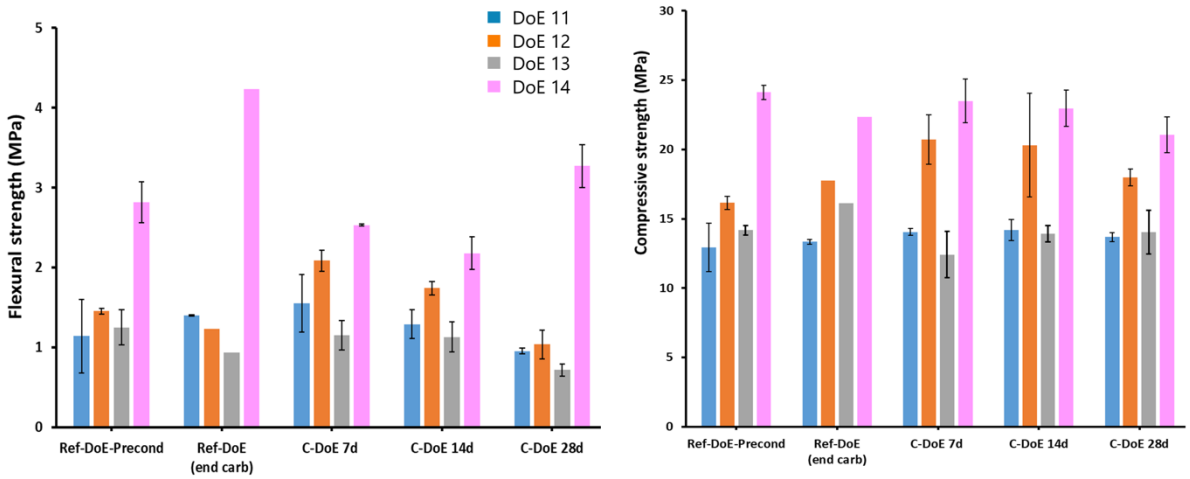

Figure 65. Evolution of flexural strength (left) and compressive strength (right) of four DoE samples over 7, 14, and 28 days of carbonation

Series A

CV Rez also studied the evolution of the compressive strength of samples (series A) with Mogul oil waste load of 5 wt.% and different surfactants and surfactant concentration cured under aerated conditions is shown in Figure 66. As with the samples cured under sealed bag conditions, the introduction of waste oil with surfactant has resulted in a reduction in compressive strength compared to the standard sample. The values varied from 17.03 to 26.41 MPa. There was no shrinkage observed with the samples cured in aerated conditions, but compared to samples cured in sealed conditions there were small cracks observed on the surface of the samples.

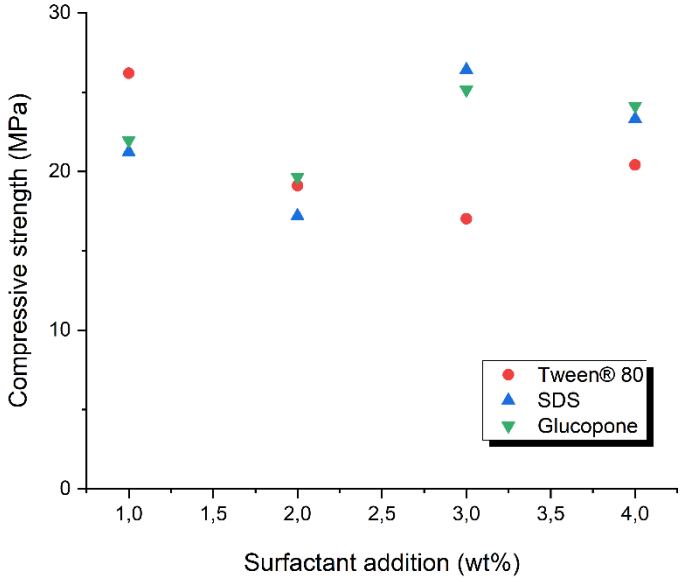

Figure 66. Compressive strength of samples with 5 wt.% Mogul oil and different surfactants and surfactant concentration in aerated curing conditions

There was no consistent pattern across the surfactants used. The inconsistent performance of Glucopone, including mixing challenges and solidification, suggests that it might not be a favourable choice for this application. Therefore, we conducted subsequent experiments with only the other two remaining surfactants.

4.3 Study of conditioning matrix durability in acid and alkaline liquid lixiviation leaching conditions

4.3.1 Metakaolin formulation

In order to analyse how stable the samples are and if there is leaching of the waste immobilised in the geopolymer, CIEMAT performed leaching tests of the samples in milliQ water with the samples cured in aerated and endogenous conditions. Tests followed the CIEMAT leach procedure, and parameters measured on the leachant are pH and carbon content

- Cylindrical geometry samples with a height of 4 cm and a diameter of 2 cm were prepared.
- The leachant must be totally renewed after 1, 3, 7, 10, 14, 21, 28, 35, 42, 72, 98, 126, 156, 182 until to reach 375 days from the start of the test.
- The ratio between the volume of leachant and the exposed area of specimen ranges from 10 to 20 cm.
- The specimen must be totally submerged in the leachant.

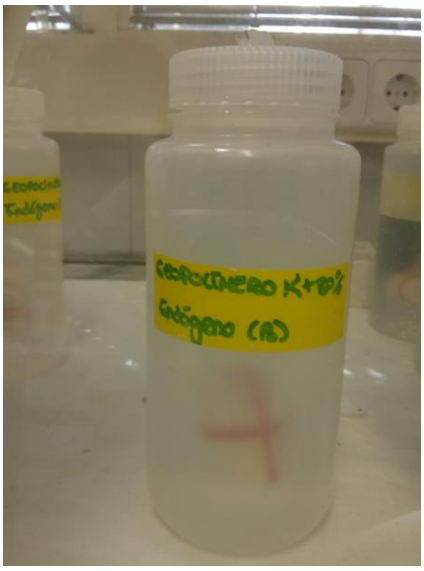

Figure 67. Geopolymer sample submerged in the leachant.

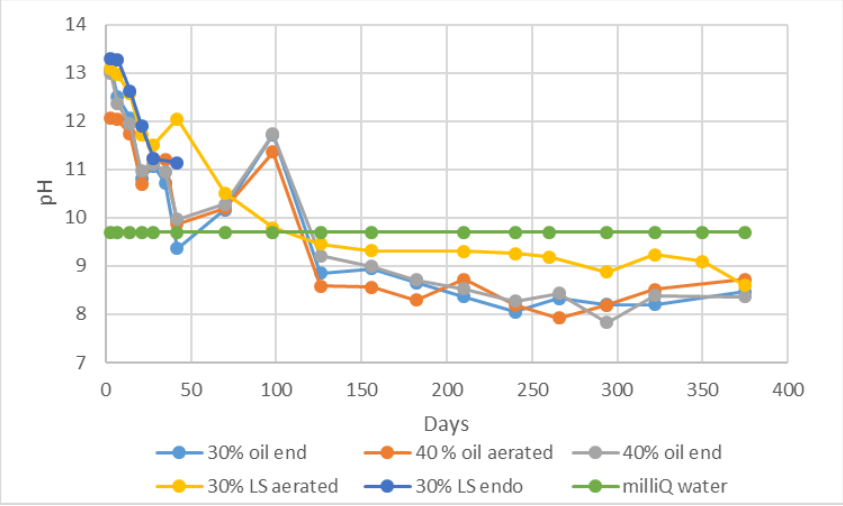

Figure 68. pH values from leachant solutions after leaching from geopolymer samples with oil and liquid scintillation cocktail as waste.

The values of pH analysed indicate that in the first stage of the study hydroxide ions are liberated to the leachant, increasing the pH of the milliQ water. The solutions analyzed from samples cured in aerated conditions generally have a higher pH.

Total organic carbon (TOC) has been measured as a parameter to know if the components of the immobilized waste leach into the environment. The following figures represents the TOC measurements in the solution in the time fixed of analysis. To ensure representativeness of the measurements, prior to chemical analysis, leaching solution is homogenised and at least 3 samples are extracted (more if significant discrepancies (> 2%) are observed).

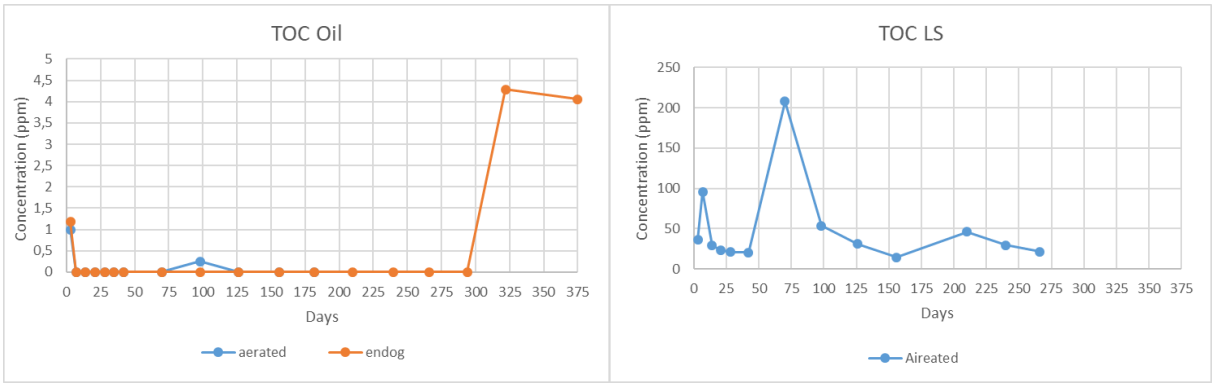

Figure 69. TOC concentration measurements in the leaching solutions in samples with oil (left) and liquid scintillation (right) immobilized in aerated and endogenous cured conditions.

As it is observed in Figure 69, the TOC measurements in the oil leachate solutions are negligible, but in the leachates of the samples containing scintillation liquid, high TOC values are observed.

Another fact that indicates the leachate solutions from the scintillation liquids leach is the formation of foam when the solutions are stirred, as can be seen in Figure 70 (left), due to scintillation liquids containing surfactant that passes into the leaching solution.

Figure 70. Foam formation after stirring the solutions from liquid scintillation lixiviation

To assess the durability of the GP formulations (MK based) in endogenous conditions, leaching of GP with Nevastane in deionized water (pH =7) has been conducted.

Leaching protocol:

The approach to the leaching experiments followed the ANDRA protocol. The principle comprises the leaching of radionuclides from solidified waste as a function of time.

The test sample must be both representative and homogeneous. For the specimen's dimensions, 4 cm cubic samples have been chosen and cylindrical specimens were opted for the other testing (D= 2.7 cm for porosity and ICP measures of leaching in water and D = 3.6 cm for permeability measures)

The volume of the leaching solution is calculated as: V_L / S >= 0.1 m

V_L = the volume of leaching solution [m^3], S = the sample surface [m^2]

The leaching methodology consisted of replenishing the leaching solution at 3, 7, 14, 28, 56 and 90 days to accelerate the leaching kinetics.

Experiments on the leaching solution: pH and ICP

Leaching in deionized water (neutral pH around 7) shows that the pH obtained from 3 up to 28 days is around 10-11, meaning that the GP matrix has released alkaline ions leading to this increase in the pH of the leaching solution (Figure 71). At 56 days, the pH starts to drop to 9.28 and stays constant at 90 days. Those pH measurements are in phase with the ICP values drops obtained. In fact, except for the high drop in the K concentration in 3 days, the pH follows the slope of K, meaning that potassium components in the geopolymer have been released, leading to this pH evolution over time.

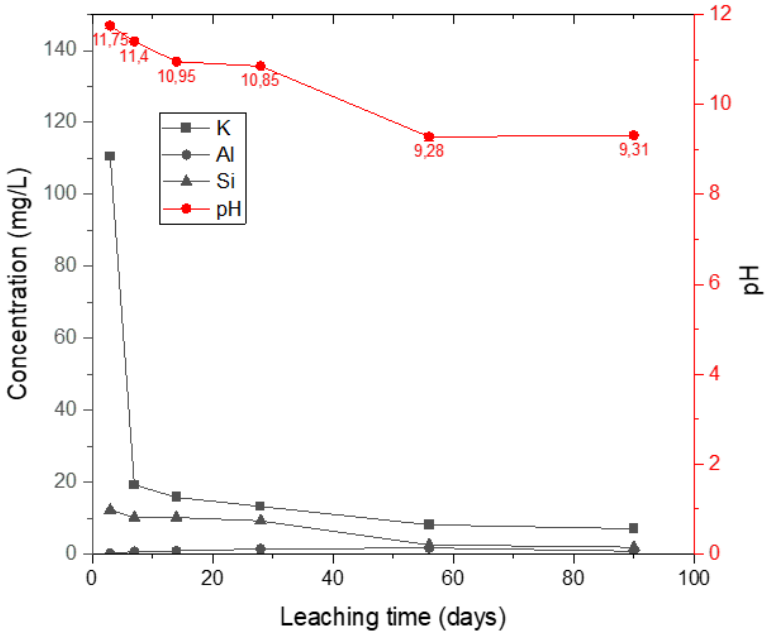

Figure 71. pH and ICP analysis of GP leaching in deionized water

Samples containing Nevastane have been colored in red (sudan III dye) in order to visually detect any oil floating on the water. However, none of the pictures have shown any red layers on the top of the beaker. Another method to detect the oil consists of drying the beaker containing the leaching solution of GP + oil. The masses before and after drying have been noted to calculate the % of oil released in volume. After 90 days of leaching, around 3.5% of the total oil contained in the specimens was released (Figure 72).

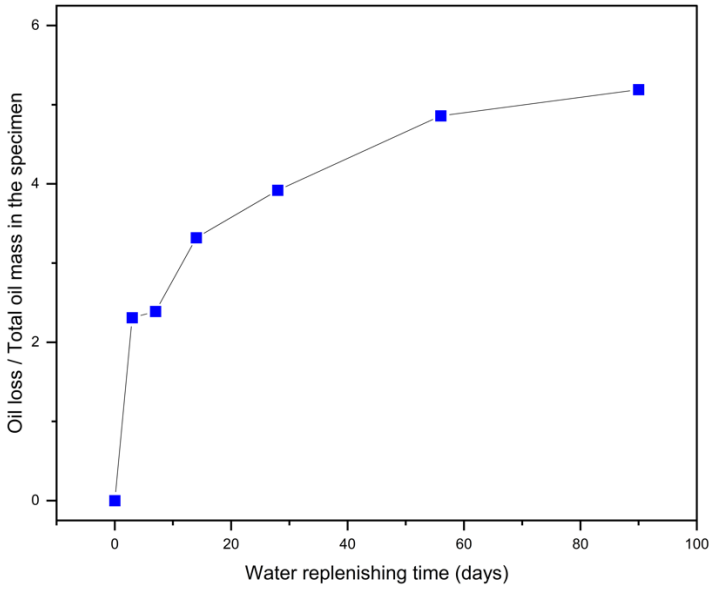

Figure 72. Oil release vol % percentage for GP leaching in deionized water

Note that, for all leaching experiments, the ICP measurements were conducted for samples with no oil (since the equipment is not adapted for oil-containing specimens). The pH values for both samples with and without oil were equal to the curve illustrated in the graphs.

GP Matrix evaluation after leaching in water (LIW):

Macroscopic testing shows no big differences (Figure 73) in terms of compressive strength where the evolution of the compressive strength obtained remains equal to within +/- 2 MPa, compared to the values at 28 days of curing before leaching experiments.

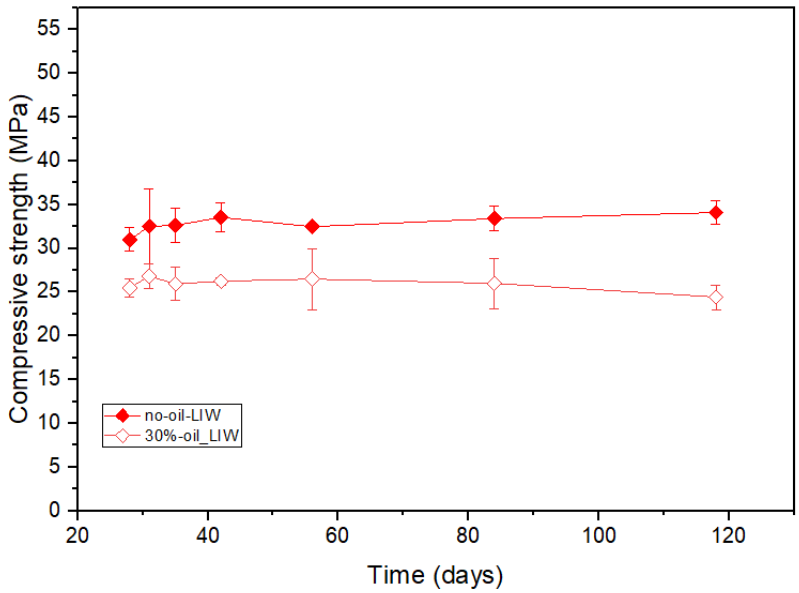

Figure 73. Compressive strength of samples leached in water

Permeability measurements show no huge changes in terms of gas permeability. The variations in the different values are in the order of $2x10^{-17}$ m^2, which is considered a low difference between samples (Figure 74).

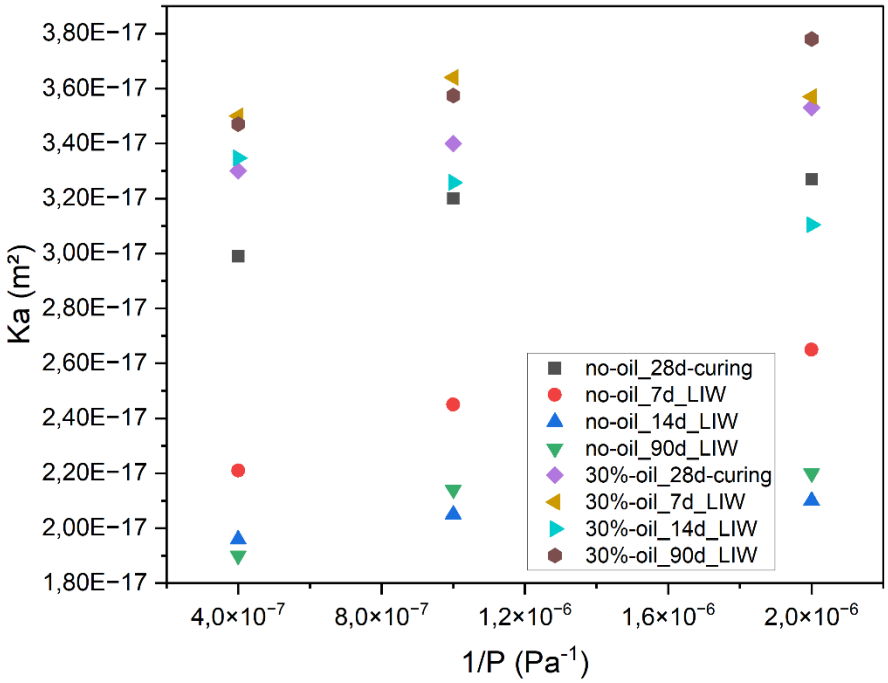

Figure 74. Permeability of different samples after 7, 14 and 90 days of leaching in water compared to the reference specimens 28 days cured

Table 35. BET surface area values for GP leaching in water (samples with no oil)

	BET surface area (m^2/g)
LIW-3d	124,2
LIW-7d	137,1
LIW-14d	140,08
LIW-28d	139,84
LIW-56d	150,11
LIW-90d	151,1

The values of Specific surface area (BET) for samples with no oil show an increase in the values, showing that there are more surfaces accessible for the gas to enter.

The values obtained from the different tests for leaching in water show that, except for the pH and ICP changes occurring, no differences on macroscopical scale have been noted. Consequently, macroscopic values obtained in compression remained constant also. This could be explained by a thin layer being leached, thus not altering the properties of the geopolymer.

Alkaline conditions:

In order to assess the durability of the GP formulations in alkaline conditions, leaching of GP with Nevastane in an alkaline solution at pH = 13 was tested. This solution is representative of the CEM V pore solution presented in the layer protecting the geopolymer, according to ANDRA. The composition of this solution is presented in Table 36:

Table 36. CEM V leaching solution composition BET

Type of water / Condition	Base concentration (g/L)					pH
	NaOH	KOH	$Ca(OH)_2$	K_2CO_3	Na_2CO_3	
CEM V (S'25 Simplified)	1,995	8,396				13,3

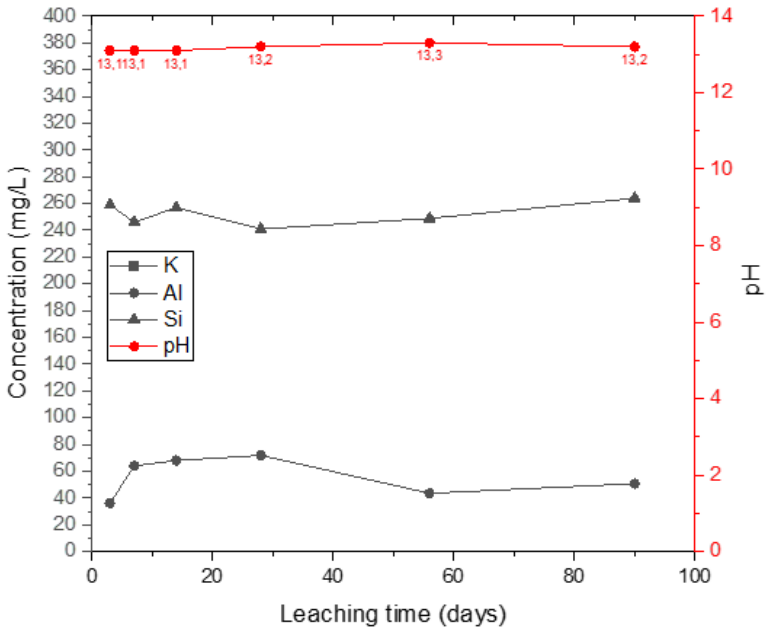

Figure 75. Concentration (ICP measurements) and pH evolution for GP leaching in alkaline solution (pH 13)

The pH evolution shows no changes compared to the initial pH of the leaching solution (*Figure 75*). The geopolymer is submerged in a compatible alkaline environment similar to its own alkalinity, although the ICP values indicate a saturation content of potassium ions in the leaching solution (>3000 mg/L). Other ions presented in the solution have shown a little variation in terms of 10-20 mg/L. Thus, the leaching solution has not shown to be aggressive to the geopolymer.

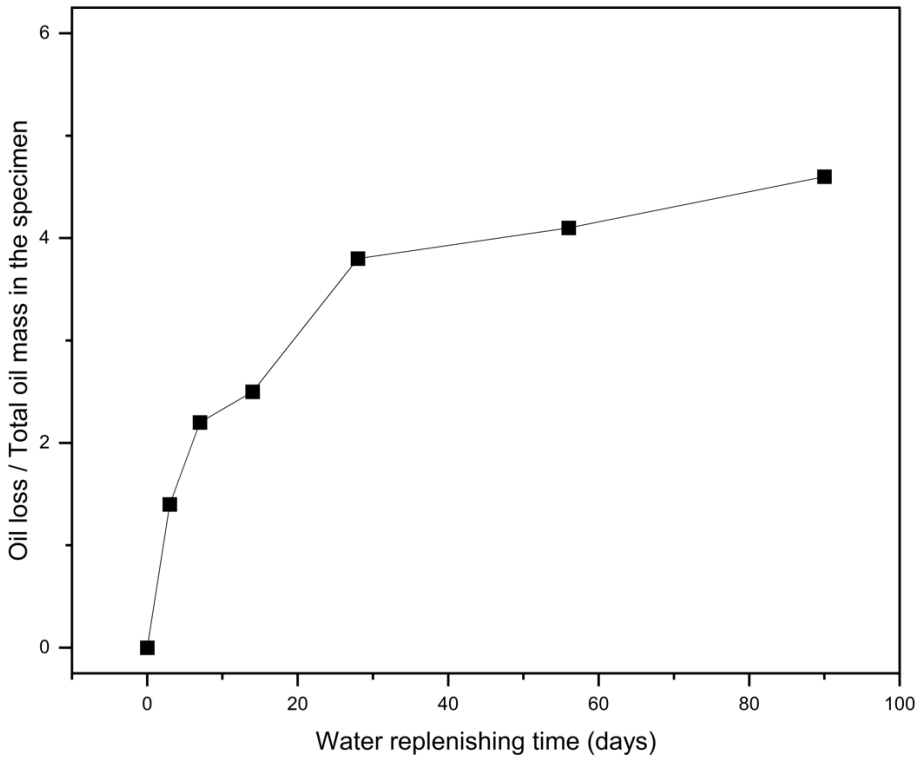

Figure 76. Oil loss for GP leached in alkaline solution (pH 13)

Similar to the leaching in the water (endogenous condition), the quantity of oil loss from day 0 to 90 days is around 5 vol.% (Figure 76) compared to the initial content (i.e. 5% of 30%). This value measured in this way show that no major release of oil has been shown (also visually not detected even after colouring the oil in red). The oil is well physically incorporated in the geopolymer matrix.

Table 37. Permeability values assessed on the samples after leaching in CEM V solution

1/P (1/Pa)	No-oil-14d	No-oil-28d	30%-oil-14d	30%-oil-28d
2e-6	6.28×10^{-16}	6.15×10^{-16}	7.14×10^{-17}	6.64×10^{-17}
1e-6	1.86×10^{-16}	2.16×10^{-16}	1.85×10^{-17}	1.38×10^{-17}
4e-7	4.34×10^{-17}	4.5×10^{-17}	4.56×10^{-18}	4.0×10^{-18}

Permeability measurements show that samples with oil show better values than samples with no oil. The improvement is 10 times. However, no aggressivity of CEM V solution is noted for the leaching.

Acid conditions:

To assess the durability of the GP formulations in acidic conditions, leaching of GP with Nevastane in hydrochloric acid with a pH = 3 has been conducted following the same protocol with renewal of leaching solution. The purpose of this testing is to understand the behaviour of K-geopolymer in an acidic environment. Note that preliminary testing with HCl at pH =1 has shown that GP matrix is aggressively attacked

Figure 77. GP leaching in HCl pH 1 after a) 1 hour b) 48 hours leaching, with no replenishing of the solutions in both cases.

pH:
Since testing is ongoing, only few results are available:

Table 38. pH measurements for samples leached in acid

Leaching in HCl	3 days	7 days	14 days
pH	12.46	11.9	12.04

Compressive strength:

Table 39. Compressive strength values for samples leached in acid solution

Compressive strength	0 days	3 days	7 days	14 days
GP with no oil	31.01	35.8	31.5	32
GP with oil	25.5	27	28.8	21.37

These first results indicate that with Oil in a geopolymer based on the MK formulation, a decrease of compressive strength starts to be highly visible at 14 days in an acid solution (pH = 3).

4.3.2 5.3.2 Blast furnace slag formulation

In SCK CEN, leaching tests of waste-forms were conducted on cylindrical samples (a diameter of 97.5 mm and a height of 25 mm) under 6 M NH_4NO_3 solution (pH~4.5). The waste-forms after 28 days of curing were saturated in water at reduced pressure for 24 hours, then immersed in the NH_4NO_3 contained in a vessel (Figure 78). A fixed ratio between the area of exposed sample surface and the volume of leachant solution is 300 cm^2/L, which ensures the pH of leachate solution is below 9.25 (pKa of NH_4^+). The leachate solution and the solid samples after 28 days of leaching were analyzed/characterized.

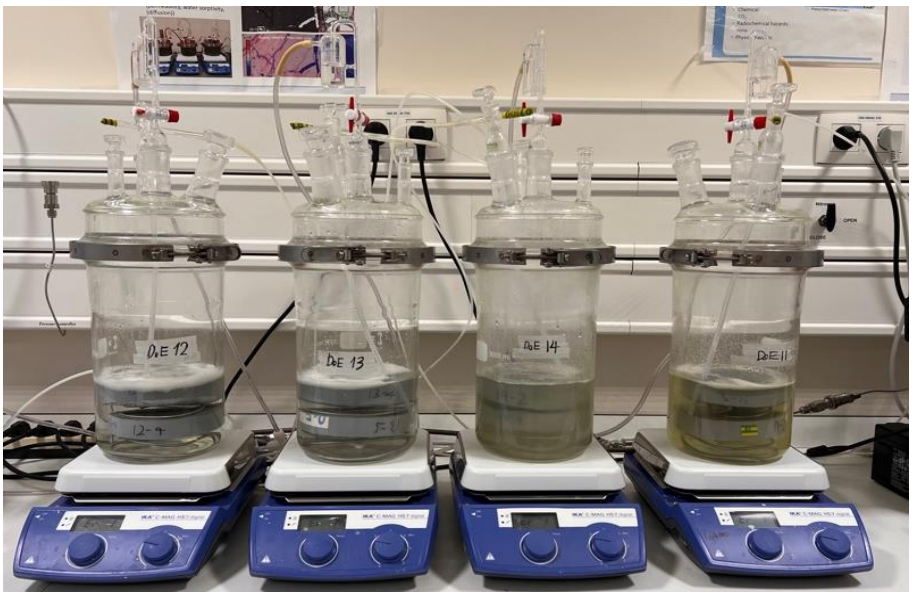

Figure 78. Leaching test setup in SCK CEN laboratory

The leaching depths of waste-forms after 28 days of exposure to 6M NH_4NO_3 were determined by using the phenolphthalein spraying method. The results shown in Figure 79 suggest a susceptibility to the leaching of the waste-forms. However, the leaching depth of waste-forms was mostly like that of reference AASs with the same w/b ratios (e.g., ~8 mm of DoE 14 and AAS 0.35). The leaching resistance of waste-forms seemed to primarily depend on w/b ratio, while the impact of oil type was not significant as differently seen in their carbonation resistance.

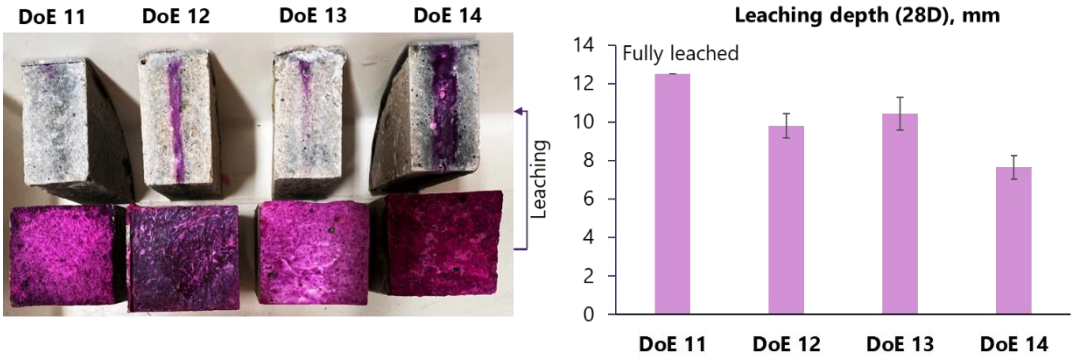

Figure 79. Leaching depth in acidic condition (pH~4.5) after 28-days exposure of waste-forms containing AASs and oils

Table 40. shows the concentration of leachable elements in the leachate solution after 28 days of leaching test, assessed by ICP-OES. Similar to the leaching of reference AASs in the same conditions, alkali (Na and K) and alkaline earth elements (Ca) were the most leached ones, whereas Al and Si mainly existed in the waste-form matrices. This suggests that the alumino-silicate framework (-Si-O-Al-O-) of waste-forms was not damaged during leaching. Compared to the leached amount of these elements of AASs with the same w/b ratios, the leached percentages of waste-forms were slightly higher. This is potentially attributed to the leaching of oil deposited near surface, benefiting the diffusion of the elements out of the matrices. However, oil presence did not significantly worsen the leaching resistance.

Table 40. Leachable elements' concentration in the leachate solution (mg/L)

Sample	Concentration in leachate solution (mg/L)						
	Ca	Na	K	Mg	Fe	Si	Al
L-DoE 11	15000 ± 380	4900 ± 700	480 ± 270	<100	<80	<60	<50
L-DoE 12	12750 ± 320	4000 ± 700	400 ± 270	<100	<80	<60	<50
L-DoE 13	12650 ± 320	4200 ± 700	400 ± 270	<100	<80	<60	<50
L-DoE 14	12140 ± 310	4400 ± 700	390 ± 270	<100	<80	<60	<50

After leaching,the water permeability of DoE 12 and DoE 13 increased to 2.27×10^{-11} and 2.57×10^{-11} m/s, respectively. Changes in C-A-S-H after leaching (decalcification, seen by ICP-OES) can lead to an alteration in microstructure (e.g., increase in porosity, crack formation), which induced the increase in the permeability. However, water permeability of the waste-forms was only slightly increased than that of AASs and insignificantly changed compared to that of cementitious materials.

In CV Rez, the cured samples were characterized and placed in demineralized water (electrical conductivity 2 µS/cm) for a specific period (2, 7, 2, 7, 14, 28, 56, and 91 days). At these times, the demineralized water was replaced and the concentration of the leached elements was analyzed. The pH and conductivity of the leachate were measured using a WTW pH/Cond 3320 Multi-Parameter Portable Meter (Xylem Analytics). Calcium values were determined by titration, while silicon and iron concentrations were determined using a Jenway 6850 UV / Vis Spectrophotometer (Cole-Parmer Instrument Company). After the leaching experiments, the samples were tested for compressive strength and porosity. No swelling was observed during the leaching experiments.

Series A - Waste loading 5 wt.%

Table 41. Composition of samples M1-M4

	Waste (wt.%)	***Waste type***	***Surfactant type***	***Surfactant (wt.%)***
M1	5	Mogul oil	SDS	0.45
M2	5	Mogul oil	SDS	0.75
M3	5	Mogul oil	Tween® 80	0.45
M4	5	Mogul oil	Tween® 80	0.75

A rapid decrease in oil leached from the samples was observed after the leaching solution analysis. No oil was leached after day 14 (same protocole than ECL : drying the beaker containing the leaching solution of GP + oil). We also observed less oil leached at samples cured in sealed bag conditions compared to those cured in aerated conditions. The cumulative leaching of oil is shown in Figure 80.

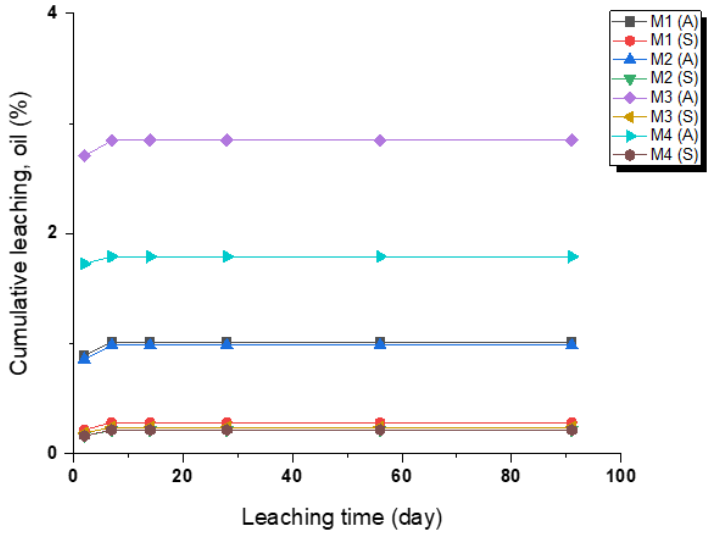

Figure 80. Cumulative oil leaching from the samples M1-M4 (A – aerated curing conditions, S – sealed bag curing conditions)

The cumulative leaching of silica and calcium is shown in Figure 81 and Figure 82. As with the leached oil, there was a significant difference between the samples cured in aerated conditions and sealed bags.

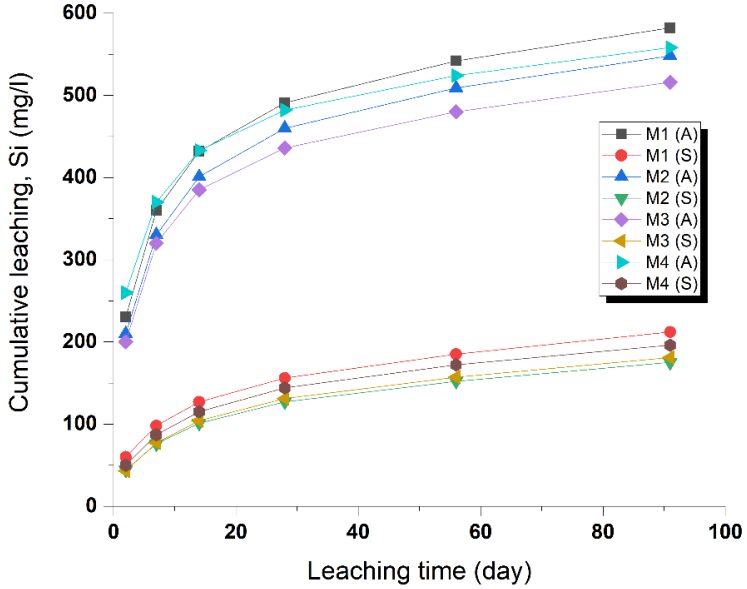

Figure 81. Cumulative leaching of silica from the samples M1-M4 (A – aerated curing conditions, S – sealed bag curing conditions)

The leached silica concentrations were consistently higher in the samples cured under aerated conditions, regardless of the types and concentrations of surfactants, with initial values ranging from 110 to 130 mg/l on day 2. Following the initial steep decrease in leached amounts (ranging from 63 to 72 mg/l) between days 7 and 14, the decline slowed, stabilising at 34 to 40 mg / l on day 91. The humid-cured samples began with initial values ranging from 32 to 38 mg/l on day 2. Similar to the dry-cured samples, the sealed bag-cured samples showed an evident reduction in leached silica between days 7 and 14, although the decrease was comparatively less pronounced. Following this initial decrease, sealed bag-cured samples maintained a relatively constant range of leached silica values, with only minor fluctuations occurring between 24 and 29 mg/l over the duration of the leaching experiment.

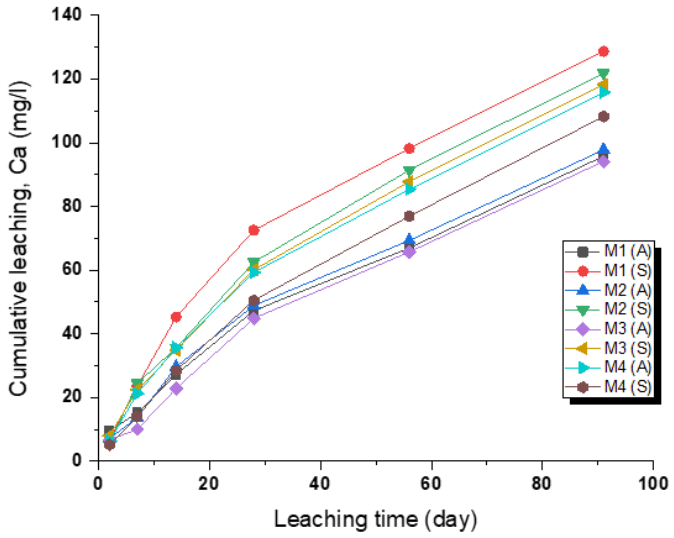

Figure 82. Cumulative leaching of calcium from the samples M1-M4 (A – aerated curing conditions, S – sealed bag curing conditions)

Throughout the experiment, calcium leaching had a consistent upward trend across all samples. The initial values, ranging from 5.2 to 9.6 mg/l on day 2, increased to a range of 28.5 to 31.3 mg/l by day 91. The impact of SDS surfactant concentration on calcium leaching was only minor, whereas higher levels correlated to a slight increased leaching. Similar tendencies were observed with Tween® 80.

Although the leached iron concentrations (Figure 83) were significantly lower in comparison to those of silica and calcium, they displayed a similar pattern, with the highest concentrations on days 2 and 7, ranging from 0.05 mg/l to 0.14 mg/l, followed by a decrease to the values below the detection limit later in the leaching experiment. This pattern remained consistent regardless of curing conditions or added surfactants.

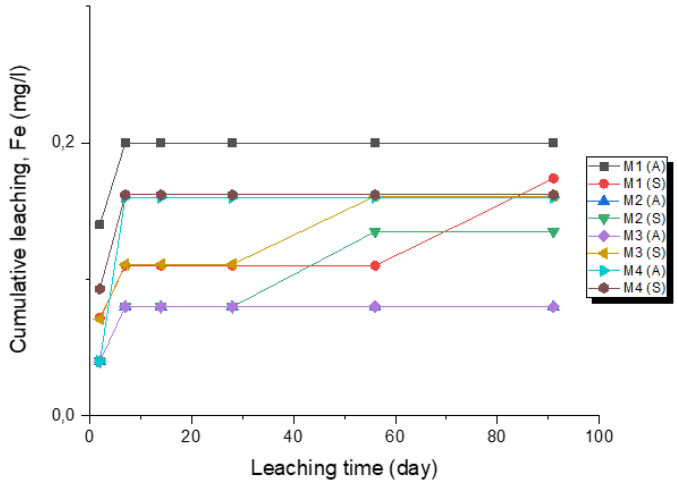

Figure 83. Cumulative leaching of iron from the samples M1-M4 (A – aerated curing conditions, S – sealed bag curing conditions)

The leachate was subjected to conductivity and pH analysis, the results of which are shown in Figure 84 and Figure 85. The conductivity values mirrored those observed in silica leaching. However, there was a greater degree of variability between samples that used different types and concentrations of surfactants. The conductivity values were consistently higher within the samples cured in the aerated conditions, from 194 to 224 µS/cm on day 2. Following a sharp decrease between days 7 and 14 to approximately half of the initial value, the values stabilised. The sealed bag cured samples displayed initial conductivity values from 141 to 164 µS/cm. There was an initial decline similar to the samples cured in aerated conditions, yet less steep followed by a slight increase. The values reached a stable range of 83 to 87 µS/cm by day 91. The differences in conductivity values between samples that used different surfactant types and concentrations of surfactants were less pronounced than with dry-cured samples. The decrease in conductivity is probably caused by the change in activity and ionic strength in the solution.

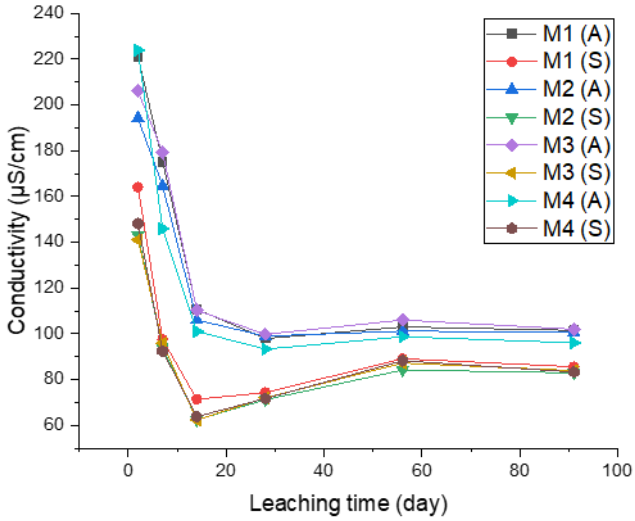

Figure 84. Electrical conductivity values during leaching

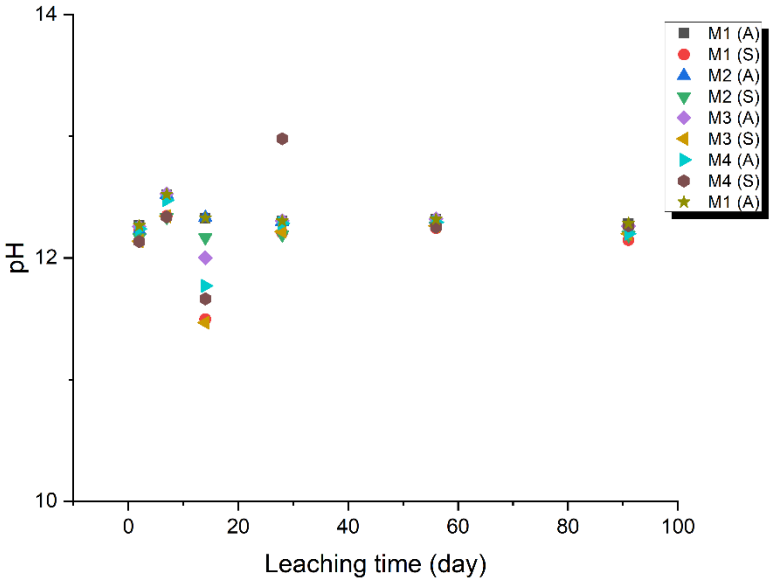

Figure 85. pH values during leaching

After completing the leaching experiments on day 91, the samples were briefly dried at laboratory temperature and analysed for compressive strength. The outcomes of this analysis have been documented in Table 42. An increased compressive strength after leaching was observed which is associated with the exposure of the samples to water (and a more advanced reaction of slag).

Table 42. Evaluation of compressive strength before and after leaching

Sample	Surfactant	Surfactant addition (wt. %)	Compressive strength before leaching (MPa)	Compressive strength after leaching (MPa)
M1 (A)	SDS	0.45	26.41	34.55
M1 (S)		0.45	29.73	29.97
M2 (A)		0.75	23.32	29.37
M2 (S)		0.75	22.30	27.56
M3 (A)	Tween® 80	0.45	17.03	31.37
M3 (S)		0.45	19.72	28.59
M4 (A)		0.75	20.42	29.75
M4 (S)		0.75	20.71	24.96

Series A - Waste loadings 10 and 20 wt. %

Table 43. The composition of samples M5-M7

	Waste (wt.%)	Waste type	Surfactant type	Surfactant (wt.%)
M5	10	Mogul oil	SDS	1.5
M6	10	Mogul oil	Tween® 80	1.5
M7	20	Mogul oil	Tween® 80	3

The cumulative leaching of oil is shown in Figure 86. Leaching of oil was observed only in the first 14 days of the leaching in all samples. No conclusive evidence emerged regarding the impact of the amount of added waste oil or curing conditions on leached oil. One sample displayed notably higher leaching of oil, which is regarded as an anomaly.

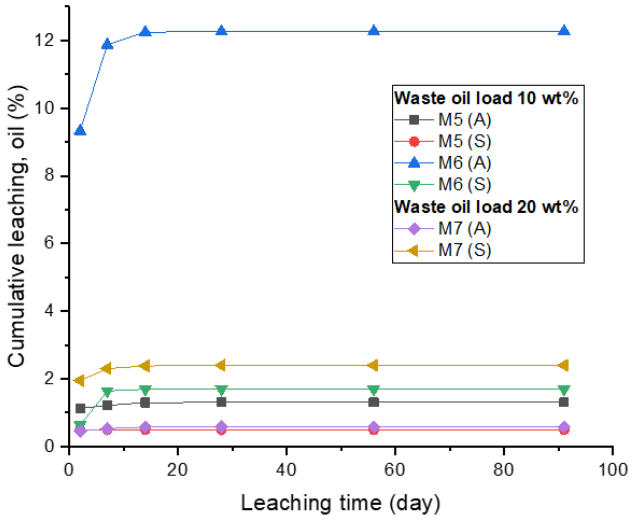

Figure 86. Cumulative oil leaching from the samples M5-M7 (A – aerated curing conditions, S – sealed bag curing conditions)

The cumulative leaching of silica and calcium is shown in Figure 87 and Figure 88.

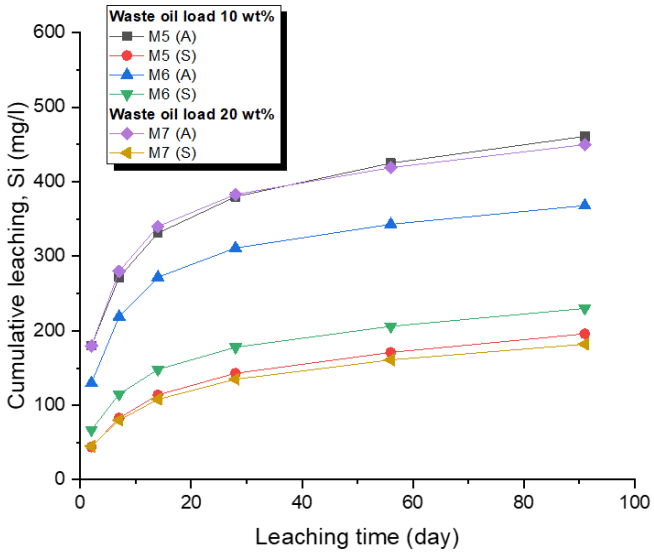

Figure 87. Cumulative leaching of silica from the samples M5-M7 (A – aerated curing conditions, S – sealed bag curing conditions)

Leached silica concentrations were, as in the previous samples, higher in the samples cured in aerated conditions with initial values ranging from 130 to 180 mg/l on day 2. The significant release of silica slowed after 14 days and then decreased to the values between 25 and 36 mg/l on day 91. The sealed bag cured samples began with initial values of 21-67 mg/l on day 2. The leaching of silica was not as significant but followed a similar pattern with the values between 25 and 44 mg/l on day 91. Higher leaching rate is probably due to microcracking generated by desiccation.

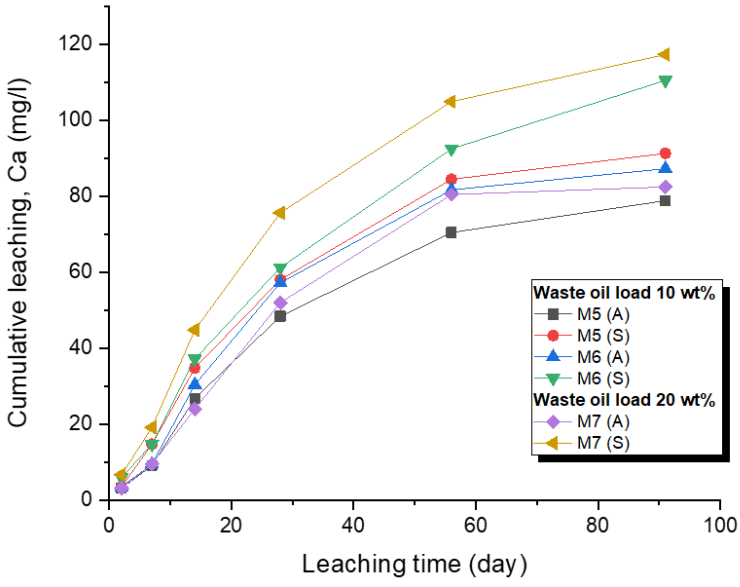

Figure 88. Cumulative leaching of calcium from samples M5-M7 (A – aerated curing conditions, S – sealed bag curing conditions)

Throughout the experiment, calcium leaching exhibited a consistent upward trend across all samples. However, the increase rate was less steep compared to samples M1-M4, and during the latter half of the leaching period, there was a noticeable slowing down in the leaching process, indicating a reduction in the amount of calcium being leached out. Samples cured in sealed bag conditions displayed higher leaching, particularly towards the end of the leaching period and varied from 3.61 – 6.81 mg/l on day one to 91-117 mg/l on day 91. The samples cured in aerated conditions started on leaching values of 3.21-3.61 mg/l on day 2 and on day 91 the values varied between 2.0 – 8.4 mg/l. The presence of iron in the leachate was detected only in one sample.

The electrical conductivity and pH of samples M5-M7 are shown in Figure 89 and Figure 90. The conductivity values were lower in the samples cured in the sealed bag condition from 153 to 178 µS/cm on day 2. Following a sharp decrease probably due to change in activity and ionic strength in the leachate as with previous samples between days 7 and 14 to approximately half of the initial value, the values stabilised. The samples cured in aerated conditions displayed initial conductivity values from 195 to 220 µS/cm on day 2 with a similar decline in values between days 7 and 14. Conductivity of samples was then stable until day 91.

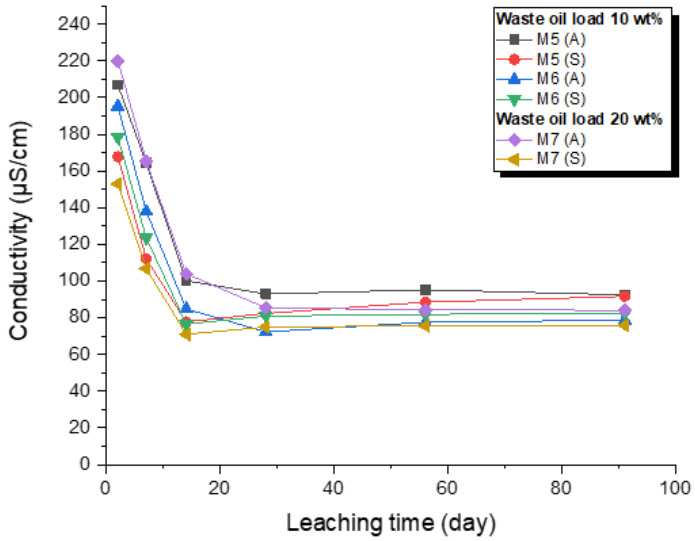

Figure 89. Electrical conductivity values during leaching

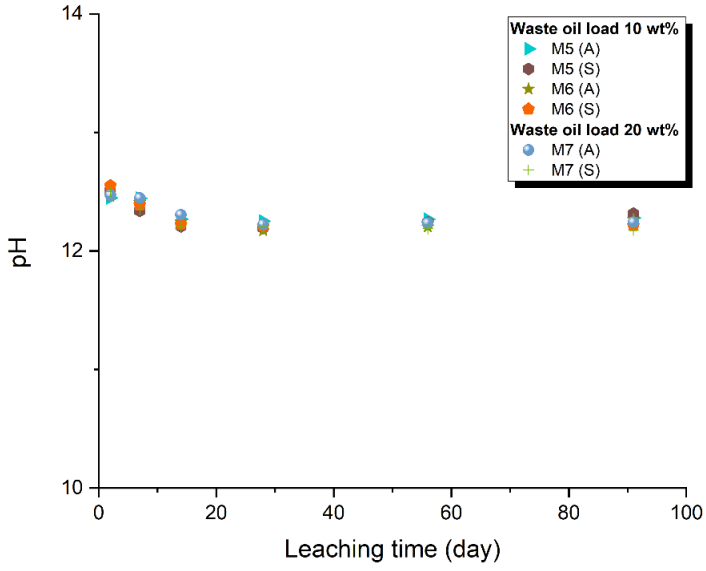

Figure 90. pH values during leaching

Series B

The samples N1-N6 and Standard from Series B cured in sealed bag condition were characterised and placed in the demineralized water for a specific duration of time (2, 7, 2, 7, 14, 28, 56 and 70 days). At these set times, the demineralized water was replaced and analyzed for concentration of the leached elements. The cumulative oil leaching is shown in Figure 91.

Table 44. Composition of samples N1-N6 and Standard

	Waste (wt.%)	Waste type	Surfactant type	Surfactant (wt.%)
N1	5	Total Nevastane EP l00	Tween® 80	0.75
N2	10			1.5
N3	15			2.25
N4	20			3
N5	25			3.75
N6	30			4.5
Standard	-	-	-	-

The cumulative leaching of oil from samples N1-N6 during leaching is shown in Figure 91. The higher quantity of oil was leached out during the initial 14 days. This trend was particularly evident in samples containing more than 10 wt.% waste loads, where the leaching rate was more pronounced. After the initial two weeks the leaching of oil slowed down. For waste loads exceeding 10 wt. %, the cumulative oil leaching ranged between 2.59 % and 3.23 % of the total oil content, whereas for lower waste load (5 and 10 wt. %), the cumulative oil leaching ranged between 0.59% and 0.97%, respectively.

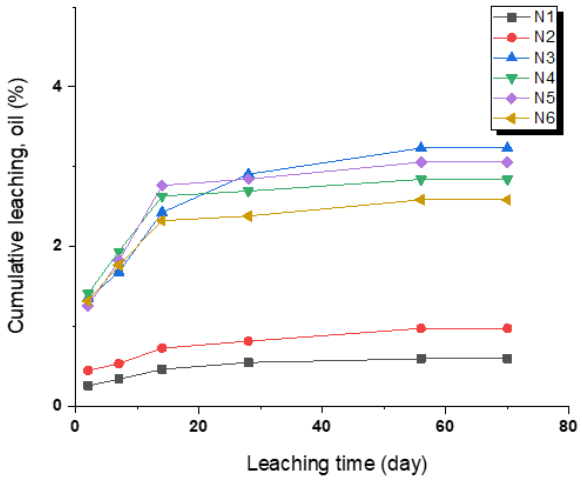

Figure 91. Cumulative leaching of oil from the samples N1-N6

Cumulative leaching of silica and calcium is shown in Figure 92 and Figure 93. As the iron leaching analysis performed in the Series A samples showed very small release of iron, it was not performed with Series B samples.

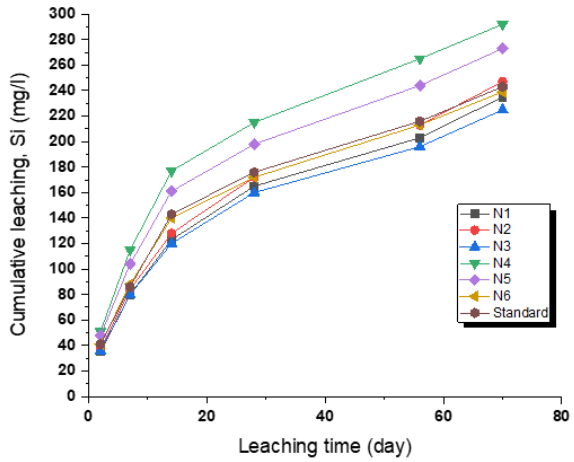

Figure 92. Cumulative leaching of silica from the samples N1-N6 and Standard

The leaching of silica, similarly to the previous samples, was faster within first 14 days of experiment and then moderately slowed down. The cumulative values of leached silica were from 225 to 292 mg/l on day 91.

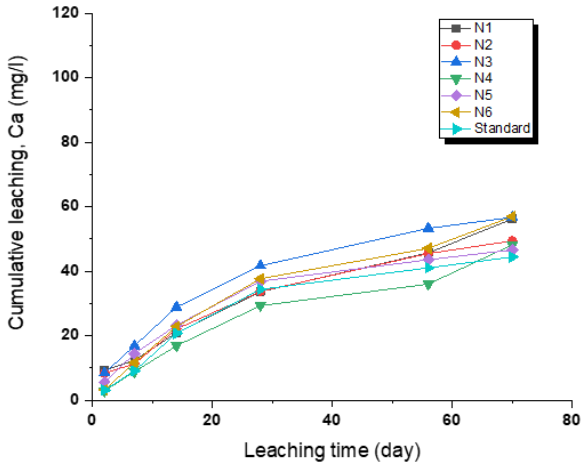

Figure 93. Cumulative leaching of calcium from the samples N1-N6 and Standard

As for calcium, a noticeable decrease in the amount of leached was observed during the latter part of the leaching period. The cumulative leached calcium amount varied between 44.4 – 56.99 mg/l on day 91. The effect of the oil present and its amount on the leaching of calcium and silica into the solution was not observed.

The electrical conductivity and pH are shown in Figure 94 and Figure 95. The conductivity values decreased probably due to change in activity and ionic strength of the solution over the course of the leaching period from values 6.17 – 7.36 mS/cm on day 2 to 1.76-2.73 mS/cm on day 91.

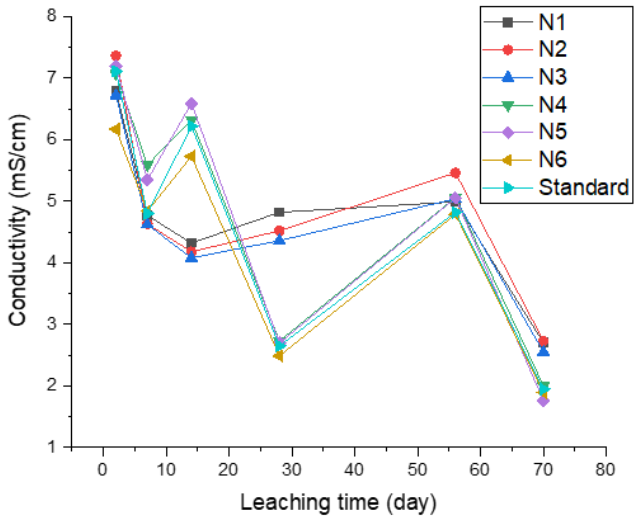

Figure 94. Electric conductivity values during leaching

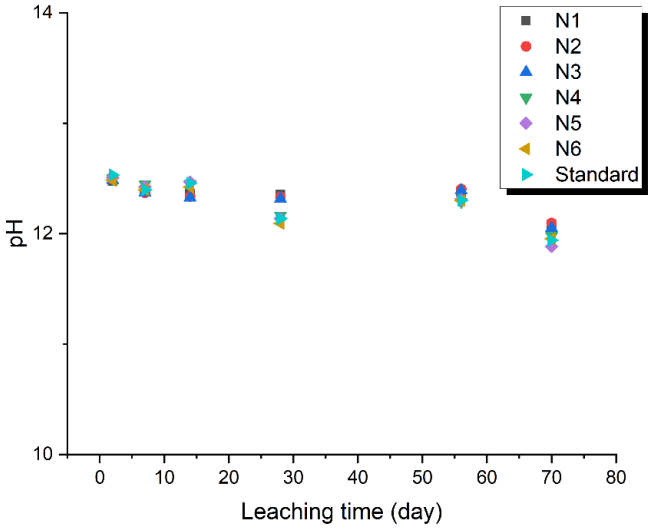

Figure 95. pH values during leaching

After the leaching period ended, the samples were weighted and measured for compressive strength. The results with comparison with the values before leaching are shown in Table 45. We observed a slight increase in compressive strength in the samples with oil after leaching. This is same as in the previous case associated with immersion in water.

Table 45. Compressive strength evaluation before and after leaching

Sample	Compressive strength before leaching (MPa)	Compressive strength after leaching (MPa)
N1	19.29	23.43
N2	8.63	10.20
N3	3.52	4.55
N4	2.15	2.83
N5	0.93	1.69
N6	1.27	1.25
Standard	34.30	30.56

The samples after leaching were also measured for porosity using the AutoPore IV 9500 mercury porosimeter. Pores measuring 1 and 0.001 µm in size were predominant within the sample matrix and are similar to those before leaching. The porosity analysis is shown in Figure 96.

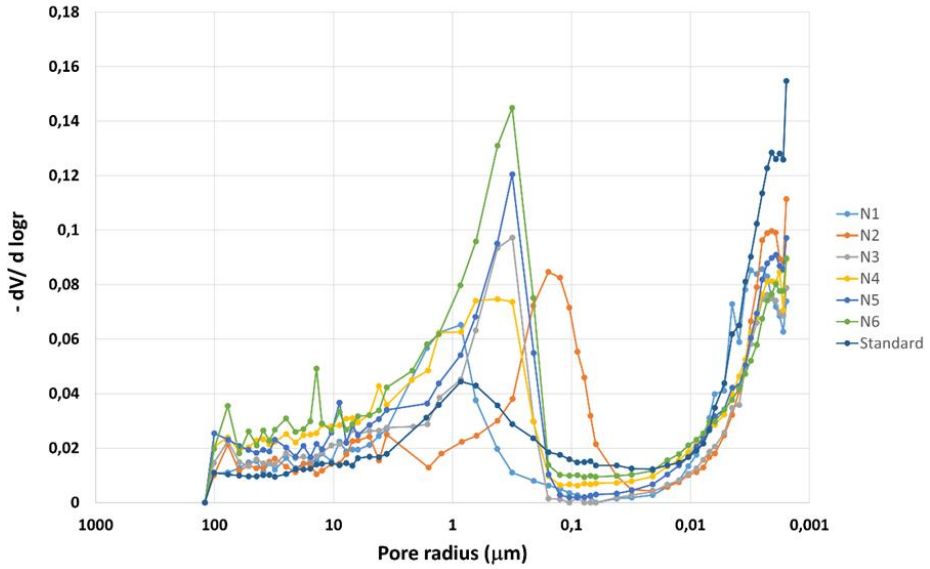

Figure 96. Porosity of samples N1-N6 and Standard after leaching

Table 46. Composition of samples N7-N9

	Waste (wt.%)	Waste type	Surfactant type	Surfactant (wt.%)
N7	5	Total Nevastane EP l00	Tween® 80	1.5
N8	10			
N9	15			

The cumulative leaching of oil from samples N7-N9 during leaching is shown in Figure 97. In all samples the cumulative oil leaching at the end of the leaching period was less than 2 %.

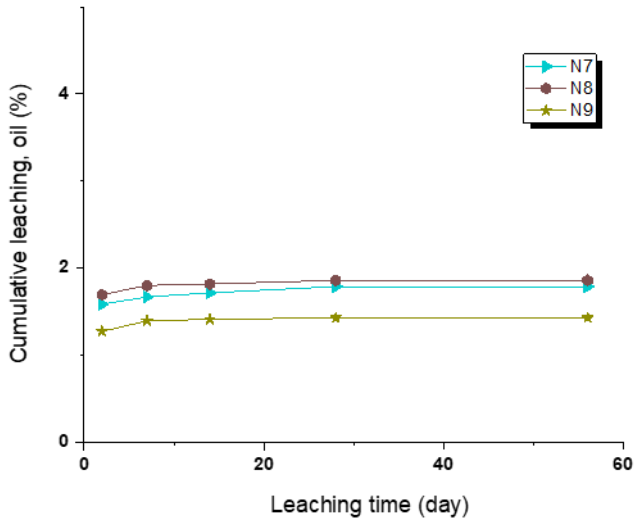

Figure 97. Cumulative leaching of oil from samples N7-N9

Cumulative leaching of silica and calcium is shown in Figure 98 and Figure 99. The cumulative values of leached silica ranged from 177 to 178 mg/l on day 91. As for calcium, the leached amount varied between 29.5 – 33.8 mg/l on day 91.

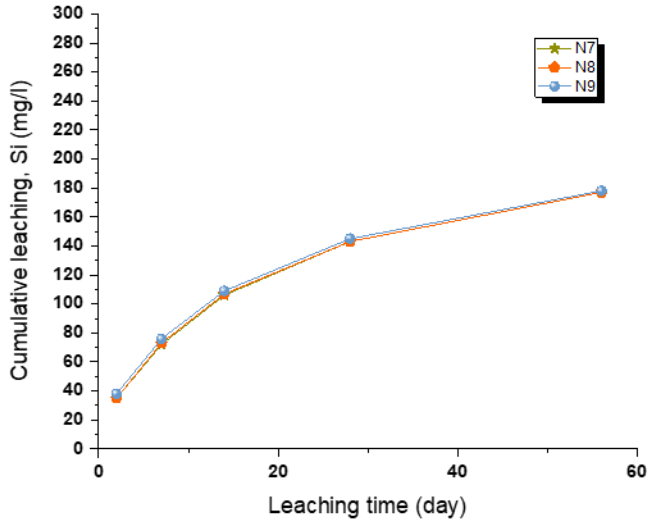

Figure 98. Cumulative leaching of silica from samples N7-N9

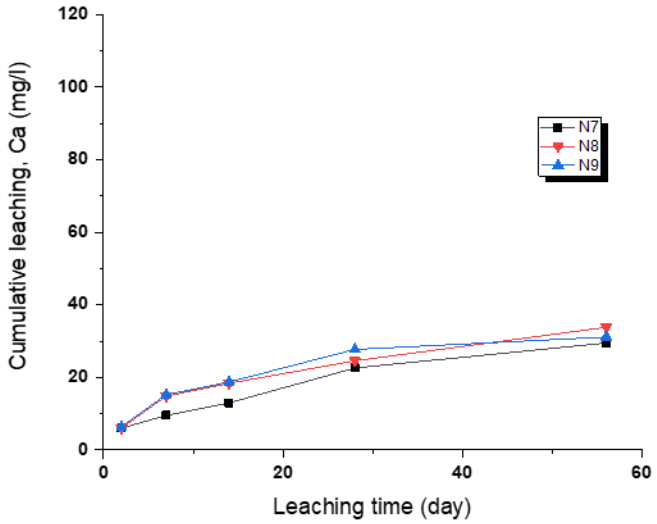

Figure 99. Cumulative leaching of calcium from samples N7-N9

The electrical conductivity and pH are shown in Figure 100 and Figure 101. The conductivity values decreased over the course of the leaching period from values 5.3 – 5.7 mS/cm on day 2 to 2.7-2.9 mS/cm on day 91. As for the previous samples, no significant change in pH was observed. This pH buffering could be caused by multiple factors. Silicate species released from the metakaolin matrix undergo hydrolysis reactions to weak acids and bases and act as buffers. Additionally, hydroxide ions from the residual alkaline activator contribute to high pH.

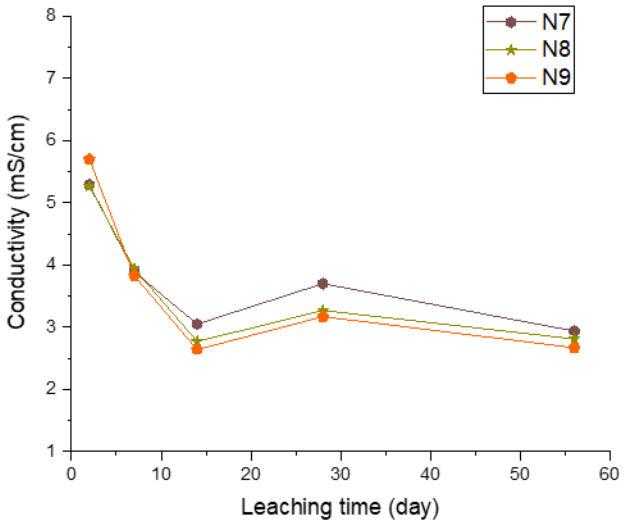

Figure 100. Electrical conductivity values during leaching

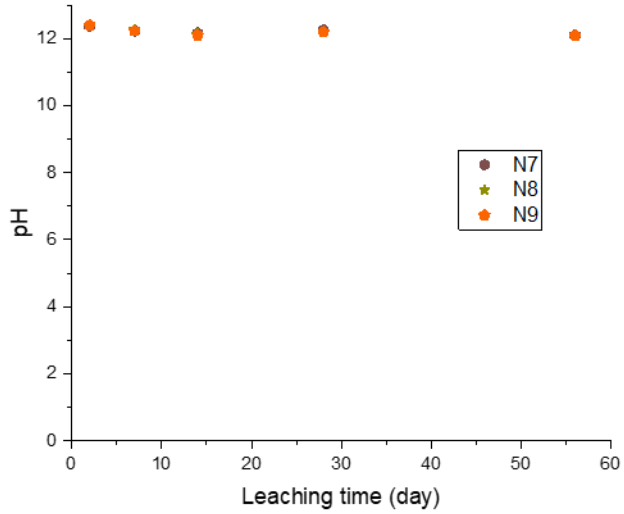

Figure 101. pH values during leaching

After the leaching period ended, the samples were weighed and measured for compressive strength. The results with comparison with the values before leaching are shown in Table 47. We observed a slight increase in compressive strength in the samples with oil after leaching.

Table 47. Evaluation of compressive strength before and after leaching

Sample	Compressive strength before leaching (MPa)	Compressive strength after leaching (MPa)
N7	2.82	3.12
N8	1.89	2.14
N9	0.95	1.03

The samples after leaching were also measured for porosity using the AutoPore IV 9500 mercury porosimeter. Pores measuring 1 and 0.001 µm in size were predominant within the sample matrix and are similar to those before leaching. The porosity analysis is shown in Figure 102.

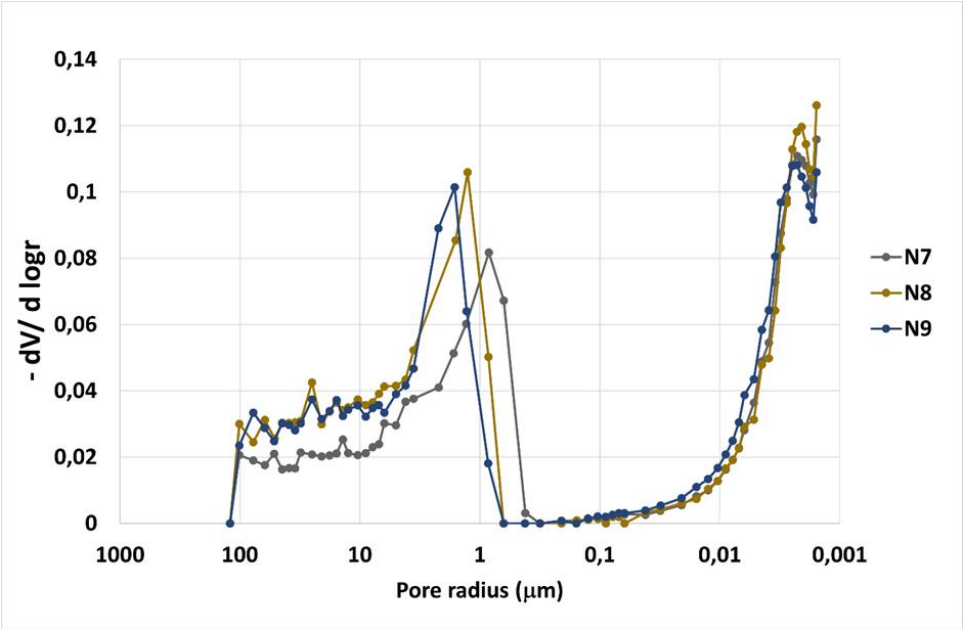

Figure 102. Porosity of samples N7-N9

4.3.3 Mix formulation

Samples in the SIIEG were used to carry out short- and middle-term leaching tests, following the reference protocol described in Milestone 35 (Experimental protocols for conditioning materials performances assessment). The leaching tests were performed on samples aged 287 days at room temperature in atmospheric conditions; the characteristics of the samples are shown in Table 48. Tests were conducted with use of the glovebox and N_2-purging of the headspace of the containers.

Table 48. Geopolymer matrix tests

Sample, №	Height, cm	Diameter, cm	Surface area, cm^2	Sample weight before leaching, g	Sample weight after leaching, g
3					
4	0.8	1.68	8.65	2.87	2.98
8	1.04	1.68	9.92	3.05	3.29
11	0.71	1.68	8.18	2.37	2.47
3S	0.975	1.68	9.57	4.02	4.38
4S	1.04	1.68	9.92	3.86	4.11
8S	0.815	1.68	8.18	3.15	3.33
11S	1.12	1.68	10.33	3.64	3.92

The surface of the sample has been cleaned of small particles or dust. The polypropylene containers have been used for leaching, and the samples were suspended in containers filled with solutions, Figure 103 and Figure 104. The quantity of solutions was 10 times the specimen's surface area. After certain intervals of time, as specified in the protocol, the specimens were withdrawn from the containers and immediately transferred to the next leaching container filled with fresh leachate. The used leaching containers containing all leached material have been closed and transmitted for analysis. Analytical data obtained for the leaching of the surrogate are based on ICP-MS results. The leachate was the solution with pH = 12.7 (NaOH/KOH/Na_2SO_4/$CaCl_2$) at 20°C, periodically renewed according to the protocol, for three months duration. The leachates have been tested for pH. The ICP-MS analyses have been performed to determine constituents Ca, Si, and Al.

Figure 103.Samples during leaching experiments

Figure 104.Leaching vials, 100 mL with sample

The measurements were conducted using a high-resolution mass spectrometer with inductively coupled plasma (HR ICP-MS Thermo Element 2) in the Laboratory of Trace Element and Isotope Analysis. External calibration has been executed using solutions with concentrations of 1, 5, 10, 50, 100, 200, 500, 1000, and 1500 mg/L. These solutions were prepared from the standard solution Inorganic Ventures IV-ICPMS-71A and Inorganic Ventures IV-ICPMS-71B. To mitigate matrix effects (signal variations due to changes in spray formation, ionisation, ion transport, etc.), Indium was used as an internal standard. 10 mg/L of indium was added to all solutions (wash, blank, calibration, and analysed), Inorganic Ventures INDIUM. Analytical reliability was ensured by measuring the standard ICP multi-element standard solution I Certipur® The instrument software calculated the relative standard deviation, Figure 105.

Figure 105.The measurements of leachate solutions

Leaching of geopolymer samples pH = 12.7 ($NaOH/KOH/Na_2SO_4/CaCl_2$)

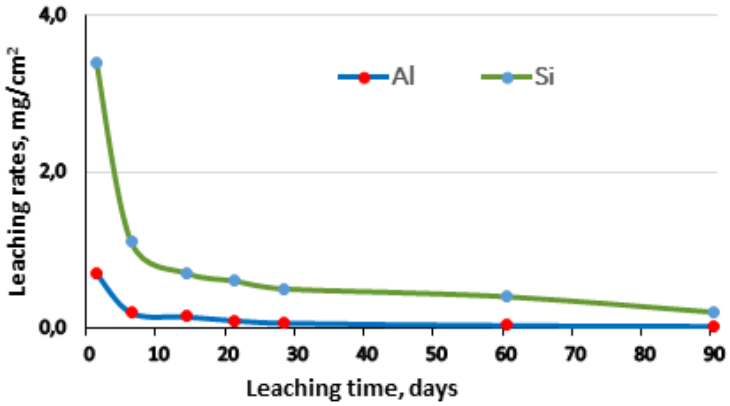

Figure 106. Leaching rate for sample of MIX formulation without organic oils for reference

During leaching, a small amount of oil was washed out from the samples, but it was impossible to analyse it because it settled in a thin rim on the walls of the glasses.

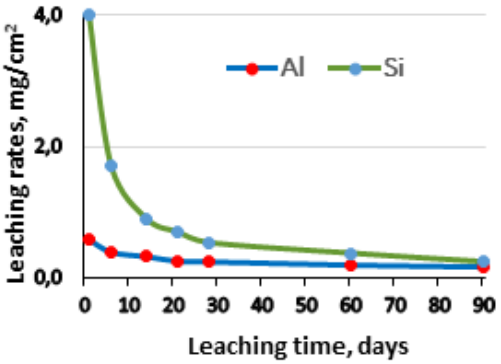

Figure 107. Leaching rate for sample of MIX formulation with 40 % oil Nevastane

With or without oil, the leaching rate evolution of Al and Si seems very close meaning that there is no evolution of the leaching resistance due to oil encapsulation by the MIX formulation.

TGA study

TGA analyses were performed to study geopolymer matrix with 10 % oil Nevastane. A comparison analysis of sample before and after leaching is presented in Figure 108.

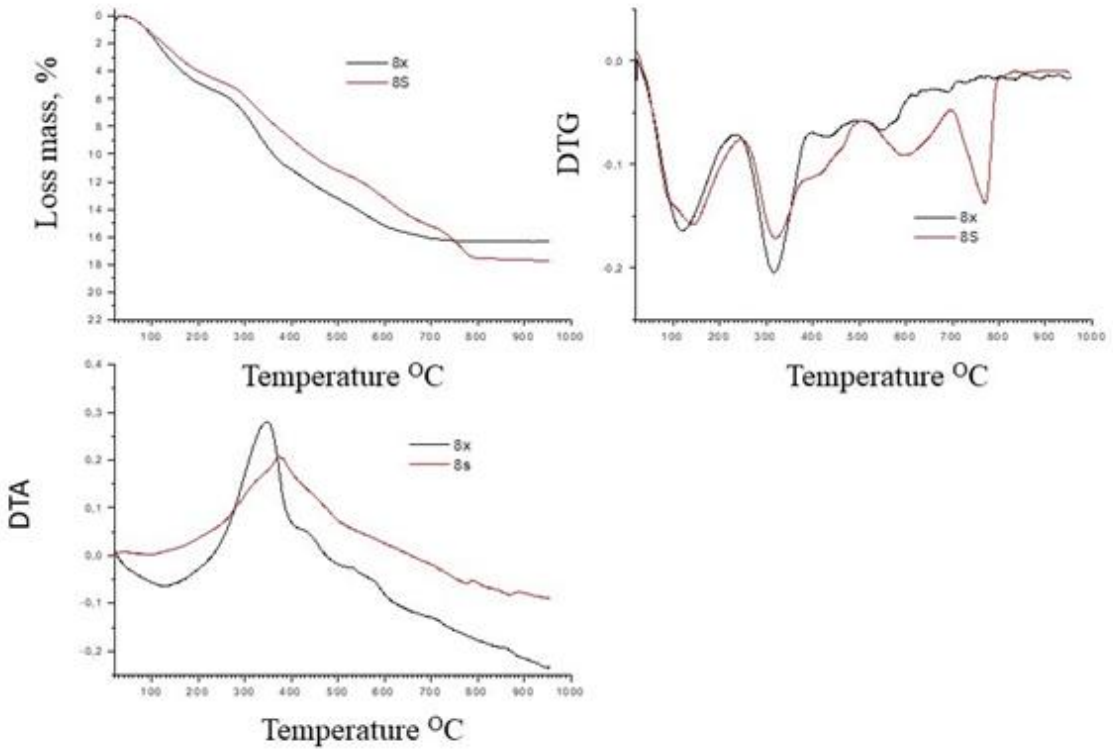

Figure 108. Geopolymer samples #8 with 10 % oil Nevastane before (8X) and after (8S) leaching

A comparison of the thermal analysis results of sample before (8X) and after leaching (8S) shows that the general appearance of the DTA, TG and DTG curves is preserved; only some details change, Figure 108. The DTA curve shows a decrease in the intensity of the exothermic effect and its shift towards higher temperatures, which is associated with the loss of a certain amount of oil in the surface layers of the sample. The TG curve also shifts towards lower temperatures. The weight loss in the range of 100°C - 200°C can be explained by the loss of water from the sample's pores, while the weight loss rate of the sample after leaching is close to that of the original sample.

Already at a temperature of 250°C, an exothermic effect begins, apparently associated with oil destruction, which is accompanied by mass loss with a maximum mass loss rate of about 350°C and an additional effect at 400°C. Further, a small effect of mass loss at 600°C appears on the DTG curve, and then a rather narrow effect of mass loss, practically not accompanied by a significant thermal effect. This effect is absent on the curve of the original sample. The nature of this effect is subject to further study.

SEM characterization

The morphology of produced geopolymer specimens was investigated after 90 days of leaching in the solution with pH = 12.7 ($NaOH/KOH/Na_2SO_4/CaCl_2$) in the air using scanning electron microscopy (SEM). Test samples were with a typical flat surface and coated with a gold layer to ensure electron conductivity. The ambient-cured sample presented some microcracks on the order of 1-3 μm in the geopolymer matrix due to the aging and drying effects.

When high humidity condensation occurs on the GP matrix, it will buffer the pH of the water film to high values. Under high pH conditions, the main dissolved CO_2 species are carbonates (CO_3^{2-}). Materials such as blast furnace slag and fly ash may enhance carbonation. After accelerated carbonation, a characterization of degraded mix-based geopolymer shows that carbonation is promoted by partial GP drying, which also induces material shrinkage with cracking, Figure 109.

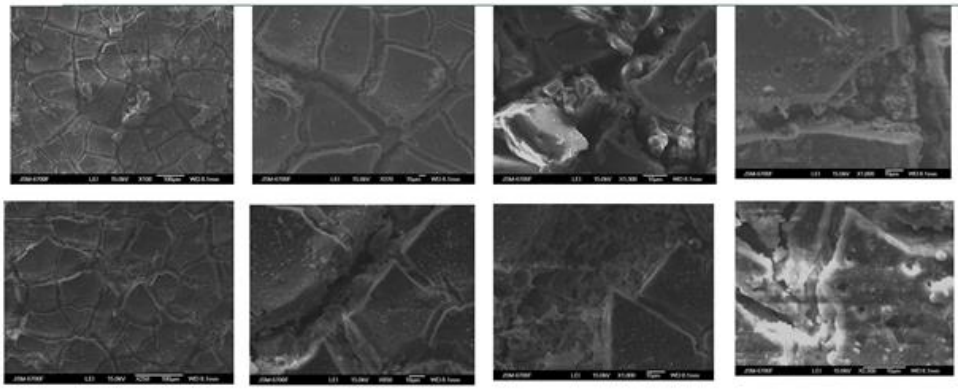

Figure 109. SEM micrographs of sample #11 formulation with 40% vol. of Nevastane oil after leaching

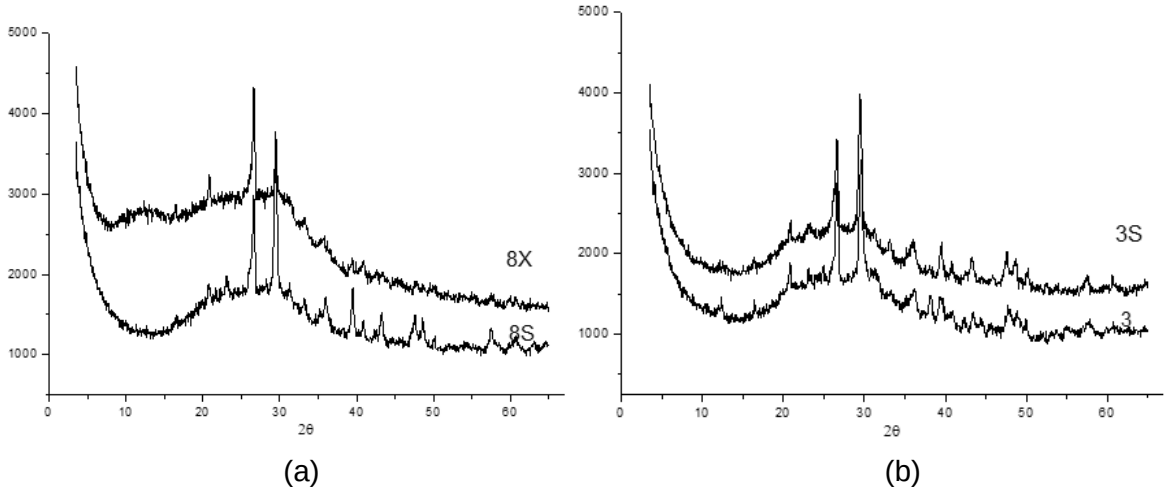

(a) (b)

Figure 110. XRD of geopolymer matrices: (a) With oil Nevastane - 10% vol. 8X before leaching and 8S after (b) without Oil 3 before leaching and 3S after

On can remark that XRD patterns before or after leaching are consistent and that the presence of Oil does not modify the capacity of the MIX based formulation for encapsulating radioactive liquid organic wastes.

4.4 Partial conclusion about durability testing

Analysis of the durability of matrices containing liquid organic waste was carried out under various ageing conditions. Firstly, analysis under aerated conditions showed that formulations based on metakaolin and blast furnace slag tend to react with environmental CO_2, generating progressive carbonation of the samples. It should be noted, however, that this carbonation does not have a deleterious effect on the compressive strength of the materials, and that the presence of oil tends to reduce the rate of carbonation through a plugging effect on porosity.

The leaching test campaigns carried out on the three formulations show the progressive leaching of the specimens. Indeed, whether analysing the leaching solutions by pH measurement or ICP, all the partners concluded that the chemical species present in the leaching solution were evolving, particularly potassium and silicon for the MK-based formulation, and calcium and silicon for the blast furnace slag-based formulation. The lower the pH of the solution, the more rapid the evolution. However, the impact of leaching on compressive strength remains very moderate (in some case, a slight increase of the compressive strength is observed), XRD analysis (on the MIX formulation in particular) shows no change in crystallographic structure, and gas permeability measurements, which are highly sensitive to changes in pore microstructure, show no major changes (on the MK formulation).

It should be noted, however, that several partners have also succeeded in measuring the release of liquid organic waste. The measurements indicate a release of some percent of the initial volume during the first few days, followed by stabilization.

5 STUDY of CONDITIONING MATRIX MATERIALS BEHAVIOUR UNDER IRRADIATION

5.1 Protocol

Gamma irradiations (^{137}Cs) were performed at Arronax facility (Nantes, France). Dose rate was estimated around 400±80 Gy/h using Fricke dosimetry. Samples were irradiated between 6 days and 2 months to achieve total doses up to 500 kGy. The samples were placed in 22 mL sealed cylindrical PEEK cells (Figure 111). A glass tube with valve mounted on the cell enables connection for the gas measurement by micro-Gas Chromatography (μGC). After sealing, the cells were filled with Argon.

Figure 111. PEEK cell (left) and the Cs-137 gamma irradiator (right).

Each cell contains four samples of the same GP batch spaced by a PEEK sample holder to avoid contact between the surfaces while ensuring gas movement, as shown in Figure 112.

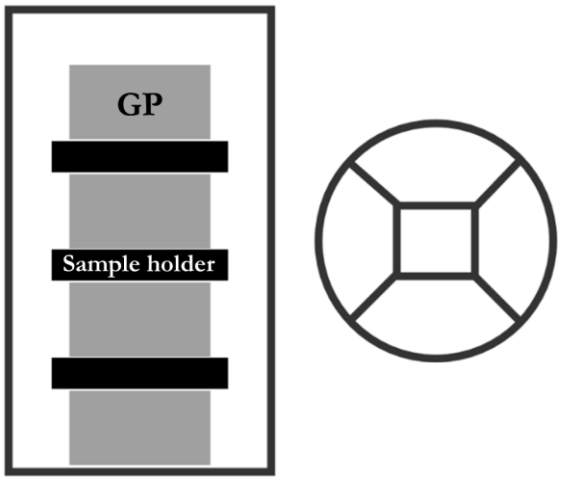

Figure 112. Representation of the set-up inside the irradiation cell and sample holder

Test method

All methods used during the study are presented below. Some methods are used specifically on certain samples, as will be outlined in the results sections.

Gas release

μGC (Agilent Technologie 490) was used to analyze the gaseous atmosphere in the cell. The H_2 channel consists of a heated injector, a 4m 5A molesieve column, using Argon as vector gas, and a TCD detector. H_2 was quantified using standards. A temperature treatment was also used to evaluate the quantity of H_2 trapped in the closed porosity. In this case, the cell removed from the irradiator was immediately placed in an oven at 70°C for 2 hours.
The gas quantification was made considering the percentage of gas (in $\%_{vol}$) determined by μGC, the gas pressure (P) after irradiation and the free volume V_{free} in the cells:

$$n(gas) = \frac{P \cdot \%_{vol} \cdot V_{free}}{R \cdot T} \quad (1)$$

where R is the gas constant and T the sample temperature.

Radiolysis results are expressed as radiolysis gas yields (G, in mol/J):

$$G(gas)_{material} = \frac{n(gas)}{D \cdot m} \quad (2)$$

where n stands for the measured amount of gas (in mole), D the absorbed dose of gamma radiation in the sample (in Gray) and m the mass of irradiated sample (in kg).

Samples containing surrogate waste were not analyzed by μGC to avoid column contamination by oil degradation product. However, a measurement of the pressure due to gas degradation product inside the cell was performed.

Leaching

Leaching tests were performed according to the ANSI ANS 16.1 procedure. The leaching tests were performed in closed vessels under semi static conditions. The leaching solution, ultrapure water, was renewed at time intervals defined by the standard protocol for a total of 4 weeks of testing, and analyzed to monitor changes in matrix elements release. Si concentration in the leachant was determined by Single Quadrupole Inductively Coupled Plasma-Mass Spectrometry (ICP XSERIES 2, ThermoFisher Scientific) after filtration with 0.45 µm pore size PTFE filter. Matrix effects were minimized by diluting the samples using a dilution factor ranging from 20 to 200 in 2% bi-distilled HNO_3 (v/v) and corrected from the use of internal standards (In). Quantification of elements concentrations was based upon calibration curves prepared from single element standard solutions (SCP Science, Canada).

The leaching behaviour can be approximated as that of a semi-infinite medium when the fraction leached is less than 20%. An effective diffusion coefficient under these circumstances can be calculated using the mass transport equation (Fick's second law), as follows:

$$D_e = \pi \left[\frac{a_n/A_0}{\Delta t_n}\right]^2 \left[\frac{V}{S}\right]^2 T \qquad (3)$$

Where D_e is the effective diffusion coefficient (cm^2/s), Δt_n is the duration of the *n*-th leaching intervals (s), V is the volume of the specimen (cm^3), S is the geometric surface area of the specimen (cm^2), and T is the leaching time representing the "mean time" of the *n*-th leaching interval.

The Leachability Index (LI) was calculated according to the standard protocol, as follows:

$$LI = \frac{1}{n}\sum_{n}^{1} \log\left(\frac{\beta}{D_e}\right)_n \qquad (4)$$

Where β is a defined constant (1.0 cm^2/s) and n is the number of leaching intervals. A material with an acceptable leaching resistance has a LI greater than 6, according to the Italian Inspectorate that is one of the strictest in Europe.

Micro-computed tomography

μCT (Easy Tom XL/RX Solution) was used to investigate the morphology of GP by a non-destructive technique. The X-ray source is tungsten (energy: 20-150 kV, intensity: 0-500 μA). The detector is a CCD camera with a resolution of 1516x1920 pixels. The sample is fixed between the source and the detector on a rotating plate. The spatial definition is in the micrometer range (4-150 μm). The 3D reconstruction was post-processed with the Xact software and the dynamic views were produced using Dragonfly 2020.2.

5.2 MK, BFS and MIX formulation behaviour under irradiation (no oil)

In this section, all the results of the analyses performed on the different GP formulations are presented. Where possible and useful, a comparison with data available in the literature is also presented.

Visual inspection of the samples after irradiation never revealed any cracks nor deformations.

Gas release

In Figure 113, the production of H_2 of each GP is reported as a function of the total absorbed dose. Considering that the production is proportional, it is possible to determine radiolytic yields as the curve's slope, the values are reported in Table 49. At IMT, lacking TGA instrumentation, it was not possible to quantify the water content of the samples after shipping, storage and irradiation. Consequently, the actual normalized G(H_2) with respect to the mass of water could not be assessed. However, Table 50 shows the normalised G(H_2) as if nothing had evaporated, this value increasing by approximately 10% for each percentage point of water loss through evaporation.

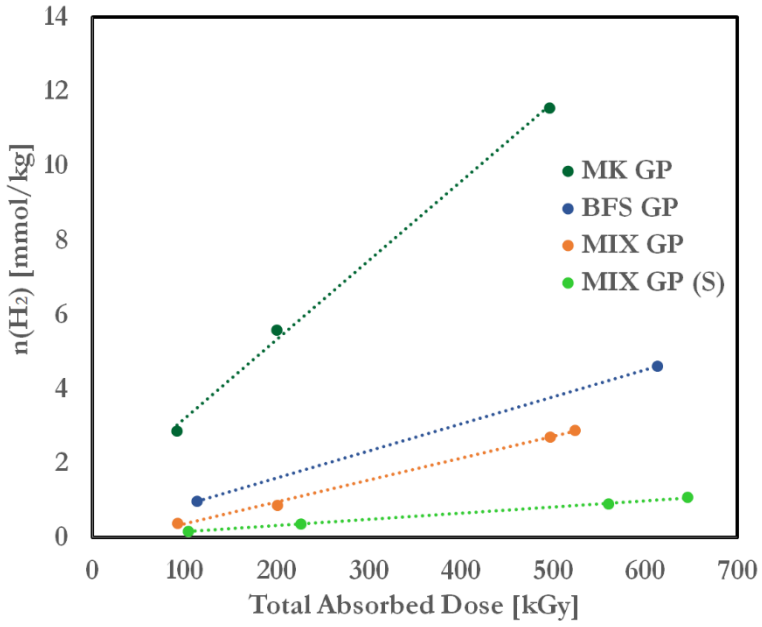

Figure 113. Production of H_2 as a function of the total absorbed dose.

Table 49. H_2 radiolytic yields of the different GPs.

Sample	Water content (w%)	G(H_2) (material) [x10^{-7} mol/J]	G(H_2) (normalized) [x10^{-7} mol/J]
MK GP	17%	(0.23 ± 0.01)	(1.34 ± 0.01)
BFS GP	17.7%	(0.07 ± 0.01)	(0.42 ± 0.01)
MIX GP	9.8%	(0.06 ± 0.01)	(0.57 ± 0.01)
MIX GP (S)	9.8%	(0.02 ± 0.01)	(0.17 ± 0.01)

Between the GPs, the MK based is the highest in H_2 production, while the MIX based with surfactant is the lowest one. All samples except MIX GP (S) have a higher normalized G(H_2) than free water (0.44×10^{-7} mol/J), BFS GP was considered also higher due to the possible error on water content. These high values are probably due to an additional H_2 production phenomenon. Indeed, G(H_2) depends not only on the water content but also on the composition and porosity of the GP samples. Indeed, a confinement effect promoting the recombination of H radicals into H_2 can also occur. The lowest value of MIX GP (S) can be related to some recombination reaction due to the addition of the surfactant[3]. Therefore, considering the huge difference between the GPs studied, further analysis is required.

[3] I. M. El-Bagory, "Protective effect of scavengers and surfactants on gamma irradiated cortisone acetate aqueous solutions," *Journal of Drug Delivery Science and Technology*, vol. 17, no. 6, pp. 437–442, 2007, doi: 10.1016/S1773-2247(07)50085-7.

Comparing those results with the one in literature for other geopolymer formulations, the radiolytic yield are on the same order of magnitude (Table 50).

Table 50. H_2 production of geopolymer in literature

Type of cement		Water [w%]	G(H_2) (material) [x10^{-7} mol/J]	G(H_2) (normalized) [x10^{-7} mol/J]	References
4 SiO_2, 1 Al_2O_3, 1 M_2O, 12 H_2O	*M* = Na	33%	0.13	0.4	Chupin[4]
	M = K	33.9%	0.25	0.75	
	M = Cs	26.8%	0.48	1.8	
Al_2O_3, 3.6 SiO_2, Na_2O *X* H_2O	*X* = 11	33.5%	0.09		Lambertin[5]
	X = 13	35.9%	0.11		

A study on the amount of H_2 remaining trapped within the porosity was also performed, increasing the temperature up to 70°C before the measurement with the μGC (Figure 114). The MIX GP (S) shows an increase of 100% in H_2 release when the temperature treatment is applied. However, H_2 release remains low with respect to the MK GP considered as reference for this test due to its open porosity structure.

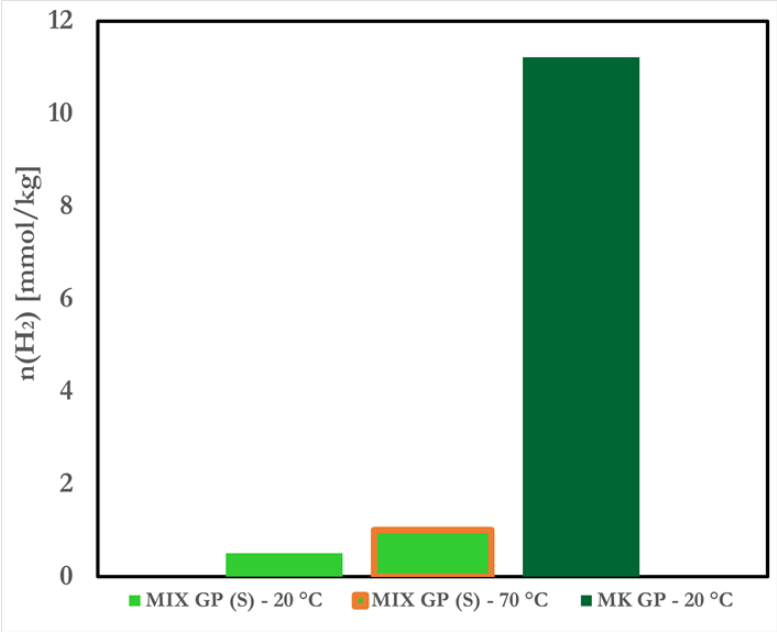

Figure 114: H_2 production measured with and without thermal treatment.

It was not possible to perform the same test on the other GPs due to time constraints, but considering the same increment, hence double the value of no thermal treatment, the new G(H_2) was estimated and reported in Table 51.

[4] Frederic Chupin. Caractérisation de l'effet des irradiations sur les géopolymères. Polymères. Université Pierre et Marie Curie - Paris VI, 2015.

[5] D. Lambertin, C. Boher, A. Dannoux-Papin, K. Galliez, A. Rooses, and F. Frizon, "Influence of gamma ray irradiation on metakaolin based sodium geopolymer," *Journal of Nuclear Materials*, vol. 443, no. 1–3, pp. 311–315, Nov. 2013, doi: 10.1016/j.jnucmat.2013.06.044

Table 51. H_2 radiolytic yields of the different GPs considering the estimated effects of a thermal treatment.

Sample	G(H_2) (material) [x10^{-7} mol/J]
BFS GP	(0.15 ± 0.01)
MIX GP	(0.11 ± 0.01)
MIX GP (S)	(0.03 ± 0.01)

Leaching

MK GP, MIX GP and MIX GP (S) were subjected to the ANSI/ANS 16.1 leaching test as presented in the methods section. The cumulative fractions of Si leached normalized by the Si content in the matrix are presented in Figure 115, Figure 116 and Figure 117.

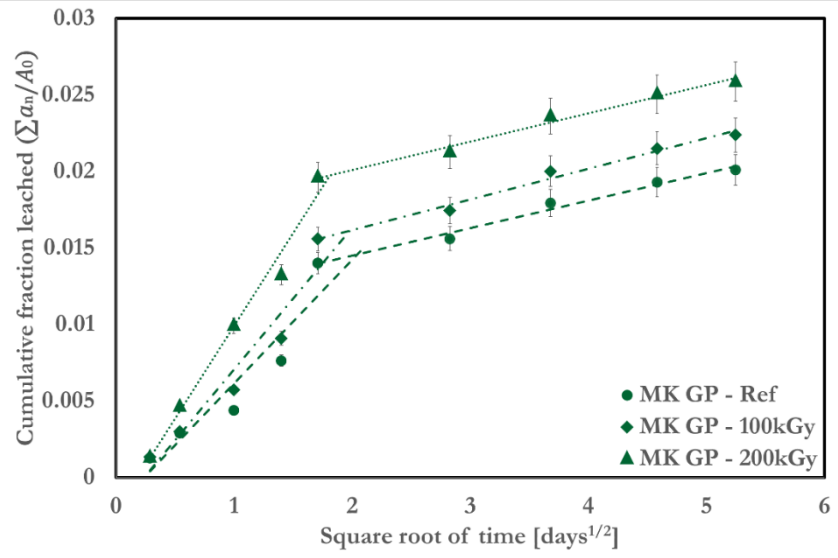

Figure 115: Cumulative leached fraction of Si from MK GP

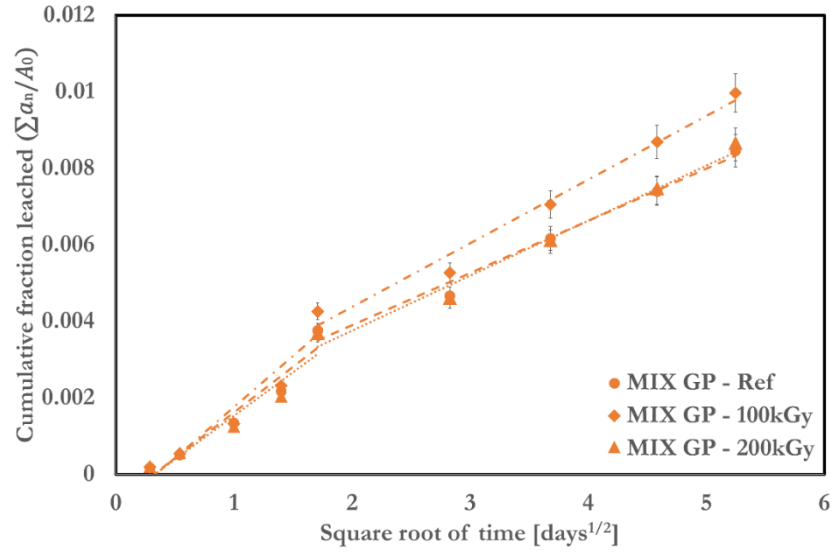

Figure 116: Cumulative leached fraction of Si from MIX GP.

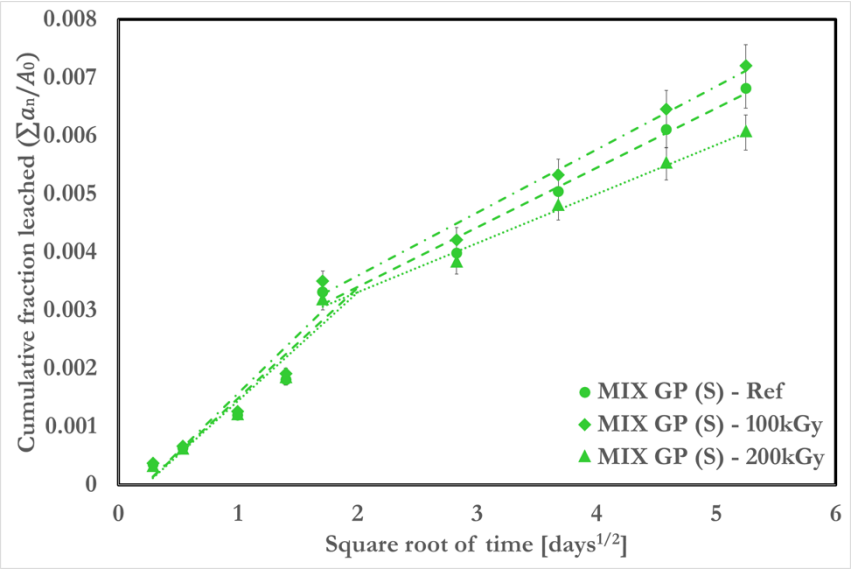

Figure 117: Cumulative leached fraction of Si from MIX GP (S).

The total fraction leached from MK GP samples were greater than MIX GP both with and without surfactant. An average of 6.3% of Si was released from MK GP samples, while 1.4 and 1.0% was released from MIX GP and MIX GP (S) samples, respectively. The cumulative Si release of MK GP is in agreement with a previous work on metakaolin based geopolymer[6].

Looking at the curves, the cumulative fraction leached cannot be represented as linear dependent with $t^{1/2}$. However, a linear dependency was observed for the initial sampling points (t < 3 days) as well as for the latter (t > 3 days), suggesting that two diffusion-controlled processes contribute to the overall leaching. The average diffusion coefficient (D_a) and leachability index for the two domains are presented in Table 52.

Table 52. Diffusion coefficients and leachability indices for Si as calculated from leaching data.

Sample	Average D_a [cm^2/s] (x10^{-12})		Leachability Index	
	1st domain	2nd domain	1st domain	2nd domain
MK GP – Ref	54.6	1.6	10.6 (0.6)	11.9 (0.3)
MK GP – 100 kGy	68.3	5.9	10.4 (0.5)	11.6 (0.7)
MK GP – 200 kGy	150.5	4.8	10.1 (0.6)	11.7 (0.7)
MIX GP – Ref	4.8	1.8	11.7 (0.8)	11.9 (0.4)
MIX GP – 100 kGy	5.6	2.4	11.6 (0.7)	11.7 (0.3)
MIX GP – 200 kGy	4.1	1.9	11.7 (0.7)	11.8 (0.3)
MIX GP (S) – Ref	3.2	1.0	11.7 (0.5)	12.1 (0.4)
MIX GP (S) – 100 kGy	3.5	1.1	11.7 (0.5)	12.1 (0.4)
MIX GP (S) – 200 kGy	2.9	0.8	11.8 (0.5)	12.3 (0.5)

D_a values in the 1st time domain (t < 3 days) were found to be greater than those in the 2nd time domain. In fact, more than 60% of the overall leaching occurred during the initial 3 days. As of now, no hypothesis can be proposed to explain the change in diffusion coefficients with time.

[6] N. Ukrainczyk and O. Vogt, "Geopolymer leaching in water and acetic acid," *RILEM Tech Lett*, vol. 5, pp. 163–173, Jan. 2021, doi: 10.21809/rilemtechlett.2020.124.

The ANSI/ANS 16.1 standards provide guidelines for calculation of leachability index, which is used as criterion for wasteform acceptance. The standard assumes that leaching is due to a single diffusion process, and therefore the leachability index is expected to be independent of time. However, in the case presented here the overall leaching is due to two concurrent diffusion processes. The leachability indices were therefore calculated for each of these time domains separately (Table 52).

All the leachability indices exceed the guidance value of 6 set by the Italian regulation, thus making all the studied GPs of "good quality".

5.3 MK, BFS and MIX formulation behaviour under irradiation (with oil)

In this section, all the results of the analyses performed on different GP formulations with surrogate waste are presented. Visual inspection of the samples after irradiation never revealed any cracks nor oil leakage.

Gas release

For the GPs samples with oil, measurement with the μGC was not possible because of the equipment's safety reason. The pressure inside each cell was measured after irradiation. The results were represented in Figure 118.

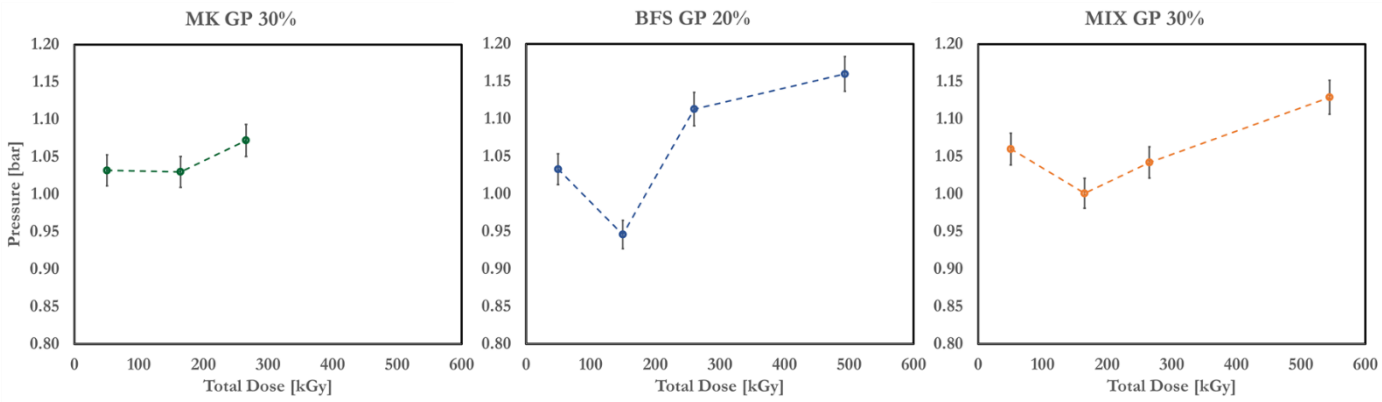

Figure 118: Pressure trend inside the cells after irradiation

While on the measurement of the gas release of GPs without waste the relation with the dose was clearly linear, here the pressure is not proportional to the dose rate. This could be due to the presence of oil inside the samples, which on one hand can produce gas under irradiation, but on the other hand fills the voids and thus reduces gas mobility.

Leaching after irradiation for MK, BFS and MIX formulation

MK GP, BFS GP and MIX GP with oil were subjected to the ANSI ANS 16.1 leaching test as presented in the methods section. The visual inspection of the samples after the leaching showed cracks in the MK GP samples. The MK GPs were always kept in a controlled environment until before irradiation, at the time of irradiation they were placed in a controlled environment filled with argon, this period could be the cause of these cracks (probably due to desiccation).

The samples were weighed before and after the leaching. In particular, after leaching the samples were put for 1 week in isopropanol and then dried for 40 hours. This process is used to remove the free water in the samples while keeping the hydrates unchanged. The mass variation of the samples is reported in Table 53.

Table 53. Mass loss after 28 days of leaching test.

Sample		Mass Before [g]	Mass After [g]	Reduction [%]
MK GP – 30%	Ref	3.2712	2.4397	25.42%
	250 kGy	3.1452	2.3688	24.69%
BFS GP – 20%	Ref	4.3300	4.5408	5.88%
	250 kGy	4.3554	4.1247	5.30%
MIX GP – 30%	Ref	3.4923	3.0655	12.22%
	250 kGy	3.0492	2.6308	13.72%

Micro computed tomography

Figure 119 shows the μCT scans of the GPs samples with oil before the irradiation. The oil particles, with a dimension bigger then 20 μm (2 times the voxel size), are underlined in red.

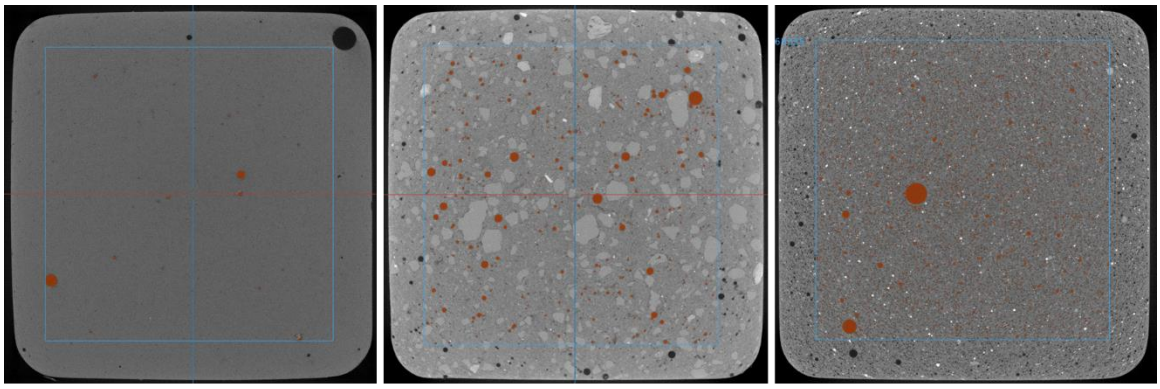

(a) MK GP (b) BFS GP (c) MIX GP

Figure 119: μCT scans of the 3 GPs formulation with oil. The oil is underlined in red, the active volume is in blue.

Table 54. presents the amount of %vol of the oil evaluated with the tomography and the difference between the added one.

Table 54. Oil percentage in the different samples.

	MK GP	BFS GP	MIX GP
%v added	30	20	30
%v μCT	0.25	2.45	3.67
%v difference	29.75	17.55	26.33

The order of magnitude of the volume of oil measure by the µCT is the same of a previous work on geopolymer[7]. Because the smaller the oil droplets, the more stable is the emulsion, having a majority of the oil in the form of droplets smaller than 20 µm means that the incorporation is very efficient in GPs. The presence of droplets smaller than 20 µm was verified using an optical microscope.

[7] M. De Campos, C. Reeb, C. A. Davy, J. Hosdez, and D. Lambertin, “Solidification/stabilization (S/S) of high viscosity organics in geopolymers,” *Journal of Nuclear Materials*, vol. 571, p. 153979, Dec. 2022, doi: 10.1016/j.jnucmat.2022.153979

Furthermore, still in De Campos' paper, they used another information derived from tomography, namely the droplet shape factor (SF), to evaluate the emulsification quality. The SF varies from 0 to 1, where 1 indicating a spherical shape of the droplet. A better emulsification is obtained when the SF is far from 1. Figure 120 shows the shape factors frequency of the different GPs analyzed. MK GP and MIX GP shape factors showed a similar behaviour with peaks at 0.63 and 0.72, meaning of a good emulsification. While the BFS GP doesn't show a broader peak between 0.8 and 1, meaning of partial coalescence and more spherical droplets.

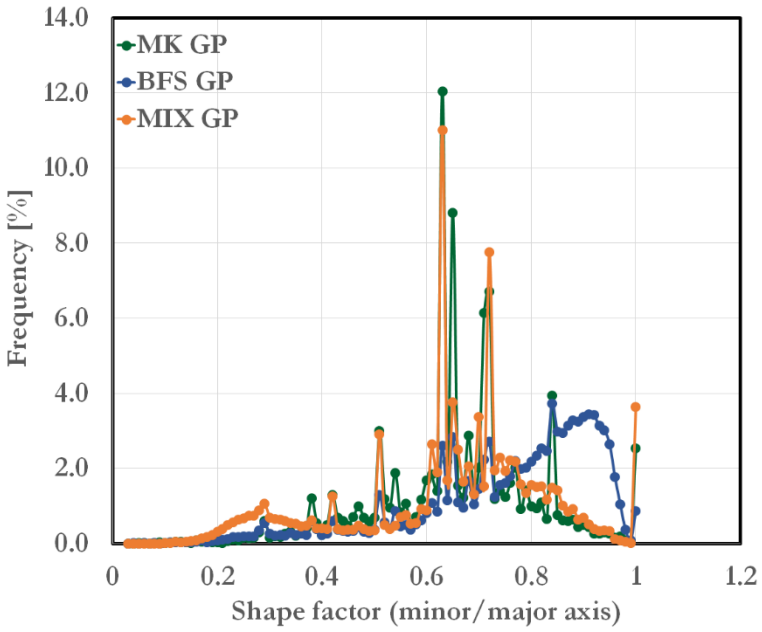

Figure 120: Shape factor of oil droplet in the different GP.

The present work shows that the different formulations of GPs without waste (oil) were not significantly affected by Cs-137 gamma irradiation. The leachability index for all formulations is way beyond the recommendations by the strict Italian regulation. The irradiation impact remains small as well for GPs with waste (oil), where no difference in weight loss was noticed for reference (non-irradiated) and irradiated samples up de 250 kGy.

POLIMI studied the variation of compressive strength of specimens of all three formulations after various combinations of ageing conditions, namely:

- static immersion in water for 28 days (all formulations);
- irradiation at 200 kGy with a Co-60 source at 2.5 kGy/h (MK- and BFS-based formulations);
- daily thermal cycling between -40 - +40 °C for 30 days (MIX-based formulation)[8].

In all cases, samples not undergoing ageing processes were stored in endogenous conditions for an equivalent time to guarantee the same total curing period across all samples considered.
Additionally, XRD and porosity measurements were also performed after the specified ageing conditions.

[8] Thermal cycling was adopted for this formulation due to the delay in the definition of the MIX-based formulation, which resulted in the impossibility of performing a 200 kGy irradiation within the timeframe of the project. The parameters of the thermal cycles are derived from Italian WAC.

MK-based formulation

Table 55.Compressive strength of MK-based samples following different ageing conditions.

Sample	Irradiation	Immersion	Compressive strength (MPa)
No waste	No	No	18.6 ± 0.9
	No	Yes	16.1 ± 0.9
	Yes	No	7.9 ± 0.6
	Yes	Yes	*NA*
LSC	No	No	8.9 ± 0.4
	No	Yes	7.1 ± 0.5
	Yes	No	4.9 ± 0.4
	Yes	Yes	*NA*
TBP/dodecane	No	No	10.0 ± 0.5
	No	Yes	6.3 ± 0.6
	Yes	No	*NA*
	Yes	Yes	*NA*

Collected data is reported in Table 55. Immersion in water appears to have a limited, but measurable, influence on mechanical resistance.

Non-representative values were obtained for irradiated samples. It should in fact be noted that since irradiation was carried out in an industrial facility, strict endogenous conditions could not be granted during dose delivery. Such samples were therefore likely degraded due to loss of humidity (confirmed by a loss of weight of 15-25% after irradiation), and not by absorbed dose itself. This hypothesis is further supported by the instability of irradiated samples towards immersion: upon contact with water, irradiated specimens tend to re-absorb water that they lost during their permanence in dry air, resulting in catastrophic cracking (hence the impossibility of evaluating compressive strength) due to capillary stresses (see Figure 121).

Figure 121. Irradiated MK-based sample showing catastrophic cracking after being immersed in water.

XRD patterns acquired on aged samples appeared identical to those of the pristine matrix, confirming the presence of a completely amorphous structure. Similarly, porosity values also remained essentially identical before and after ageing, as reported in Table 56.

Table 56. Porosity of MK-based samples (both with and without waste) after immersion, irradiation of combination of both. Reference values of non-aged samples are also reported. Uncertainty of the method was assessed at 3%.

Sample	Irradiation	Immersion	Porosity
No waste	No	No	34.9%
	No	Yes	35.2%
	Yes	No	34.5%
	Yes	Yes	35.3%
LSC	No	No	36.0%
	No	Yes	35.7%
	Yes	No	35.8%
	Yes	Yes	34.3%
TBP/dodecane	No	No	34.5%
	No	Yes	31.6%
	Yes	No	36.4%
	Yes	Yes	33.0%

BFS-based formulation

Table 57. Compressive strength of BFS-based samples following different ageing conditions.

Sample	Irradiation	Immersion	Compressive strength (MPa)
No waste	No	No	55 ± 5.1
	No	Yes	39.6 ± 4.2
	Yes	No	51 ± 5.0
	Yes	Yes	32.6 ± 3.3
LSC	No	No	3.8 ± 0.4
	No	Yes	3.1 ± 1.0
	Yes	No	3.7 ± 0.8
	Yes	Yes	3.5 ± 0.6
TBP/dodecane	No	No	5.6 ± 0.6
	No	Yes	3.2 ± 0.5
	Yes	No	5.9 ± 0.8
	Yes	Yes	5.1 ± 0.7

From data reported in Table 57 it can be seen that compressive strength is affected by water immersion, and less significantly by irradiation at 200 kGy. As already mentioned, the drastically lower values obtained in presence of waste are likely due to the inhomogeneous structure of the samples rich of macroscopic cavities resulting from the preparation protocol.

MIX-based formulation

Table 58. Compressive strength of MIX-based samples following different ageing conditions.

Sample	Thermal cycle	Immersion	Compressive strength (MPa)
No waste	No	No	44.1 ± 2.3
	No	Yes	39.5 ± 2.0
	Yes	No	47.8 ± 2.6
LSC	No	No	23.1 ± 1.2
	No	Yes	18.9 ± 1.1
	Yes	No	23.8 ± 1.4

The data summarized in Table 58, show no significant differences after ageing, but compressive strength is halved in presence of the waste (30 v%).
XRD patterns acquired on aged samples appeared identical to those of the pristine matrix, confirming the presence of an essentially amorphous structure, with a small presence of quartzite, mullite and calcite. The presence of calcite could also be ascribed to the reaction with atmospheric CO_2.

Similarly, porosity values also remained essentially identical before and after ageing, as reported in Table 59.

Table 59. Porosity of MIX-based samples (both with and without waste) after immersion or thermal cycling. Reference values of non-aged samples are also reported. Uncertainty of the method was assessed at 3%.

Sample	Thermal cycle	Immersion	Porosity
No waste	No	No	26.1%
	No	Yes	25.4%
	Yes	No	25.2%
LSC	No	No	27.9%
	No	Yes	23.3%
	Yes	No	24.7%

5.4 Partial conclusion about irradiation testing

It is important to study the behaviour of materials under irradiation, both to quantify potential dihydrogen production and to investigate the impact of irradiation on the residual properties of the material. The tests carried out during this phase enabled us to classify the different formulations according to their hydrogen production (MK based being the most prone to hydrogen release and MIX the least) and to show that up to 200 kGy, the effect of irradiation on leaching is very moderate, whether or not organic liquid is incorporated. Post-irradiation strength tests carried out at POLIMI on the MK formulation show a marked reduction in compressive strength, although it is not possible to separate the effect of irradiation and the effect of drying, which as we saw in the first chapters is important for this matrix. Other literature has shown less effect of irradiation on the bulk properties of geopolymers, but this remains the subject of ongoing investigation.

6 STUDY of RADIONUCLIDES BINDING and LEACHING

6.1 Protocols

Leaching behaviour over 1 month of immersion was studied by POLIMI on MK-, BFS- and MIX-based samples doped with stable elements representative of some of the most common activation and fission products. In some cases, the leaching behaviour was also studied on specimens irradiated at 200 kGy, to investigate possible degradation due to absorbed dose.

To guarantee the representativeness of results, all leaching tests were performed on samples with the same overall curing period, in order to negate possible age-dependent effects. Therefore, samples not undergoing irradiation were stored at >90% RH for the time period required for the irradiation of their analogues.

The standard protocol ANSI/ANS-16.1-2019 was followed by employing cylindrical samples of 2.5 cm diameter and 4 cm height. The leachant was ultrapure water at room temperature (20 ± 2 °C), which was periodically renewed according to the intervals specified by the protocol. After the appropriate leaching interval, leachates were acidified with ultrapure nitric acid, diluted appropriately and analyzed via inductively coupled plasma optical emission spectroscopy (ICP-OES) or ICP-mass spectrometry (ICP-MS). Cumulative fractional releases of the considered contaminants (Cs, Sr, Ni, Co, Ce, Eu, Nd, Th and U) were used to compute leachability indices as specified by the ANSI/ANS protocol.

The experiments investigated the sorption of ^{63}Ni and ^{14}C radionuclides on the BFS and GP matrices were conducted by UJV. 1 g and 0.5 g inactive samples were activated by the leaching solutions with grain sizes of below 0.5 mm were tested (activity of ^{63}Ni: 26 000-30 000 CPM, activity of ^{14}C: 17 000-22 000 CPM).

Hidex liquid scintillation spectrometer (Figure 13) (which detects sources of both α and ß radiation) was used for the measurement of the samples. The measurement process involved the weekly sampling of the leachates (0.5 ml) over a period of 7 – 49 days with the addition of the scintillation cocktail (4 ml).

Two parameters – the linear distribution coefficient *Rd* and the sorption efficiency *η* – can be calculated from the resulting data CPM (counts per minutes) with the following formula:

$R_d = (A_0-A_n)/A_0 * V/m$

$\eta=(A_0-A_n)/A_0$

A_0 = activity of the liquid phase of the reference sample without the sorbent presence [CPM] – results from Hidex

A_n = activity of the liquid phase in the presence of sorbent [CPM] – results from Hidex

V = volume of the liquid phase = 5 ml

m = sorbent weight [g]

In this report only the results of sorption efficiency will be presented.

The approach to the leaching experiments followed the ANSI method ANSI/ANS-16.1.1986 (The measurement of the leachability of solidified low-level radioactive wastes by a short – term test procedure). The principle comprises the leaching of radionuclides from solidified waste as a function of time.

The test sample must be both representative and homogeneous. It must have a cylindrical shape with a length to diameter ratio of 0.2 – 5. The preparation approach is unique for each type of waste. Leaching solution: DEMI water with the appropriate characteristics is used for determination purposes – conductivity < 5 microohms/cm at 25°C.

A constant temperature within the range 17.5 – 27.5 °C must be maintained during the testing procedure.
The volume of the leaching solution is calculated as: V_L / S = 10 ± 0.2 cm

- V_L = the volume of leaching solution [cm^3]
- S = the sample surface [cm^2]

The method:

The prepared sample is placed in the specified volume of the leaching solution. Once the time interval has elapsed, the leaching solution is replaced with a clean solution and the activity of the solution is determined. The procedure is repeated at set intervals: 1d, 2d, 3d, 4d, 5d, 19d, 47d and 90d.

A Hidex liquid scintillation spectrometer (which detects sources of both α and ß radiation) was used to measure the samples. The measurement process involved the extraction of leachates (1 ml) at set intervals and the addition of 4 ml of scintillation cocktail.

The Leachability index Li was calculated according to the ANSI method. The Leachability index comprises a dimensionless value that is calculated from the experimentally obtained effective diffusivity value for a given radionuclide. It characterizes the leaching properties of a given solidified material.

$$L_i = \frac{1}{10}\sum_{10}^{1}\left[\log(\beta / D_i\right]$$

were

ß = defined constant 1.0 cm^2/s
D_i = effective diffusivity for a given radionuclide cm^2/s,

Figure 122. Leaching samples: ^{63}Ni (left) ^{14}C (right)

6.2 Metakaolin formulation

Leaching behaviour over 1 month of immersion was studied by POLIMI on doped MK-based samples loaded with the above-mentioned organic liquids (TBP/dodecane and Ultima Gold liquid scintillation cocktail), both irradiated and non-irradiated. For reference, MK-based samples without waste were also considered. Obtained leachability indices values of the contaminants are reported in Table 60. Release of matrix constituents was also assessed as an indicator of stability. Cumulative fractional release of K, Si and Al at 1 month is reported in Table 61.

Table 60. Leachability indices for the MK-based formulation (irradiated and non-irradiated) determined for the considered contaminants according to ANSI/ANS-16.1-2019.

Sample	Irradiation	Ce	Co	Cs	Eu	Nd	Ni	Sr	Th	U
No waste	No	11.1 ± 0.2	11.3 ± 0.3	9.5 ± 0.2	11.2 ± 0.3	10.9 ± 0.2	10.1 ± 0.3	11.4 ± 0.5	10.0 ± 0.2	11.0 ± 0.2
	200 kGy	10.8 ± 0.1	12.4 ± 0.4	9.6 ± 0.4	11.7 ± 0.3	10.4 ± 0.1	10.4 ± 0.4	9.1 ± 0.2	10.1 ± 0.5	9.0 ± 0.7
LSC	No	10.2 ± 1.1	9.8 ± 0.1	9.5 ± 0.1	12.5 ± 0.1	9.5 ± 1.1	10.7 ± 0.2	8.8 ± 0.2	10.4 ± 0.2	11.6 ± 0.6
	200 kGy	11.1 ± 0.3	10.4 ± 0.2	9.6 ± 0.2	12.7 ± 0.3	11.2 ± 0.2	9.2 ± 0.8	9.3 ± 0.1	10.5 ± 0.3	10.8 ± 0.5
TBP/ dodecane	No	10.7 ± 0.6	10.0 ± 0.1	9.5 ± 0.1	12.3 ± 0.3	11.0 ± 0.3	8.2 ± 0.8	8.8 ± 0.2	10.1 ± 0.3	11.7 ± 0.3
	200 kGy	11.4 ± 0.3	11.0 ± 0.1	9.6 ± 0.2	12.4 ± 0.3	11.1 ± 0.3	10.5 ± 0.3	8.9 ± 0.7	10.2 ± 0.3	10.5 ± 0.5

Table 61. Cumulative fractional release of matrix constituents after 1 month of leaching for the MK-based formulation (irradiated and non-irradiated).

Sample	Irradiation	K (%)	Si (%)	Al (%)
No waste	No	14.0 ± 0.9	0.59 ± 0.08	0.12 ± 0.04
	200 kGy	15.4 ± 1.2	0.22 ± 0.07	0.09 ± 0.02
LSC	No	14.8 ± 1.3	0.54 ± 0.08	0.14 ± 0.04
	200 kGy	15.3 ± 0.8	0.24 ± 0.05	0.09 ± 0.01
TBP/ dodecane	No	24.7 ± 1.8	1.03 ± 0.09	0.29 ± 0.02
	200 kGy	26.4 ± 1.5	0.51 ± 0.09	0.26 ± 0.03

No significant differences were noted in leachability indices determined for sample with no waste and with either LSC or TBP/dodecane. Irradiation at 200 kGy also resulted in no appreciable worsening of nuclide retention. As expected, Cs presents among the lowest index due to its high mobility and solubility even at high pH. With regard to matrix constituents, K presented the highest cumulative release after 1 month of immersion. This is expected as K is present as a cation with high solubility and is present in non-framework sites and pore fluid within the geopolymer. Also in this case, irradiation at 200 kGy did not show significant effects towards matrix stability. On the other hand, samples loaded with TBP/dodecane showed the lowest stability towards immersion with respect to the release of matrix constituents.

Release of the organic component of the LSC waste during the leaching period of 1 month was also evaluated via periodic chemical oxygen demand (COD) measurements on collected leachates. This measure was performed only for the specimens containing LSC waste, as in this case the leachates proved to be homogeneous. In the case of TBP/dodecane waste, the negligible solubility of the waste in water would hinder obtaining a representative and homogeneous sample for COD determination. Nevertheless, no organic droplets were evidenced by visual inspection of the leachant surfaces. Correlation between measured COD and actual organic waste content in the leachates was determined through calibration with a standard solution prepared ad hoc. Cumulative LSC release is reported in Figure 123 for both irradiated and non- irradiated samples. A significant increase of organic release was noted for the former sample.

From collected data, it is unclear whether irradiation at 200 kGy significantly affects stability of the wasteform. It should in fact be noted that, since irradiation was carried out in an industrial facility, strict endogenous conditions could not be guaranteed during dose delivery. Hence, differences in organic release could be attributed to the different storage conditions between samples, which are known to affect the properties of the matrix. However, this hypothesis is in contrast with the leaching behaviour of contaminants, which did not show difference between irradiated and non-irradiated samples. Considering both these factors, it may be hypothesized that lower waste retention could be attributed to the radiolysis of the waste, and not to the degradation of the matrix. Lower molecular weight degradation products of LSC could in fact be of higher mobility, resulting in an increase of waste leaching.

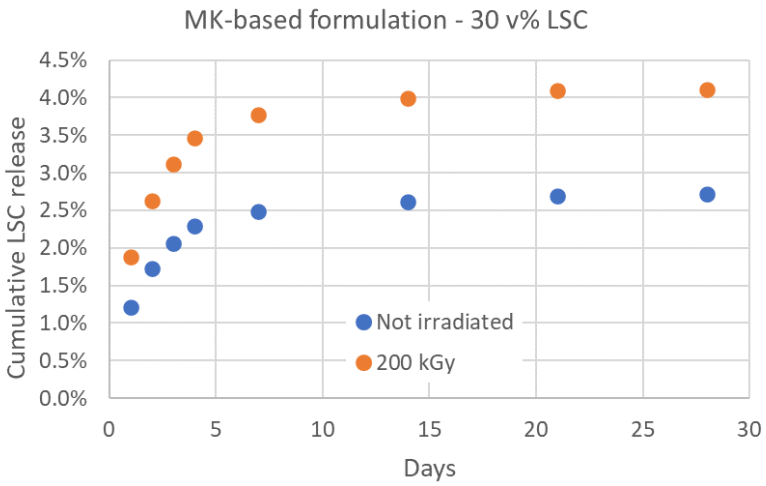

Figure 123. Cumulative fractional release of LSC waste for the MK-based formulation (irradiated and non-irradiated) over 1 month of immersion in water. Relative standard uncertainty of measurement points is ≈5%.

Sorption tests (MK Based formulation matrix)

The results of the sorption tests can be found in Figure 124 and Figure 125 for metakaolin based matrix.

For sorption efficiency ŋ of ^{63}Ni, a significant increase in the ŋ were evident for the initial sampling period (day 14). The values were relatively stable from day 14 onwards. Slightly higher *ŋ* values are obtained for 1 g samples. This evolution means that almost all the ^{63}Ni is absorbed by the matrix.

For sorption efficiency *ŋ* of ^{14}C, low efficiency values are obtained with a decrease over the time. The evolution seems to show that after a small sorption of ^{14}C during the 7 first days, this last is progressively released.

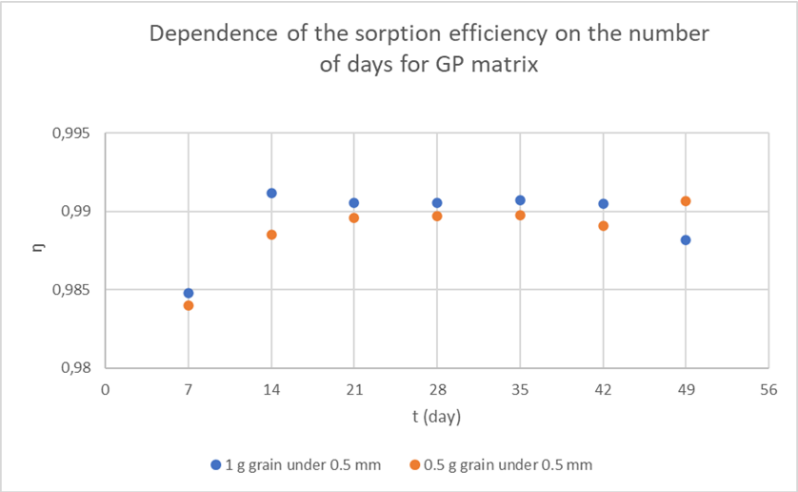

Figure 124. Time dependence of η (^{63}Ni sorption on the GP matrix)

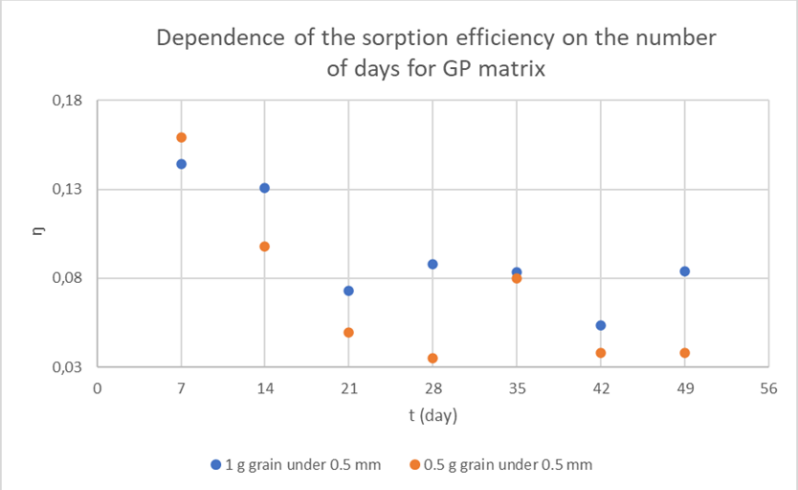

Figure 125. Time dependence of the η (^{14}C sorption on the GP matrix)

Leaching tests

The results of the leaching tests are presented in Figure 126 and Figure 127 for both metakaolin based matrix (GP) and BFS matrix for two kind of RLOW. Even if the variability seems important at the beginning of the measurements, CPM count for ^{63}Ni and ^{14}C is almost stable (no leaching of radionuclides)

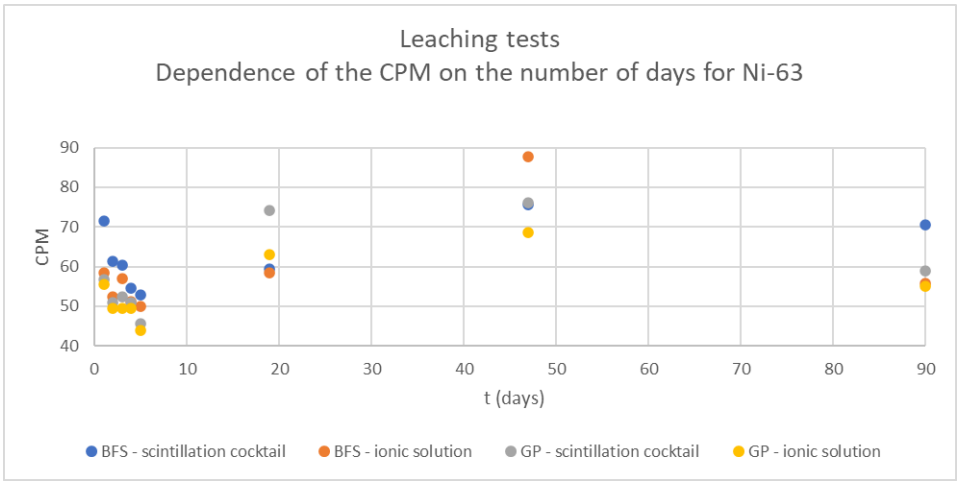

Figure 126. Leaching tests - Dependence of the CPM on the time for ^{63}Ni

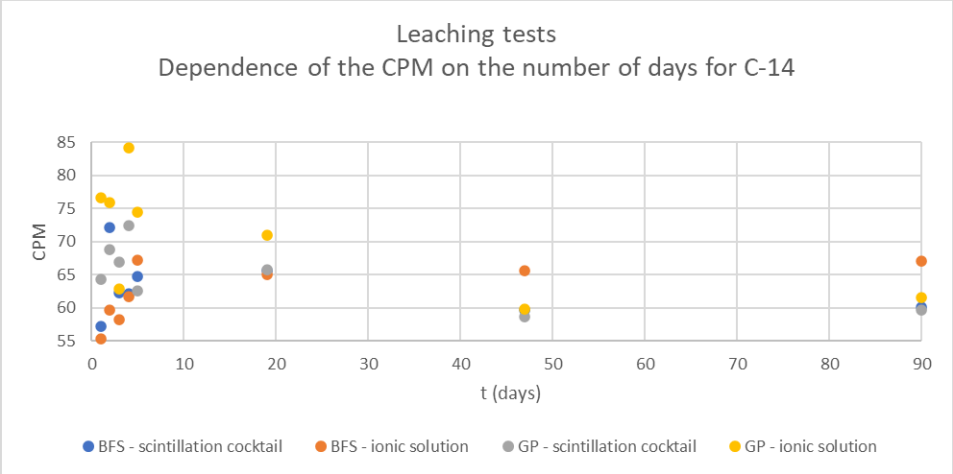

Figure 127. Leaching tests – Dependence of the CPM on the time for ^{14}C

For both radionuclides (^{63}Ni and ^{14}C) and both formulae (MK based and BFS based), the required minimum value of the leachability index *Li* = 8 was reached.

6.3 Blast furnace slag formulation

Leaching behaviour over 1 month of immersion was studied by POLIMI on doped BFS-based samples loaded with the above-mentioned organic liquids (TBP/dodecane and Ultima Gold liquid scintillation cocktail), both irradiated and non-irradiated. For reference, BFS-based samples without waste were considered. Obtained leachability indices values of the contaminants are reported in Table 62.

Release of matrix constituents was also assessed as an indicator of stability. Cumulative fractional release of Na, Ca, Si and Al at 1 month is reported in Table 63.

Table 62. Leachability indices for the BFS-based formulation (irradiated and non-irradiated) determined for the considered contaminants according to ANSI/ANS-16.1-2019.

Sample	Irradiation	Ce	Co	Cs	Eu	Nd	Ni	Sr	Th	U
No waste	No	11.5 ± 0.7	11.8 ± 1.5	9.1 ± 0.9	10.6 ± 1.2	10.5 ± 0.7	9.0 ± 0.9	9.1 ± 0.9	12.7 ± 1.4	12.7 ± 1.1
	200 kGy	11.2 ± 0.8	11.9 ± 0.8	9.3 ± 0.4	10.8 ± 1.5	10.3 ± 1.3	8.8 ± 0.6	9.3 ± 0.6	13.4 ± 0.7	12.8 ± 1.2
LSC	No	10.9 ± 0.9	11.4 ± 1.1	9.0 ± 0.3	11.1 ± 1.1	10.7 ± 0.9	9.0 ± 0.8	9.6 ± 0.6	13.1 ± 0.9	12.6 ± 1.0
	200 kGy	10.9 ± 1.0	11.9 ± 1.6	8.8 ± 0.5	11.2 ± 1.0	10.6 ± 1.1	9.0 ± 1.0	9.2 ± 0.9	13.3 ± 1.0	12.6 ± 1.4
TBP/ dodecane	No	10.8 ± 1.4	11.4 ± 1.6	9.0 ± 0.5	11.3 ± 1.1	10.8 ± 1.2	8.8 ± 1.3	9.5 ± 0.5	13.2 ± 1.2	12.4 ± 1.4
	200 kGy	10.4 ± 1.0	11.2 ± 1.1	9.1 ± 0.5	11.0 ± 0.7	10.3 ± 0.9	8.6 ± 1.0	9.4 ± 0.3	13.2 ± 0.9	12.6 ± 1.1

Table 63. Cumulative fractional release of matrix constituents after 1 month of leaching for the BFS-based formulation (irradiated and non-irradiated).

Sample	Irradiation	Na (%)	Ca (%)	Si (%)	Al (%)
No waste	No	3.2 ± 0.1	0.34 ± 0.08	0.41 ± 0.06	0.40 ± 0.08
	200 kGy	4.0 ± 0.1	0.18 ± 0.09	0.52 ± 0.01	0.50 ± 0.06
LSC	No	4.5 ± 0.2	0.38 ± 0.09	0.60 ± 0.04	0.61 ± 0.02
	200 kGy	4.2 ± 0.1	0.39 ± 0.12	0.51 ± 0.06	0.48 ± 0.04
TBP/ dodecane	No	6.5 ± 0.3	0.30 ± 0.04	1.18 ± 0.10	1.05 ± 0.09
	200 kGy	6.6 ± 0.1	0.23 ± 0.08	0.81 ± 0.03	0.85 ± 0.07

No significant differences were noted in leachability indices determined for sample with no waste and with either LSC or TBP/dodecane. Irradiation at 200 kGy also resulted in no appreciable worsening of nuclide retention. As expected, Cs presents the lowest index due to its high mobility and solubility even at high pH. With regard to matrix constituents, Na presented the highest cumulative release after 1 month of immersion. This is expected as Na is present as a cation with high solubility. Also in this case, irradiation at 200 kGy did not show significant effects towards matrix stability. On the other hand, samples loaded with TBP/dodecane showed the lowest stability towards immersion with respect to the release of Na, Si and Al.

Release of the organic waste during the leaching period could not be quantitatively assessed since the leachates were not uniform and a representative sample could not be obtained. Qualitative appearance of the leachate confirmed, however, a visible release of the encapsulated waste, as illustrated in Figure 128.

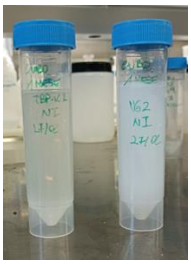

Figure 128. Leachates deriving from BFS-based samples loaded with TBP/dodecane (left) and LSC (right).

Results of sorption testing performed by UJV on BFS formulation can be found in Figure 129 and Figure 130. Similarly, to the MK based matrix, the BFS based formulation shows an important sorption of ^{63}Ni even if the kinetics seems lower. For ^{14}C, the sorption efficiency coefficient remains low (below 0.25).

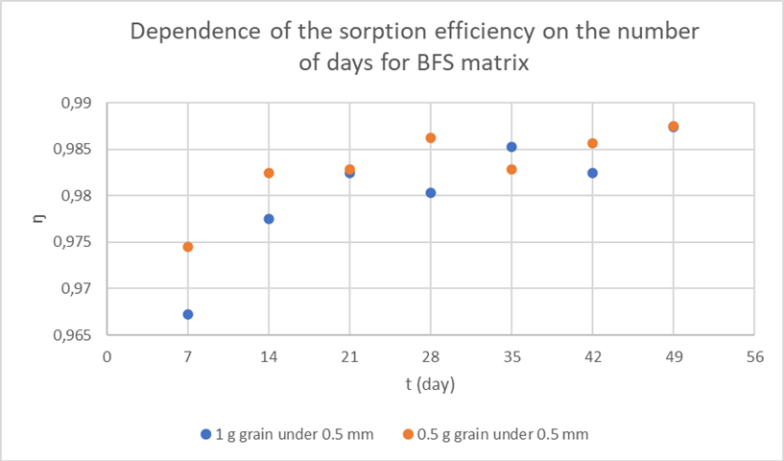

Figure 129. Time dependence of the η (^{63}Ni sorption on the BFS matrix)

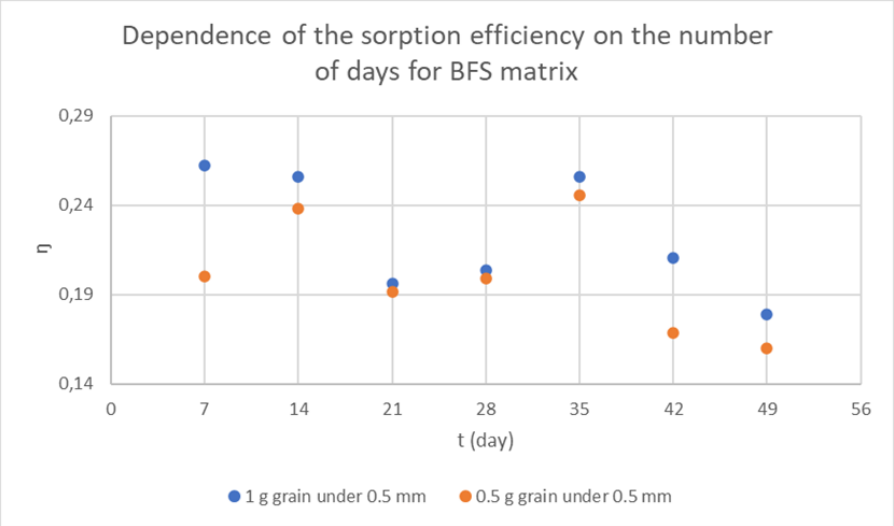

Figure 130. Time dependence of the η (^{14}C sorption on the BFS matrix)

Leaching tests

Results of the leaching tests of BFS formulation with ionic solution of liquid scintillation cocktail have been presented previously with MK based results. Nevertheless, based on the results the BFS matrix exhibited the highest Li compared to the MK matrix.

6.4 Mix formulation

Leaching behaviour over 1 month of immersion was studied by POLIMI on doped MIX-based samples loaded with Ultima Gold liquid scintillation cocktail. As mentioned earlier, samples loaded with TBP/dodecane could not be prepared due to incorporation issues. For reference, MIX-based samples without waste were considered. Obtained leachability indices values of the contaminants are reported in Table 64.

Release of matrix constituents was also assessed as an indicator of stability. Cumulative fractional release of Ca, K, Si and Al at 1 month is reported in Table 65.

Table 64. Leachability indices for the MIX-based formulation determined for the considered contaminants according to ANSI/ANS-16.1-2019.

Sample	Ce	Co	Cs	Eu	Nd	Ni	Sr	Th	U
No waste	10.2 ± 0.6	12.1 ± 0.1	8.9 ± 0.1	12.0 ± 0.5	10.3 ± 0.3	9.8 ± 0.4	8.5 ± 0.2	9.9 ± 0.2	11.3 ± 0.2
LSC	10.2 ± 0.7	10.2 ± 0.4	9.8 ± 0.9	9.5 ± 0.5	11.7 ± 1.2	10.4 ± 0.7	10.1 ± 1.0	9.6 ± 0.1	10.9 ± 0.1

Table 65. Cumulative fractional release of matrix constituents after 1 month of leaching for the MIX-based formulation.

Sample	Ca (%)	K (%)	Si (%)	Al (%)
No waste	0.06 ± 0.02	18.9 ± 1.5	0.49 ± 0.08	0.42 ± 0.05
LSC	0.02 ± 0.01	20.0 ± 1.2	0.66 ± 0.10	0.51 ± 0.24

No significant differences were noted in leachability indices of contaminants determined for sample with no waste and with LSC. With regard to matrix constituents, K presented the highest cumulative release after 1 month of immersion. Similar stability was noted also in presence of LSC waste for all matrix constituents.

Release of the organic waste during the leaching period could not be quantitatively assessed since the leachates were not uniform and a representative sample could not be obtained (see Figure 131).

Figure 131. Leaching of organic content from MIX-based sample loaded with LSC.

6.5 Partial conclusion about radionuclide binding and leaching

Through test campaigns carried out by two project partners, absorption and leaching tests were carried out using samples or leaching solutions containing radionuclides. For the MK-based matrix, the results show a release of LSC which appears to be more significant after irradiation, even if the values are low, thus increasing the measurement uncertainty. Still on MK-based materials, the absorption of ^{63}Ni is much greater than that of ^{14}C. The results for BFS are similar, with ^{63}Ni again showing greater adsorption.

In terms of leaching, the presence of radionuclides does not alter leaching sensitivity, which remains very moderate, with leachability indices close to 10 for all formulations and all contaminants.

7 STUDY of THERMAL BEHAVIOUR and FIRE HAZARD

7.1 Thermo-Mechanical Characterization of LOW simulant/formulation

The presence of liquid organic wastes in addition to the water content may determine significant variation of the thermophysical and mechanical properties of material formulation due to heterogeneous composition.

The behaviour of the surrogate materials (the formulation of which is summarized in Table 17) is unknown from a thermo-mechanical point of view, and particularly in conditions of high thermal gradients (and fire hazard). Moreover, the thermal characterization is felt important for the performance and durability assessment of waste matrices. The experimental characterization consisted of two phases: 1) thermal test, and 2) compression test (on both fresh and thermal aged samples.

7.1.1 Experimental protocol

It is worthy to remember that the LOW substances/mixtures used in all the three formulations (i.e. NNL, BFS and KIPT ones) are characterised by a flash point of about 146°C, 240°C and 220°C, limiting the thermal characterization and impeding reaching 800°C, as per IAEA, SSR-6 (Rev.1), 2018.

Based on this, the need arose to first test inert materials and only numerically simulate the fire behaviour of the surrogates. In doing that, firstly a test protocol was developed with reference to inert Portland type cement matrices with w/c ratio of 0.29, subsequently the effects of the elevated temperature or fire flame condition was investigated either by means of experimental campaign or by numerical simulations.

Thermal tests were carried out according to the Hot Wire parallel method on (aged/unaged) cylindrical concrete samples at temperatures from 50°C to 800°C. Tests were repeated for statistical soundness. Specimens were prepared according to ASTM C335 and ISO 8497 standards.

The cylindrical samples dimensions were: 400 mm length, and 100 mm external diameter. Each sample was equipped with at least two type C thermocouples (TC) positioned at a radial distance of 0.05 and 0.03 m from the centroid and a central wire resistor. The measurement error, as from the calibration procedure resulted in less than 2%. Thermal test procedure consisted of:

1. Positioning of the sample in the oven
2. Uniform heating up the electric oven until the specified test temperature.
3. Monitoring and control the temperature ramp by data acquisition system (DAS)
4. Acquisition of temperature values by DAS when steady state condition is reached for at least 300s.

The temperature increase was controlled through a PID system (GEFRAN© GF Promer) connected to a DAS. The interface with a PC is obtained via Labview©, while a Lexan© membrane faceplate was provided a frontal IP65 rating. The Fourier equation for 1D steady-state heat flow was used to calculate the thermal conductivity (k) value based on the rate of temperature increase and power input, at each specific test temperature.

Figure 132 and Figure 133 show the heating phase and k-trends for aged/unaged material respectively.

Figure 132. Cylindrical sample in the oven

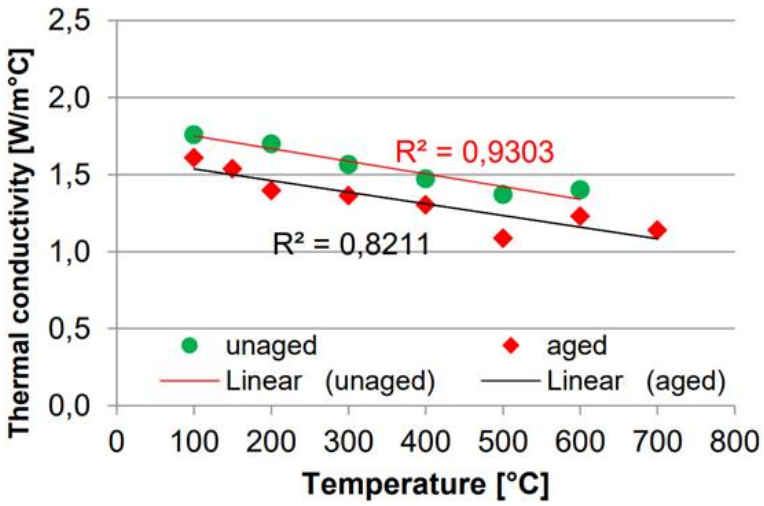

Figure 133. Thermal conductivity vs temperature for Portland cement type material

Results are like the ASCE and Eurocode trends: 20% monotonic decrease in thermal conductivity (of both aged/unaged material) is attributable to the increase in porosity[9] [10]. The k of siliceous aggregate is higher than that of the carbonate one in the temperature range of 200 – 800°C: the higher the crystallinity, the higher thermal conductivity and its rate of decrease with temperature.

7.1.2 Thermal testing of MK and MIX formulation

In the following, the results obtained by performing thermal cycling tests on MK based formulation and MIX formulation are summarised. As before-mentioned the selected formulation to assess RLOW/conditioning matrix thermal behaviour associated with elevated temperature (fire hazard) have a flash point of about 146°C, 240°C and 220°C impeding therefore a safe execution of the thermal testing (ASTM D 635-03) at 800° C, as per IAEA, SSR-6 (Rev.1), 2018. However, the fire behaviour was simulated numerically.

Thermal cycling and compression tests were carried out experimentally per each specimen formulation with/without LOW simulants. The following tests were therefore performed:

- Differential Scanning Calorimetry (DSC) analysis according to the BS-EN ISO 11357-1:2023-TC to investigate the thermal behaviour of materials by measuring the heat flow associated with transitions in the sample as a function of temperature.
- Thermal Ageing Analysis to examine the thermomechanical characteristics of various formulations.

Differential Scanning Calorimetry (DSC) analysis

DSC analysis was carried out in compliance with BS-EN ISO 11357-1:2023-TC. 20 samples before and after ageing have been analyzed.

The analysis involved heating the samples at a constant rate in a controlled atmosphere to prevent oxidation. The thermal stability, phase transitions, and overall thermal behaviour of different formulations were obtained from data processing done by the Pyris© software interface.

[9] J. Li, 2013 Progress in Nuclear Energy and IAEA TECDOC-1701;
[10] Shi, C., et al. 2004 Critical Reviews in Environmental Science and Technology; Natsuda, M. et al. (1992) Journal of Nuclear Science and Technology

The program set-up of DSC analysis was as follows:

- I° heating from -20°C to 120°C, 20 °C/min in N_2
- cooling from 120°C to -20°C, -20°C/min in N_2
- II° heating from -20°C to 120°C, 20 °C/min in N_2

The overall information of investigated samples is collected in Table 66 below.

Table 66. Characteristics of sample tested

ID Sample	Sample Status	Formulation	RLOW	Onset Temperature [°C]
235-0100	Aged	MK Based	-	113.2
235-0200	Aged	MK Based	Nevastane Oil	113.8
235-0300	Aged	MK Based	-	111.6
235-0400	Aged	MK Based	Nevastane Oil	109.9
235-0500	Aged	MK Based	-	113
235-0600	Aged	MK Based	TBP	113.1
235-0700	Aged	MIX formulation	-	104.5
235-0800	Aged	MIX formulation	ShellSpirax	110.6
235-0900	Aged	MIX formulation	-	105
235-1000	Aged	MIX formulation	ShellSpirax	102.3
273-0100	No - Aged	MK Based	-	109.63
273-0200	No - Aged	MK Based	Nevastane Oil	109.16
273-0300	No - Aged	MK Based	-	109.94
273-0400	No - Aged	MK Based	Nevastane Oil	108.49
273-0500	No - Aged	MK Based	-	111.37
273-0600	No - Aged	MK Based	TBP	109.16
273-0700	No - Aged	MIX formulation	-	110.46
273-0800	No - Aged	MIX formulation	Nevastane Oil	102.57
273-0900	No - Aged	MIX formulation	-	110.56
273-1000	No - Aged	MIX formulation	Nevastane Oil	112.34

The DSC thermograms of no-aged (an example of results is provided in Figure 134) and aged samples did not show any significant transition in the temperature range analysed, except for a partial degradation of the materials characterised by an onset temperature ranging from 100° to 115° C probably caused by boiling of the pore water.

Similar trends were observed expect for the samples 273-0800, 235-0800 and 235-1000 which have shown an endothermic transition in the first heating.

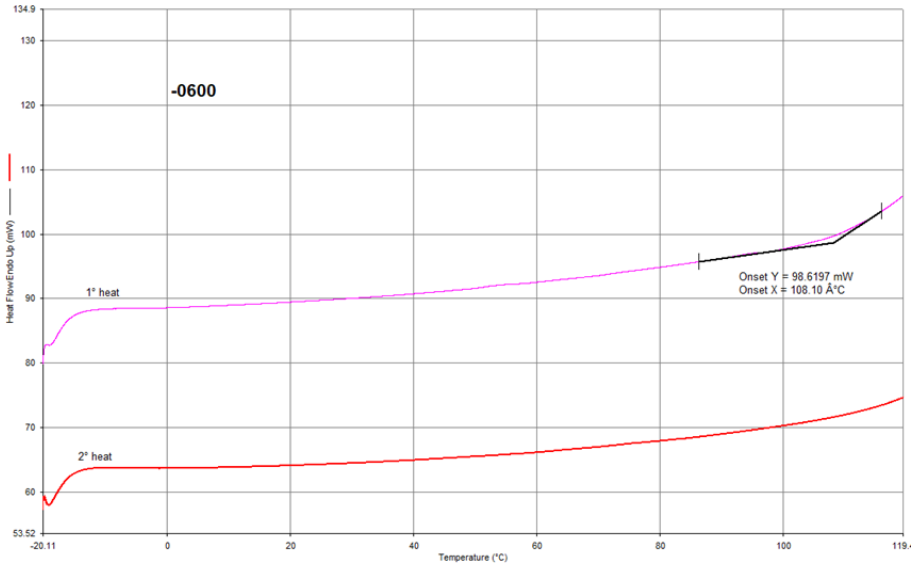

Figure 134. DSC Thermogram of MK based sample without and with (b) Nevastane oil

Thermal Ageing Analysis

The specimens labelled from 235-0100 to 235-1000 were subjected to a thermal aging followed by DSC and compression tests to assess the thermomechanical performances of each formulation. Thermal ageing was performed according with CEI EN 60068-2-14 standard (Nb test); the following thermal cycle was used, repeated 15 times for a total aging time of 100 h:

- from -20° to +40°C, 3°C/min.
- permanence at +40°C for 3h.
- from +40° to -20°C, 3°C/min.
- permanence at -20°C for 3h.

Figure 135. Thermal ageing setup

Samples aged by thermal cycling have been scanned showing cracking for sample with and without RLOW. For example, in Figure 136 micro-cracks are clearly visible at location indicated with yellow arrows.

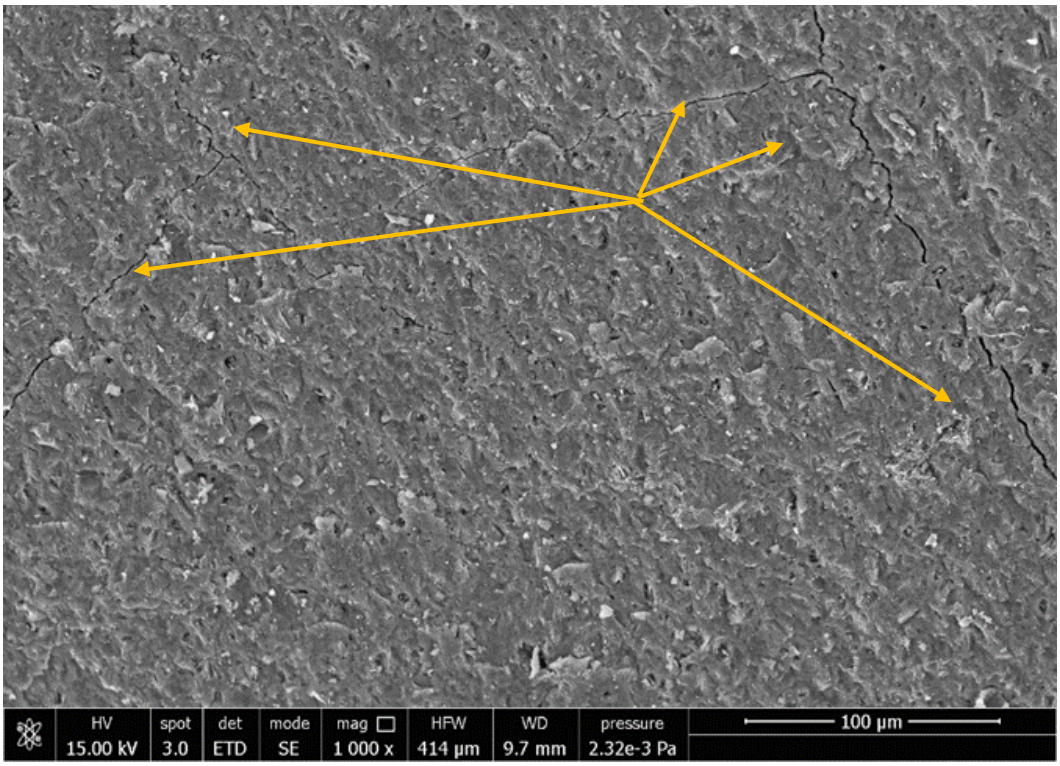

(a)

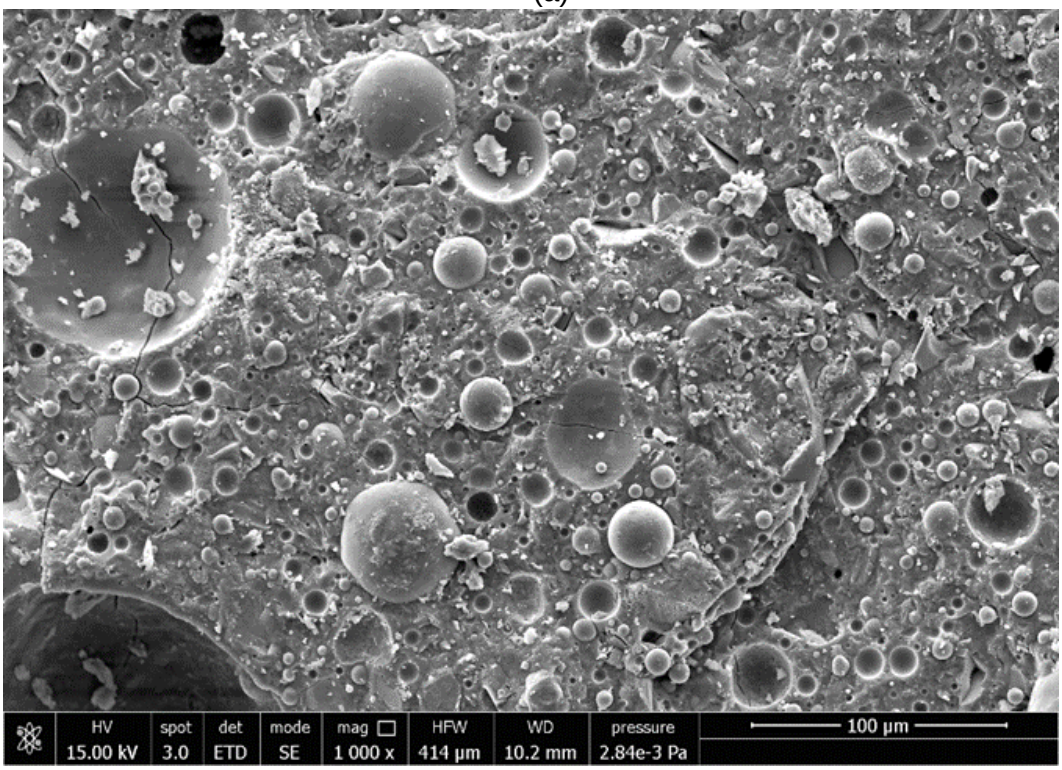

(b)

Figure 136. SEM micrographs of thermally aged materials: (a) MK formulation (b) MIX formulation

- **TGA**

TGA analysis was performed on samples 235-0600 and 235-1000 to verify the degradation behaviour; the following thermal program was used:

- heating from +30°C to 60°C, 20 °C/min in O_2
- isothermal at +60°C for 30 min in O_2
- heating from +60°C to 800°C, 20 °C/min in O_2

In the following Figure 137, the TGA thermograms of samples 235-0600 and 235-1000 are reported. During isothermal at +60°C, the sample 235-0600 shows a mass loss of 9.4% of water and Hydrocarbon material probably derived from degradation of Kerosene, while sample 235-1000 shows a mass loss of 3.6% of water.

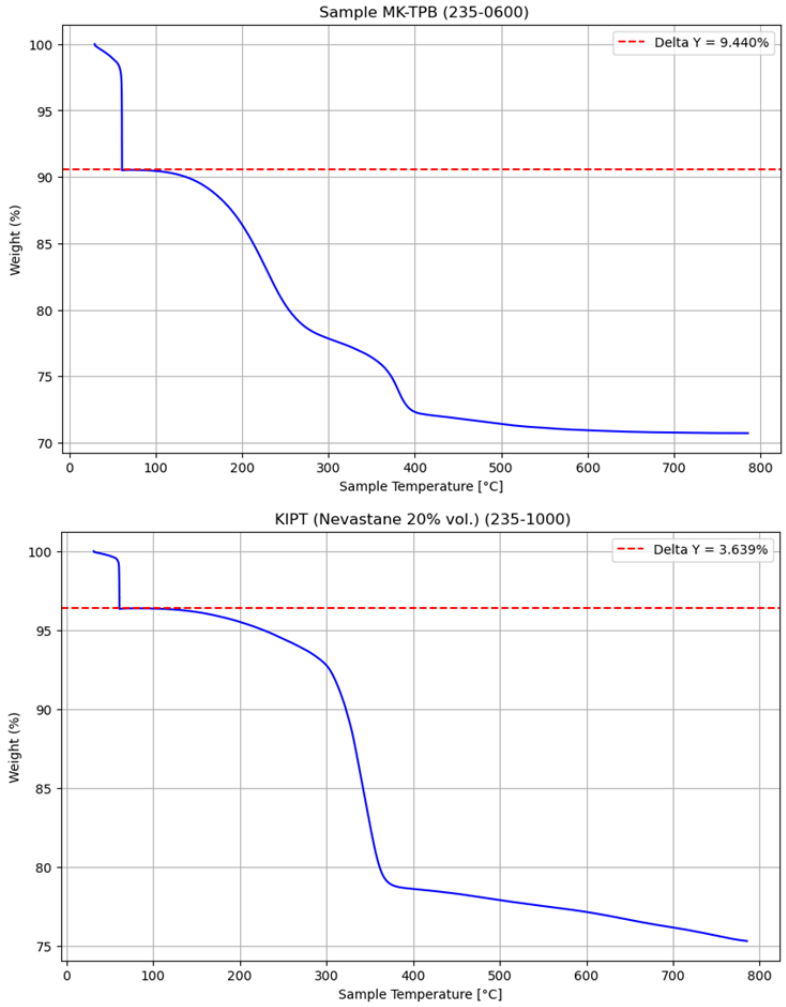

Figure 137. TGA thermograms of samples 235-0600 and 235-1000

At temperature above 400°C, the weight loss increases up to about 30%. It seems nevertheless that MK sample with TPB is more prone to weight loss than MIX formulation especially in the range before 300°C. The loss of strength caused was about 22.17% and 8.6% for 235-0600 and 235-1000 respectively. The results are summarised in Table 67.

Table 67. Ultimate stress of fresh and TTa MK-based and Mix formulation

Formulation	Fresh	Ultimate Stress [MPa]	TTa	Ultimate Stress [MPa]	Strength loss [%]
MK-based	273-600	6.0	235-600	4.2	22.15%
Mix Formulation	273-1000	7.88	235-1000	7.2	8.6%

7.2 In-Fire Test Analysis

The fire resistance tests were carried out according to the ASTM D 635-03 by heating at 800°C the MK-based, the BFS-based and the Mix formulation samples without oil. Thermocouples type K allowed to monitor the testing conditions. Figure 138 shows the fire test execution and the induced samples shape. NNL samples suffered extensive damage highlighted hourglass shape, KIPT samples showed an increase in the porosity, and BSF samples suffered slight cracking. The compressive strength of samples after in-fire condition are summarised in Table 68. The ultimate strength as numerically calculated by means of FE preliminary analysis, assuming homogenised behaviour of samples NNL, BFS and KIPT with oil, are of the order of kPa.

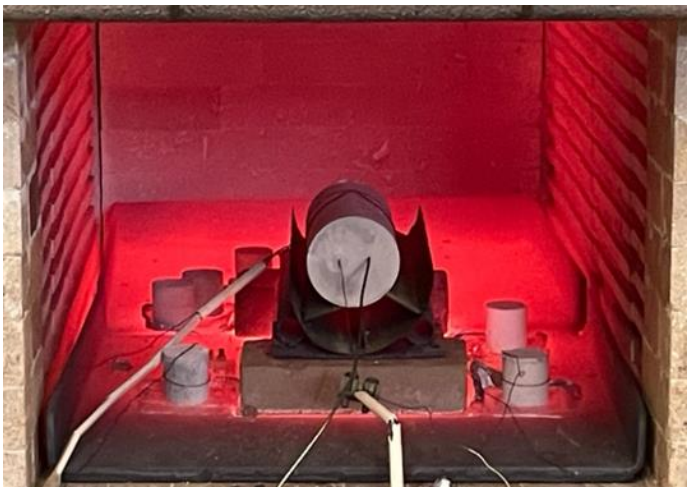

(a)

MK Based MIX formulation BFS Based

(b)

Figure 138. Fire test execution(a) and sample shape at the end of the fire test (b)

Table 68. Ultimate stress of fresh and Post-Fire (PF) MK Based, BFS Based and MIX formulations without oil

Formulation	Ultimate Stress [MPa]- Fresh	Ultimate Stress [MPa]- PF	Strength loss [%]
MK Based	15,36	0,00	100,00%
	8,38	0,00	100,00%
BFS Based	10,48	3,15	69,95%
	10,23	2,00	80,47%
MIX	10,24	6,02	41,19%
	14,65	4,71	67,87%

7.3 Partial conclusion about high temperature testing

The study of the high-temperature behaviour of materials encapsulating organic liquid waste is important to address safety issues, particularly in the event of fire or thermal cycling. To this end, several analyses have been carried out by UNIPI on samples from other partners, limited by the number of samples available. The DSC analyses show for all the samples (MK based formulations and MIX one) and for the different LOW used (limited to Oil) a first evolution of the behaviour at a temperature slightly higher than 100°C which corresponds to the vaporization of the water contained in the samples. TGA (thermal gravimetric analysis) tests reached 800°C, but only two samples (MK with TPB/Kerosen, MIX formulation with Nevastane, and BFS with TPB/Aliquat) could be studied. Nevertheless, they showed significant differences in behaviour above 200°C, indicating that the MK formulation is less resistant to high temperatures.

On the SEM images, the appearance of cracks is noticeable after thermal cycling between -20°C and +40°C. This cracking also translates into a reduction in strength, which appears to be the case (the scale of the compression testing campaign is not sufficient to present consolidated data, and the moisture control during these tests is also uncertain).

8 SYNTHESIS AND CONCLUDING REMARKS

The aim of this report was to present the main results obtained from the studies carried out on tasks 5.4.2 to 5.4.7 on conditioning matrix performance studies. These tasks involved 12 partners who studied the behaviour of geopolymer matrices developed in WP5.3 to immobilize radioactive liquid organic waste.

In order to study the ability to immobilize this type of waste over long timeframes, the various test campaigns focused primarily on analyzing the durability of matrices containing waste, as well as their ability to withstand both irradiation from the waste and accidental or seasonal thermal stress.
The first stage, involving the production of test samples, enabled us to study the robustness of the proposed formulations, and highlighted the need in some cases to adapt the formulations to the materials available in the various countries. This stage also highlighted the difficulty of incorporating certain liquid wastes (notably LSC and TPB/kerosene blends) into BFS-based formulations and the MIX formulation. The use of surfactants seems to facilitate this incorporation, although not all of the surfactants tested were able to demonstrate effectiveness.

In order to study matrix aging in detail under realistic conditions, the compressive strengths of the various formulations were measured as a reference state, but microstructural analyses provided crucial information. Indeed, all the analyses show that, for all 3 formulations, waste encapsulation is mainly based on physical phenomena, and that there is no modification of the crystalline microstructure of the materials in the presence of organic waste. The waste is thus trapped in the porosity of the matrix and not chemically bound to it. The analyses also show a finer and more extensive pore structure for the metakaolin-based geopolymer which potentially explains the possibility of incorporating a greater quantity of waste into this material while maintaining acceptable strength (greater than 10 MPa).

Aging tests under aerated conditions or in contact with a leaching solution (basic, neutral or acidic) showed that, as for other porous materials, ionic and gaseous exchanges took place. The penetration of CO_2 into the matrix has an effect on the pH of the interstitial solution of the materials, but has no deleterious effect (in the formulations tested, i.e. MK based and BFS based) on strength or on water and gas transfer properties. The presence of LOW seems even to slow down this process. In solutions, ionic exchange rates are significantly affected by the pH of the leaching solution, and exchange is faster when the pH of the solution is far from the one of the interstitial solutions of the materials (basic). As in the case of carbonation, although ionic exchange is measurable, it does not appear to have any impact on matrix strength. Furthermore, oil release rates remained very low (below 5% of the amount of waste incorporated) and leaching indices always remained above the acceptance criteria (6 or 8 depending on the country) even after irradiation of the matrices (tested up to 250 kGy). Irradiation tests revealed also higher hydrogen production for the metakaolin-based geopolymer, due to a higher initial water content than for the other formulations.

Initial results on thermal behaviour of the formulations tested (MK and MIX) show the microcracking of matrices under thermal cycling. Based on thermal gravimetric analysis, the MIX formulation seems to offer a higher resistance to temperature in the range between 200°C and 300°C. Nevertheless, the quantity of available data and post-mortem analysis remains insufficient to draw a robust conclusion.

In addition to summarizing the results obtained, it is also important to mention that:

- MK-based formulations are sensitive to drying/wetting cycles, which can rapidly lead to massive and violent cracking. As the waste is only physically encapsulated, matrix cracking will lead to higher waste release.
- The irradiation rates studied in this WP remain relatively modest, and these tests should be extended to higher irradiation rates.
- A study of the compatibility of the waste with respect to the fresh rheology of the matrices needs to be carried out in order to obtain compatible viscosities and to avoid bleeding or strong heterogeneity of the complex (RLOW and GP matrices)
- Behaviour at high temperatures and under fire-like conditions needs to be studied in greater depth due to the important role of the thermal gradients in reducing the strength capacity of these matrices.